Compressive Strength of Geopolymer Concrete Composites: Modeling and Comprehensive Systematic Review

Hemn Unis Ahmed (hemn.ahmed@univsul.edu.iq)
University of Sulaimani
Azad A. Mohammed
University of Sulaimani
Ahmed S. Mohammed
University of Sulaimani https://orcid.org/0000-0003-4306-3274

Research Article

Keywords: Geopolymer Concrete, Mix Proportion, Compressive Strength, Curing Condition, ANN Modelling, M5P-tree modeling

Posted Date: June 29th, 2021

DOI: https://doi.org/10.21203/rs.3.rs-611987/v1

Compressive strength of Geopolymer concrete composites: Modeling and comprehensive systematic review

Hemn Unis Ahmed [*1], Azad A. Mohammed[1], Ahmed S. Mohammed[1]

(1) University of Sulaimani, College of Engineering, Department of Civil Engineering, Kurdistan Region, Iraq

*Corresponding author: Tel: +964-7501119884; e-mail: hemn.ahmed@univsul.edu.iq

Abstract

The growing concern about global climate change and its adverse impacts on societies is putting severe pressure on the construction industry as one of the largest producers of greenhouse gases. Given the environmental issues associated with cement production, geopolymer concrete has emerged as a sustainable construction material. Geopolymer concrete is cementless concrete that uses industrial or agro by-product ashes as the main binder instead of ordinary Portland cement; this leads to being an eco-efficient and environmentally friendly construction material. Compressive strength is one of the most important mechanical property for all types of concrete composites including geopolymer concrete, and it is affected by several parameters like an alkaline solution to binder ratio (*l/b*), fly ash (*FA*) content, SiO_2/Al_2O_3 (*Si/Al*) of the FA, fine aggregate (*F*) and coarse aggregate (*C*) content, sodium hydroxide (*SH*) and sodium silicate (*SS*) content, ratio of sodium silicate to sodium hydroxide (*SS/SH*), molarity (*M*), curing temperature (*T*), curing duration (*CD*) inside the oven and specimen ages (*A*). In this regard, a comprehensive systematic review was carried out to show the effect of these different parameters on the compressive strength of the fly ash-based geopolymer concrete (FA-GPC). In addition, multi-scale models such as Artificial Neural Network (ANN), M5P-tree (M5P), Linear Regression (LR), and Multi-logistic Regression (MLR) models were developed to predict the compressive strength of FA-GPC composites. For the first time, in the modeling process, twelve effective parameters including l/b, FA, Si/Al, F, C, SH, SS, SS/SH, M, T, CD, and A were considered the modeling input parameters. Then, the efficiency of the developed models was assessed by various statistical assessment tools like Root Mean Squared Error (RMSE), Mean Absolute Error (MAE), Scatter Index (SI), OBJ value, and the Coefficient of determination (R^2). Results show that the curing temperature, sodium silicate content, and ratio of the alkaline solution to the binder content are the most significant independent parameters that influence on the compressive strength of the FA-GPC, and the ANN model has better performance for predicting the compressive strength of FA-GPC in compared to the other developed models.

Keywords:

Geopolymer Concrete; Mix Proportion; Compressive Strength; Curing Condition; ANN Modelling; M5P-tree modeling

1 Introduction

It is widely known that the production of Portland cement needs a considerable amount of energy and at the same time contributes to generating a huge volume of the total carbon dioxide (around 7%) to the atmosphere directly and indirectly, the heating of limestone releases CO_2 directly which is called calcination (50%), while the burning of fossil fuels to heat the kiln indirectly results in CO_2 emissions, this is around 40 percent of cement emissions and finally around 10% for quarrying and transporting [1-3]. In addition, around 2.8 tons of raw materials are needs for the manufacture of one ton of cement; this is a resource-exhausting process that consumes a large number of natural resources such as limestone and shale for the production of clinkers for cement [4]. Furthermore, approximately one trillion liters of mixing water is required to be used in the concrete industry annually [5]. In the same context, the cement industry is the most energy-intensive construction material after aluminum and steel manufacture. In a typical cement plant alone, around 110-120 kWh is used for each ton of produced cement [6]. However, cement-based concrete is still the main important material used in the construction industries worldwide [7]. Therefore, a highly efficient application of renewable and non-renewable raw materials is essential for the economic development [8]. Sustainable development of a novel material to replace the Portland cement has become increasingly substantial as the globe goes on to face serious environmental problems [9, 10].

A convenient, suitable replacement to conventional concrete is geopolymer technology that was developed first by Davidovits in France, 1970 [11]; the ancient Roman civilizations have used geopolymer for building their monumental and castles in ancient times [12]. Geopolymers are members of the family of inorganic alumino-silicate polymer synthesized from alkaline activation of various aluminosilicate materials or other industrial or agro by-product materials rich in silicon and aluminum like fly ash (FA), ground granulated blast furnace slag (GGBFS), metakaolin (MK), palm oil fuel ash (POFA), rice husk ash (RHA) [13]. The microstructure of geopolymer materials is amorphous, and their chemical constituents are similar to the natural zeolitic materials [14]. The chemical reaction between alkali solution and base material containing aluminosilicate is called geopolymerization process; the final product of the geopolymerization process gives a three-dimensional polymeric chain and ring structure Si-O-Al-O bonds as shown in the Scheme.1. [15], with an empirical formula of $\{M_n[-(SiO_2)_z-AlO_2]_n.wH_2O\}$, when; M is an alkali action, n is the percent of polymerization, and w is the content of water [16]. In addition, the chains in aluminosilicate could be in the form of poly-(sialate) with the ratio of Si to Al is equal to 1.0 (-Al-O-Si- chain), poly (sialate-siloxo) with the ratio of Si to Al is equal to 2.0 (-Al-O-Si-Si- chain), and poly (sialate-disiloxo) with the ratio of Si to Al is equal to 3.0 (-Al-O-Si-Si-Si- chain) [17].

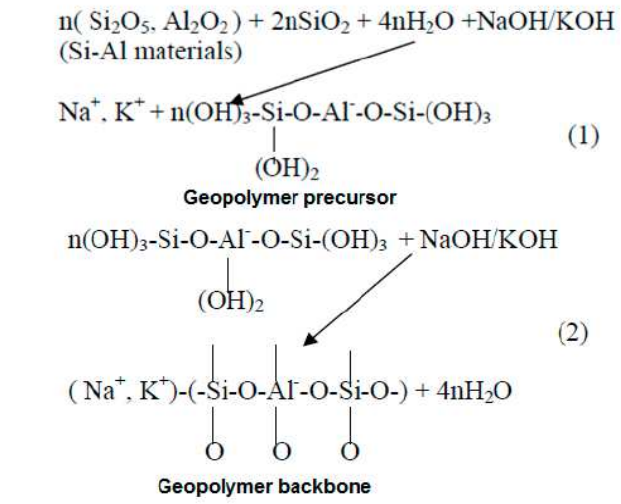

Scheme.1. Chemical reactions during geopolymerization process [15]

The mechanism of geopolymerization could be briefly explained as follows; in the first stage, dissolution of the silicate and aluminum elements of the binder inside the high alkalinity aqueous solution produces ions of silicon and aluminum oxide. In the second stage, a mixture of silicate, aluminate, and aluminosilicate species, which through a contemporaneous operation of poly-condensation-gelation further condensation, finally produces an amorphous gel [18]. Several of factors could influence the performance of geopolymer concrete (GPC), such as type of binder, concentration of the alkaline solution, the molarity of sodium hydroxide, ratio of sodium silicate to sodium hydroxide, extra water, mix proportion and curing method [19]. The chemical composition of the ash-based geopolymer and alkaline activators are effect on the final product of the geopolymerization process, and this geopolymerization is usually accelerated at higher temperatures [20, 21]. Thus, it can be said that, the geopolymer is a third generation of cementing materials after lime and cement [22], and it is an eco-friendly and green material that has low green gas emission of around 70% lower than the Portland cement concrete due to the high consumption of waste materials inside their mix proportions [23]. The mix proportions of the GPC are consist of aluminosilicate binder, fine and coarse aggregates, alkaline solutions, and water. The polymerization between these ingredients produces solid concrete almost like normal concrete [24]. Binder source materials of the geopolymer concrete are those rich in alumino-silicates such as FA, GGBFS, RHA, MK, POFA, or any hybridization between these ashes with or without Portland cement. FA is the most commonly used source binder materials for making GPC due to its low cost, abundance availability, and higher potential for preparation geopolymers [25, 26]. FA is the finely chopped residue that produced from the combustion of pulverized coal and is imparted from the combustion chamber by using exhaust gages by using electrostatic precipitators or other devices for the filtration of the particles before the flue gages reach the chimneys [27, 28]. Generally, based on the source of the coal being burned, FA is divided into two classes, namely class F fly ash which is produced from burning anthracite or bituminous coal, and class C fly ash which is mainly produced from the

burning of lignite coal sources, the former type has lower calcium content in compared to class C fly ash [29]. Further, the main components of FA are typical consist of SiO_2, Al_2O_3, Fe_2O_3, and CaO with a lower percent of some other minerals, which is shown in Table 1. The total percent of SiO_2, Al_2O_3, and Fe_2O_3 for the class F fly ah is over 70%, with the content of CaO less than 10%, while for the class C fly ash total content of SiO_2, Al_2O_3 and Fe_2O_3 should be between 50% to 70% with the percent of CaO greater than 20% [30, 31]. In addition, FA is considered as a dangerous material because it contains many trace elements, such as Mn, Ti, Cr, V, Co, As, Pb, and Mo. The intensity of the toxic trace elements in FA could be 5-10 times greater than those in the raw material sources [32-34] and it has small amounts of polycyclic aromatic hydrocarbon and dioxins [35, 36]. Therefore, the erroneous discarding of FA and any other by-product or waste materials will increment the occupation of land and destroy the environment and ecology [37-39]. Thus, to tackle these problems of FA and any other waste materials; efforts have been made towards re-use of them in an efficient and green way, for instance, high volume researchersresearchersresearchersresearchers have used FA have used FA have used FA have used FA to replace Portland cement in different types of concrete and cementitious composites [40-46]. More recently, FA has been utilized as an alternative source to make geopolymer paste [47, 48], mortar [49, 50], and concrete [51, 52]. For the production of FA-GPC, some reactions take place between alkali liquids and FA. Condensation among the resultant of Al^{3+} and Si^{4+} patterns, go ahead by other complex nucleation, oligomerization, and polymerization, which lastly produce new amorphous three-dimensional network structure with a novel aluminosilicate based polymer as shown in Fig.1 [53].

Alkaline solution or liquids in the GPC are a mixture of sodium hydroxide or potassium hydroxide with sodium silicate or potassium silicate with water. The alkaline solutions include concentrated aqueous alkali hydroxide or silicate solution with soluble alkali metals that are usually sodium or potassium-based consumed in the production of alkali activators for balancing the negative charge of the alumina if four-fold coordination with the silica [2]. The purity of the sodium hydroxide is almost above 97%, and pellets and flakes are the two main states of the sodium hydroxide, while a range of SiO_2 is varying from 28 to 37%, Na_2O is varying from 8 to 18%, and the percent of water is between 45 to 64% for the sodium silicate for the reviewed researches as shown in Table 2. These solutions generate a geopolymeric binder by activating and extracting Si and Al atoms from the binder source materials [2].

Fig.1. the schematic graphical representation that shows the transition of fly ash to fly ash-based geopolymer cement/concrete [53]

One of the most important mechanical properties of all types of concrete composites, including FA-GPC, is the compressive strength (*fc′*), and it can be found by following the standard test methods of ASTM C39 [54] BS EN 12390-3 [55]. *fc′* gives a general performance about the quality of the concrete [56]. However, in the structural design and construction field, the compressive strength of the concrete at 28 days is essential. Therefore, achieving an authoritative model for predicting the compression strength of GPC is essential regarding the possibility of changing or validating the GC mix proportions [57, 58]. By selecting appropriate mixing proportions, economic and efficient designs will be accomplished. Therefore, various researches have been tried to shorten the time of choosing a proper mix of proportions to get the targeted properties; among them is modeling with developing empirical equations. There are different ways to model construction materials' characteristics, including statistical techniques, computational modeling, and nowadays developed techniques such as regression analysis [59, 60]. A variety of factors affect the *fc′* of the FA-GPC; this leads to different compression strength results; consequently, predicting *fc′* is a challenging task for researchers and engineers. Therefore, there is a need for numerical and mathematical models [61]. Due to the good ability of machine learning regarding prioritization, optimization, forecasting and planning were widely used in the various engineering fields [57]. In the literature, machine learning systems were used to model the various characteristics of different types of concrete composites such as compression strength of green concrete [62], splitting tensile and flexural strength of recycled aggregate concrete [63], modulus of elasticity of recycled concrete aggregate [64, 65], the *fc′* of high volume fly ash concrete [66], the *fc′* of eco-friendly GPC containing natural zeolite and silica fume [67], splitting tensile strength of fiber-reinforced concrete [68], the *fc′* of self-compacting concrete modified with nanosilica [69], and so on.

In the literature, there is a lack ofsystematic and comprehensive reviews to show and measure the effects of several mixture proportion parameters and different curing regimes on the compressive strength of

FA-GPC. Therefore, in this study, for the first time influence of several parameters like an alkaline solution to binder ratio (*l/b*), fly ash (*FA*) content, SiO_2/Al_2O_3 (*Si/Al*) of the FA, fine aggregate (*F*), and coarse aggregate (*C*) content, sodium hydroxide (*SH*) and sodium silicate (*SS*) content, the ratio of sodium silicate to sodium hydroxide (*SS/SH*), molarity (*M*), curing temperature (*T*), curing duration (*CD*) inside the oven and specimen ages (*A*) were investigated to show their influences on the *fc′* of the FA-GPC, and then multi-scale models such as Artificial Neural Network (ANN), M5P-tree (M5P), Linear Regression (LR), and Multi-logistic Regression (MLR) models were developed to predict the *fc′* of the FA-GPC composites at different mixture proportions.

Table.1. Chemical composition of fly ash

References	Sp.Gr.	SiO_2	Al_2O_3	Fe_2O_3	CaO	MgO	K_2O	Na_2O	SO_3	LOI
[70]	-	53.3	26.49	10.86	1.34	0.77	0.8	0.37	1.7	1.39
[71]	-	77.1	17.71	1.21	0.62	0.9	-	0.8	2.2	0.87
[72]	-	62.9	25.8	3.1	2.3	0.3	-	-	-	1.7
	-	66.6	25.9	0.9	0.4	0.1	-	-	-	1.3
	-	77.2	15.2	2.5	0.6	0.3	-	-	-	0.7
	-	43.4	26.2	17.4	5.4	1.4	-	-	-	0.7
	-	52.7	33.4	9	1	0.6	-	-	-	0.4
[73]	1.95	62.5	29.02	4.22	1.1	-	-	0.2	0.22	0.52
[74]	-	62.1	25.5	4.28	3.96	1.27	-	-	0.73	-
[75]	1.95	62.5	29.02	4.22	1.1	-	-	0.2	0.22	0.52
[76]	2.13	57.9	31.1	5.07	1.29	0.97	1	0.09	0.05	0.8
[77]	2.42	65.6	26.5	5.49	0.31	0.76	0.23	0.36	0.31	0.41
[78]	2.12	70.3	23.1	1.4	0.2	0.6	0.9	0.4	0.2	2
[79]	-	47.8	24.4	17.4	2.42	1.19	0.55	0.31	0.29	1.1
[80]	2.2	62.3	28.1	2.1	0.5	1	1	0.5	0.4	2.5
[81]	-	52	33.9	4	1.2	0.81	0.83	0.27	0.28	6.23
[82]	-	49	31	3	5	3	1	4	0	0
[83]	-	48	29	12.7	1.76	0.89	0.55	0.39	0.5	1.61
[84]	-	32.1	19.9	16.91	18.75	3.47	2.38	0.69	2.24	0.07
[85]	-	51.5	23.63	15.3	1.74	1.2	0.84	0.38	0.28	1.78
[86]	2.04	59.2	24.36	7.074	2.235	1.4	3.37	0.378	-	1.517
	2.3	62.3	21.14	7.347	1.568	2.35	0.73	2.445	-	2.071
[87]	2.05	64.9	26.64	5.69	0.33	0.85	0.25	0.49	0.33	0.45
[88]	-	47.8	24.4	17.4	2.42	1.19	0.55	0.31	0.29	1.1
[89]	-	59.7	28.36	4.57	2.1	0.83	-	0.04	0.4	1.06
[90]	2.36	37.6	14.79	18.56	19.61	2.7	0.98	0.73	4.81	-
[91]	-	53.7	27.2	11.17	11.17	1.9	0.54	0.36	0.3	0.68
[92]	2.54	42.4	21.3	15.7	13.2	2.3	2	0.9	1	0.4
[93]	-	50.7	28.8	8.8	2.38	1.39	2.4	0.84	0.3	3.79
[94]	-	50.7	28.8	8.8	2.38	1.39	2.4	0.84	0.3	3.79
[95]	-	50.5	26.57	13.77	2.13	1.54	0.77	0.45	0.41	0.6

Table.2. Purity of NaOH and compositions of Na_2SiO_3

References	Sodium Hydroxide	Sodium Silicate		
	Purity %	SiO_2	Na_2O	Water
[70]	98	29.4	14.7	55.9
[71]	97	34.31	16.37	49.28
[72]	98	29.4	14.7	55.9
[74]	98	32.4	13.7	53.9
[76]	98	34.64	16.27	49.09
[77]	98	35.06	16.95	47.99
[79]	98	29.4	14.7	55.9
[81]	99	28	8	64
[87]	99	45		55
[88]	98	29.4	14.7	55.9
[89]	98	34.64	16.27	49.09
[90]	99	34.72	16.2	49.08
[91]	98.5	30.1	11.4	58.6
[96]	97	36.7	18.3	45
[97]	98	29.93	12.65	56.42
[98]	99	29.4	14.7	55.9
[99]	99.51	28	9	63

2 Research Significance

Investigate the effects of several mixture proportion parameters and different curing regimes on the *fc′* of FA-GPC and develop and develop multi-scale models to predict the *fc′* of FA-GPC are the main scope of this study. Thus, the effect of several parameters such as an alkaline solution to binder ratio (*l/b*), fly ash (*FA*) content, SiO_2/Al_2O_3 (*Si/Al*) of the FA, fine aggregate (*F*) and coarse aggregate (*C*) content, sodium hydroxide (*SH*) and sodium silicate (*SS*) content, ratio of sodium silicate to sodium hydroxide (*SS/SH*), molarity (*M*), curing temperature (*T*), curing duration (*CD*) inside oven and specimen ages (*A*) were quantified. A wide range of experimental data (510 laboratories tested data) with different *l/b*, *FA*, *Si/Al*, *F*, *C*, *SH*, *SS*, *SS/SH*, *M*, *T*, *CD*, and *A*, were collected and analyzed to broaden the horizon of researchers and construction industry to have considerable information about the influence of these different parameters on the compression strength of FA-GPC. Regarding the modeling process, for the first time, twelve input parameters were considered to develop predictive models aiming: (i) to guarantee the construction industry to use the provided models without any theoretical; (ii) to carry out statistical analysis and recognize the influence of various parameters on the *fc′* of FA-GPC; (iii) to quantify and provide a systematic multiscale model to predict the compression strength of FA-GPC; (iv) to discover the most authoritative model to predict the compression strength of FA-GPC from four

different model techniques (ANN, M5P, LR, and MLR) by applying statistical assessment tools such as MAE, RMSE, SI, OBJ, and R^2.

3 Methodology

In the literature, there is a wide range of data regarding GPC with different source binder materials, including *FA*, *GGBFS*, *RHA*, *SF*, *MK*, and *RM*. In this paper, the authors focus on those studies that used FA as the source binder materials. The authors extract about 510 laboratories-tested datasets from 175 previous research types of research with different mixture proportion parameters, curing regimes, and specimen ages to investigate the influence of these parameters on the fc′ of the FA-GPC composites as for developing the models. The input datasets were consists of the *l/b* range from 0.25-0.92, *FA* range from 254-670 kg/m^3, *Si/Al* range from 0.4-7.7, *F* range from 318-1196 kg/m^3, *C* range from 394-1591 kg/m^3, *SH* range from 25-135 kg/m^3, *SS* range from 48-342 kg/m^3, *SS/SH* range from 0.4-8.8, *M* range from 3-20, *T* range from 23-120°C, and *CD* range from 8-168 hr. as can be seen in Table 3. The models used twelve input parameters, which not allowed authors to use more datasets in the developed models. For instance, those researches were ignored if the mix proportions and any other model parameters of the research were not provided. The larger group of a dataset, which included 340 datasets, was used to create the models. The second group consists of 85 datasets used to test the proposed models, and the last group, which includes 85 datasets, was used to validate the provided models [57, 69]. The data collection, comprehensive review, and modeling work are summarized in a flow chart, as depicted in Fig.2.

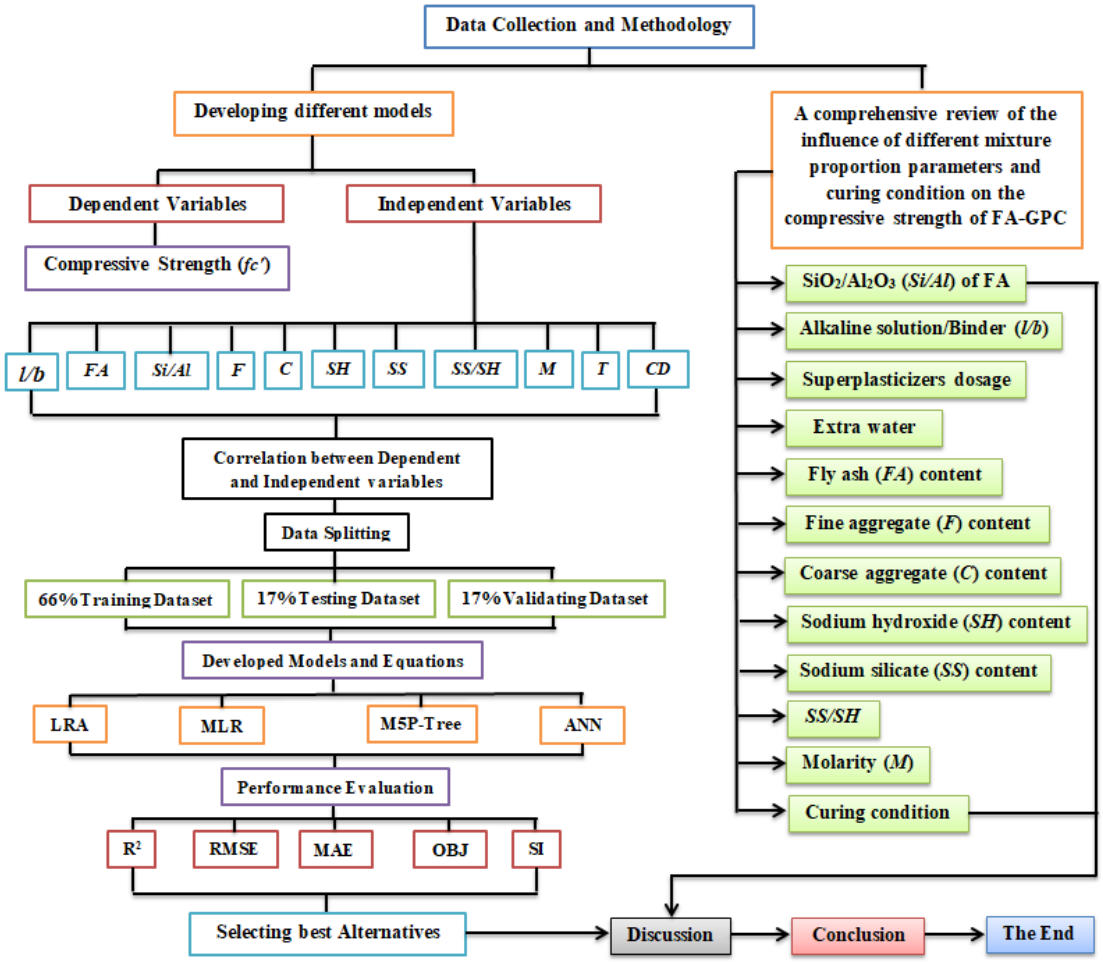

Fig.2. The flow chart diagram followed in this study

Table.3. Summary of different FA-GPC mixes

References	(*l/b*)	*FA* (kg/m^3)	(*Si/Al*)	*F* (kg/m^3)	*C* (kg/m^3)	*SH* (kg/m^3)	*SS* (kg/m^3)	(*SS/SH*)	M	T (°C)	CD (hr.)	A (Day)	*fc'* (Mpa)
[70]	0.35	476	2	554	1294	48-120	48-120	0.4-2.5	8-14	24-90	8-96	3-94	17-64
[71]	0.5-0.6	300-500	1.5-5.1	471-664	1000-1411	42-120	90-215	1.5-2	12-16	70	24	7	16-64
[72]	0.6	385	2.4	601.7	1203	66	165	2.5	12	80	24	3-28	74-81
[73]	0.45	350-400	2.1	505-533	1178-1243	45-52	112-129	2.5	8-16	24	-	3-28	7-41
[74]	0.45-0.55	300-350	1.8	698-753	1048-1131	38-55	96-118	2.5	10	100	24	7-28	26-36
[75]	0.45	298-430	2.4	533-590	1243-1377	38-55	96-138	2.5	8-14	10-90	24	3-28	19-43
[76]	0.81	409	3.0	686	909	129	204	1.58	15	80	24	28-96	22-27

[77]	0.4	394	2.3	646	1201	45	112	2.5	16	24-60	24	3-28	8-50
[78]	0.35	408	1.9	554	1294	41	103	2.5	8-14	60	24	7	40-64
[79]	0.3-0.45	400	2.2	830-895	830-895	32-52	85-129	2-3.3	12-18	50	48	7-28	16.36
[80]	0.3-0.5	400-475	1.5	529-547	1235-1280	34-57	85-142	2.5	14	24	-	7-56	7-44
[81]	0.35	408	1.6	647	1202	41	103	2.5	14	24-60	24	28	27-40
[82]	0.6	390	1.6	585	1092	67	167	2.5	8-18	24	-	28	23-32
[83]	0.35-0.38	408	2.1	660	1168-1201	41	103	2.5	10-16	24-50	24	28	25-72
[84]	0.55	356	2.8	554.4	1293	43-78	117-152	1.5-3.5	10	60	48	7-28	23-35
[85]	0.45	500	2.4-2.9	575	1150	64	160	2.5	14	24	-	28	44-52
[86]	0.4	350	0.4	650	1250	41	103	2.5	8	24-60	24	3-28	6-32
[87]	0.35	408	1.9	640-647	1190-1202	41	103	2.5	14-16	60	24	28	42-62
[88]	0.3	670	1.9	600	970	80	120	1.5	3-9	50	72	3-7	59-61
[89]	0.6	450	1.9	500	1150	135	135	1	10	40	24	7-96	18-49
[90]	0.4	400	1.7	554	1293	45	113	2.5	14	100	72	3-28	14-36
[91]	0.4	400	1.7	554	1293	45	113	2.5	14	100	72	3-28	29-45
[92]	0.37-0.4	408	1.9	647	1201	62-68	93-103	1.5	14	60	24	28	32-38
[93]	0.4	420-440	2.3-3.3	340-575	660-1127	60-68	150-169	2.5	12	80-120	72	7	21-61
[94]	0.35	356-444	1.9	554-647	1170-1248	36-44	89-111	2.5	14	60	24	7-28	24-63
[95]	0.35	409	3	549	1290	41	102	2.5	10	24	-	7-112	10-41
[96]	0.38-0.46	350-400	2.1	540-575	1265-1343	38-53	95-132	2.5	16	24-90	24	3-28	2.6-44
[97]	0.35	408	1.5	554	1294	41	103	2.5	8	24	-	7-28	12-16
[98]	0.35-0.65	254-420	2.1	318-1198	394-1591	25-76	69-165	1.5-3.5	8-16	24-120	6-72	3-28	13-60
[99]	0.4	400	1.9	651	1209	45	114	2.5	14	24	-	3-96	5-33

[100]	0.35	334	4.3	555-632	1175-1329	58	58	1	13	90	8	7	17-61
[101]	0.4	440	2.4	723	1085	64	112	1.75	12	60	48	3-28	23-35
[102]	0.7-0.9	412-420	1.5-3.9	693-706	918-936	39-92	241-342	2.6-8.8	15	80	24	3-96	22-57
[103]	0.55	310	2.5	649	1204	48.8	122	2.5	10	80	24	28-96	44-47
[104]	0.5	420	2.6-2.9	630	1090	60	150	2.5	12	80	24	7	32-41
[105]	0.37	424	1.5	598	1169-1197	63	95	1.5	14	70	24	3-96	2-58
[106]	0.5	368	2.3	554	1293	52	131	2.5	16	100	24	28	41
[107]	0.3	450	2.1-2.6	788-972	945-972	67	67	1	10	70	24	7-28	25-41
[108]	0.4	410	5.6	530	1044	67	117	1.74	10	24-75	26	7-180	4-36
[109]	0.45	500	2.3	550	1100	64.3	160.7	2.5	14	70	48	28	49.5
[110]	0.4	400	1.9	651-656	1209-1218	40-46	100-114	2.5	14	24	–	28-90	25-41
[111]	0.58	380	1.6	462	1386	62	156	2.5	10	60	24	28-56	18-23
[112]	0.5	414	2.2	588	1091	69-104	104-138	1-2	10-20	24-60	24	7-28	19-54
[113]	0.4	394	1.9	554	1293	45	112	2.5	12	24-60	24	7-28	8-28
[114]	0.3-0.4	428	2.1	630	1170	44-57	114-122	2-2.5	8-14	60-90	24	3-7	20-49
[115]	0.3	563	1.5	732	5994	44	124	2.8	10	75	16	28	3345
[116]	0.5	400	3.1	650	1206	50-70	140-154	2-2.75	14	60	168	7-28	30-36
[117]	0.4-0.6	345-394	7.7	554	1294	45-83	94-148	1.5-2.5	8-16	24	-	28	7-22
[118]	0.4	400	2.0	644	1197	53	107	2	10	24	-	3-56	5-23
[119]	0.4	394	1.8	554	1293	45	112	2.5	8	24	-	7-28	3-18
[120]	0.4	350	1.8	483	1081	40	100	2.5	14	24	-	7-28	3-23
[121]	0.45	436	1.7	654	1308	56	140	2.5	8	24	-	3-12	8-18
[122]	0.65	639	2.6	639	959	121	304	2.5	8_12	24	-	7-28	6-32
[123]	0.35	500	1.6	623	1016	70	105	1.5	14-16	24	-	3-28	7-27
[124]	0.41	350	2.1	645	1200	41	103	2.5	8	24	-	3-56	7-21

Remarks (Ranged are Varies Between)	**0.25-0.92**	**254 - 670**	**0.4 - 7.7**	**318 - 1196**	**394 - 1591**	**25 - 135**	**48 - 342**	**0.4 – 8.8**	**3 - 20**	**23 - 120**	**8 - 168**	**3 - 112**	**2 - 64**

*(***l/b***) is the alkaline liquid to binder ratio, (***FA***) is a fly ash content (Kg/m^3), (***Si/Al***) is a (SiO_2/Al_2O_3) ratio of fly ash, (***F***) is a fine aggregate content (Kg/m^3), (***C***) is a coarse aggregate content (Kg/m^3), (***SH***) is a sodium hydroxide content (Kg/m^3), (***SS***) is a sodium silicate content (Kg/m^3), (***SS/SH***) is the ratio of sodium silicate to sodium hydroxide of the mix, (***M***) is the molarity (concentration of sodium hydroxide) of the mix, (***T***) is the curing temperature of the specimens and this is may be ambient curing or heat curing inside an oven (°C), (***CD***) is the curing duration inside an oven (hr.), (***A***) is the age of samples at the time of testing (days) and ***fc'*** is the measured compressive strength (MPa).

4 Effect of mixture proportion parameters on the compressive strength of FA-GPC

4.1 Chemical composition of fly-ash (SiO_2/Al_2O_3) (*Si/Al*)

In the literature, a variety of fly ashes with slightly different chemical compositions, specific surfaces and specific gravity were used to prepare the GPC. Based on the ASTM C618 [29], ash with the summation of their SiO_2+Al_2O_3+Fe_2O_3 greater than 70% can be known as fly ash. To investigate the effect of mixed compositions on the *fc'* and microstructure of FA-GPC an experimental laboratory research work has been conducted by Thakur and Ghosh [125]. They reported that the compression strength was improved almost linearly with *Si* content up to 4, and then it was decreased, as illustrated in Fig.3.

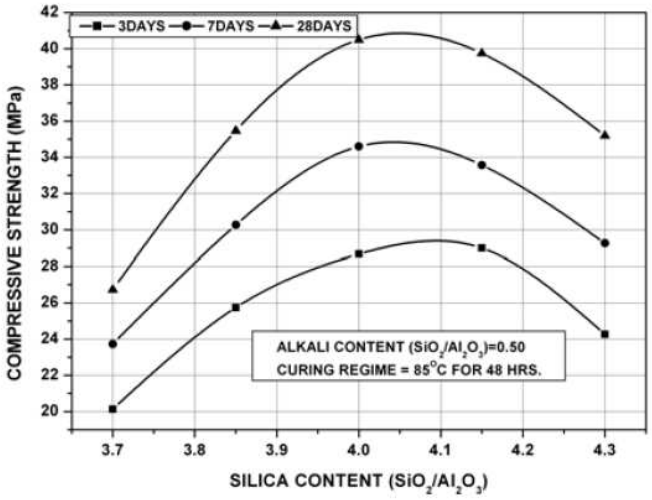

Fig.3. Effect of different SiO_2/Al_2O_3 on the *fc'* of FA-GPC [125]

A research study was carried out on the FA-GPC by Al-Azzawi et al. [71], who used five different fly ashes. The fly ashes have different chemical compositions with the ratio of *Si/Al* of 1.58, 1.66, 2.44, 2.57, and 5.08. At the constant mixture proportions and same curing conditions, the highest compression

strength was recorded for the fly ash with *Si/Al* ratio of 1.66, which it is 34 MPa. This value is significantly higher than the other fly ashes by 20.5%, 38.2%, 41.2%, and 44.1% for the *Si/Al* of 1.58, 2.44, 2.57 and 5.08, respectively. This result may be attributed to the different properties of different fly ashes that lead to different extent of geopolymerization between the alkaline activator and the fly ashes, which influences the *fc′* of the GPC. In addition, the different extent of the geopolymerization process affects the microstructure of the FA-GPC, which in turn affects the compressive strength of the GPC [71]. In the same context, an experimental study had been conducted to investigate the mechanical and durability properties of FA-GPC with the inclusion of two different types of fly ashes. At ambient curing temperature, the *fc′* was 51.6 and 44.8 MPa at the age of 28 days for the *Si/Al* ratio of 2.43 and 2.95, respectively. At the same time, the CaO content for the *Si/Al* of 2.43 was greater than 2.95 [85]. This result was attributed to the lower content of CaO and low activity of fly ash [126, 127].

Furthermore, to investigate the long-term permeation characteristics of the GPC, four different types of fly ashes were used to prepare FA-GPC. Their results claimed that the highest *fc′* was achieved for the GPC with the *Si/Al* of 1.71, and the lowest compression strength was recorded to *Si/Al* of 1.8, while the other fly ash types fell between the two. Moreover, all their GPC mixtures archived almost 70% of their one-year compression strength at 3 days; for instance, the GPC with *Si/Al* of 1.71 displayed about a 20 MPa strength increment between three and 365 days [102]. These results revealed that there is a continuation in the geopolymerization process which leads to improvement in the compressive strength of different types of FA-GPC. This output is in contrast to the past studies on FA-GPC, which have recorded little subsequent improvement in the *fc′* for the heat curing conditions [70, 128, 129].

In addition, another research study had been carried out on the mechanical characteristics of geopolymer concrete which they used three different fly ashes with different chemical compositions. In the controlled heat curing conditions and constant mixture proportions, *fc′* values were 32.1, 41, and 36.6 MPa for the Si/Al of the fly ash of 2.9, 2.78, and 2.6, respectively [104]. Scanning Electron Microscopy (SEM) examined the results behind different compressive strength values. They reported that the samples made from the fly ash with Si/Al of 2.78 have the highest degree of reacted fly ash spheres, which participated in the greatest compression strength. This result was reported by other researchers who claimed that the total reacted *Si/Al* is crucial to the progress in the polymerization of the FA-GPC process [70, 128]. In addition, it was observed that with the increase of *Si/Al* ratio, compression strength was improved [80, 130]. Similar observations have been made by Thokchom et al. [131], who founded that with the increase in *Si/Al* ratio of binder source materials, residual compressive strength of the GPC was improved when the specimens exposed to different temperature degrees, as shown in Fig. 4. The GPC with 2.2 ratios of *Si/Al* still retained nearly 63% of its compression strength even after exposure to 900 °C, while the GPC mixture prepared with 1.7 ratios of *Si/Al* indicated the residual compressive strength of 50%. This result was further investigated by SEM tests which revealed that the GPC specimens prepared with 1.7 *Si/Al* ratio have entire disruption of the matrix due to sintering of phases inside the samples; however, interconnected matrix the most of the initial pores being blocked in the

heating process. While GPC made with *Si/Al* of 2.2 presents a relatively undisturbed matrix except at little places [131].

Lastly, an experimental research program was performed to investigate the mechanical properties of high early strength FA-GPC. They used five different fly ash source materials with various *Si/Al* ratio and CaO content. Their results indicated that the highest *fc′* was recorded for a mixture with 2.18 of *Si/Al* and 4.96 CaO content [107], and from the Fig.5 variation of compression strength of the FA-GPC with different percentage of CaO and SiO_2+Al_2O_3 of fly ash could be clearly seen, which emphases the idea that the CaO, SiO_2, and Al_2O_3 content has a direct effect on the mechanical properties of fly ash-based geopolymer concrete. The high CaO FA-GPC mixture can explain this result gains strength as a result of two main different mechanisms, namely geopolymerization and hydration with the controlled curing conditions [132], an increment in the SiO_2 and Al_2O_3 content of the fly ash resulted in an increase *fc′* of the FA-GPC linked to the geopolymerization process. While the availability of CaO prohibits the geopolymerization process as a consequence decrease the compression strength of the GPC.

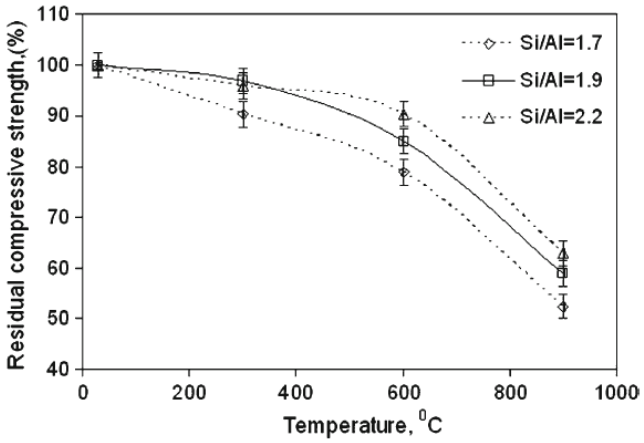

Fig.4. Variation of residual compression strength of different Si/Al ratio of FA-GPC with temperature [131]

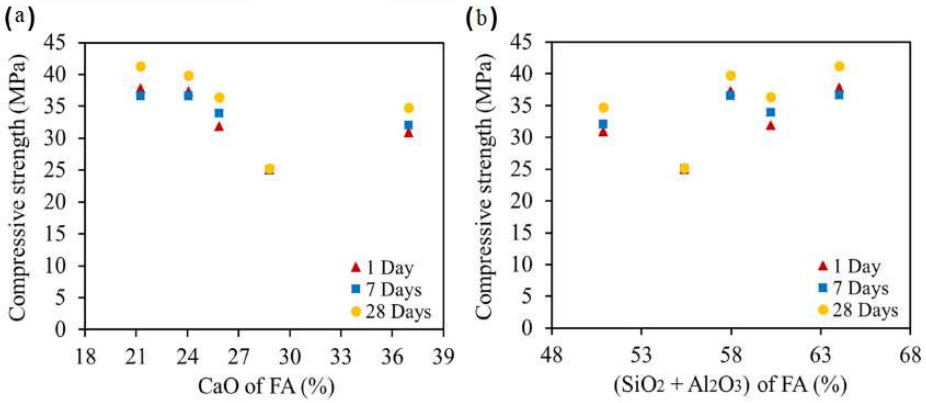

Fig.5. Variation of *fc′* of FA-GPC versus: (a) calcium content and (b) silica and alumina contents [107]

4.2 The alkaline solution to the binder ratio (*l/b*)

The alkaline solution is the summation of the sodium hydroxide and sodium silicate content, while the binder content is the total weight or volume of the fly ash or other source binder materials in the mixture proportions of the GPC. Based on the findings of Aliabdo et al. [79], when the chemical admixture content, additional water content, *SS/SH,* and *M* were kept constant at 10.5 Kg/m^3, 35 Kg/m^3, 0.4, and 16, respectively, the *fc′* of the FA-GPC was increased with the increment in the *l/b* ratio up to 0.4; then the effect reverses as shown in Fig.6. This increment in the compression strength of the FA-GPC was 52%, 78%, and 68% for mixes with 0.35, 0.4, and 0.45 alkaline liquid to fly ash ratio, correspondingly, as compared with that mix that has 0.3 alkaline liquid to fly ash ratio. Similar observations have been made by Shehab et al. [74], who found that the higher percentage of *l/b* improves the *fc′* of the FA-GPC at the age of 7 and 28 days. In the same context, experimental work was performed to investigate the effect of different parameters on the mechanical properties of FA-GPC, and they noticed that the *fc′* was significantly increased as the *l/b* increased up to 0.55 and beyond that negatively affected. The recorded compression strength was 39, 47, 58, and 44 MPa for the l/b ratio of 0.35, 0.45, 0.55, and 0.65, respectively when the other variable parameters are constant at 100 °C curing condition. Also, they observed that when the curing temperature is 80 °C and 60 °C, the compressive strength was the same as before, which improved up to 0.55 of *l/b* ratio [98].

In contrast to the results mentioned above, some studies reported that with increasing *l/b* ratio will cause a reduction in the *fc′* of the FA-GPC, for instance, an experimental research study have been performed to investigate the behavior of low-CaO fly and bottom ash-based geopolymer concrete with different *l/b* ratio cured at ambient temperature. They observed that the *fc′* of the geopolymer concrete at 28 days is 18.8, 27.2, and 34.3 MPa at *l/b* ratio of 0.5, 0.35, and 0.3, respectively [80]. This result argued to the fact that water content in the reaction medium of the GPC mixture was increased as any increase in the *l/b* ratio which leads to decreasing friction between the particles and, as a consequence reducing the *fc′* of the GPC [133]. However, the same GPC with *l/b* ratio of 0.25 is the only exception to this general trend, as a slight reduction in the *fc′* was actually observed due to the lack of suitable workability of the GPC mixture in the fresh state, which caused placement problems during concrete casting compared to the other l/b ratio mixtures, therefore, as a result, affected the compressive strength negatively [80]. Similar results can also be found in other studies even though the different alkaline solution to binder ratio was used [26, 77, 114]. In the same context, Fang et al. [118] claimed that the increment of *l/b* ratio strongly influences the early-age compression strength of FA-GPC but no significant effect on the later ages of the GPC. This result argued that decreasing l/b ratio will lead tohat decreasing l/b ratio accelerating in the alkaline activation process of fly ash-slag geopolymer concrete due to the decrease of consistency GPC mixture [134]. In this case, the Calcium Aluminate Silicate Hydrate (C-A-S-H) gel and Sodium Aluminate Silicate Hydrate (N-A-S-H) gel can be generated quickly in the geopolymer concrete mixture with low *l/b* ratio and, as a consequence, participated in the development of early-age compressive strength of fly ash-slag geopolymer concrete [135, 136].

Lastly, it was observed that the compressive strength decreased with increasing in the *l/b* ratio for the lower sodium hydroxide concentrations (molarity) cured at ambient temperature; for instance, when the molarity is 8 *M*, the compression strength was 11, 7.6, and 7.5 MPa at l/b ratio of 0.4, 0.5, and 0.6, respectively. However, when the molarity increased to 14 M, the *fc'* of FA-GPC improved to 18.1, 21.5, and 21.5 MPa, at 0.4, 0.5, and 0.6 *l/b* ratios, correspondingly [117], as shown in Fig.7. Furthermore, the increase in the *l/b* ratio from 0.5 to 0.6 results in the decrease in the *fc'* of the GPC by about 6.1%, 8.8%, 13.8%, 22.2%, and 14% for the molarity of the sodium hydroxide concentration of 8, 10, 12, 14, and 16 *M*, correspondingly. This result argued to the fact that increasing molarity of the alkaline liquid will lead to the presence of more solid part compared to the water content, which significantly influences the geopolymerization process and, as a consequence, compression strength was improved [137].

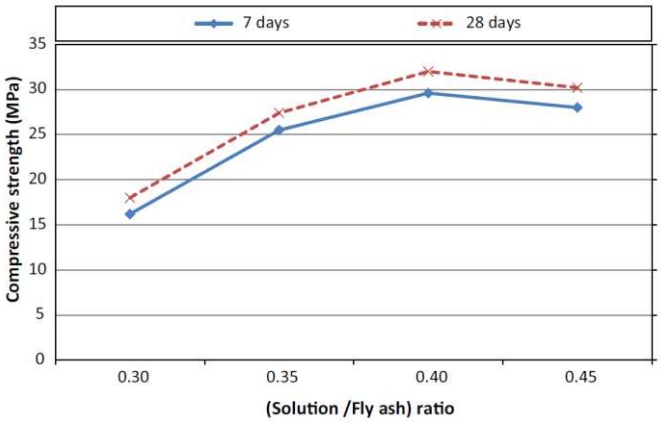

Fig.6. Effect of *l/b* on the *fc'* of the FA-GPC [79]

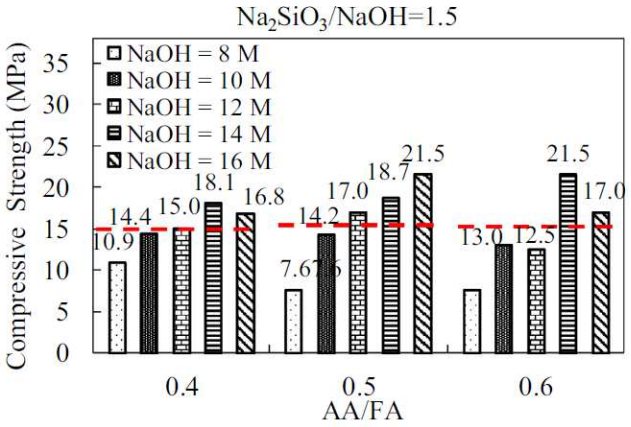

Fig.7. Effect of *l/b* and molarity on the *fc'* of the FA-GPC with *SS/SH* of 1.5 [117]

4.3 Superplasticizer Dosage and Extra Water

Superplasticizer and water content are two key factors that govern the workability behavior of the FA-GPC and hence affect the hardened characteristics of the geopolymer concrete. The alkaline solution, which is consists of sodium hydroxide and sodium silicate, is more viscous than water; hence their use in the GPC makes the mixture more sticky and cohesive than the traditional concrete [138]; therefore, extra water and superplasticizer are used to improve workability in GPC mixture.

To investigate the effect of superplasticizer dosage on the *fc′* of FA-GPC, Hardjito et al. [139] set an experimental program using different dosages of high-range water-reducing admixtures. Their results revealed that workability of the FA-GPC was improved with the inclusion of superplasticizer on the one hand; on the other hand, superplasticizer addition to the geopolymer, concrete mixture has very little effect on the compression strength up to nearly 2% of fly ash by mass as shown in Fig.8. After 2% of superplasticizer dosage, the value of compressive strength was decreased with increasing the superplasticizers dosage; for instance, the *fc′* was decreased by 19% when the dosage of superplasticizer increased from 2% to 3.5%. Moreover, according to the findings of this research study [139], with the increment of extra water content to the GPC mixture, compressive strength was significantly declined at different curing temperatures. This result is same as the results of Barbosa et al. [140] who their works were carried out on the geopolymer concrete pastes.

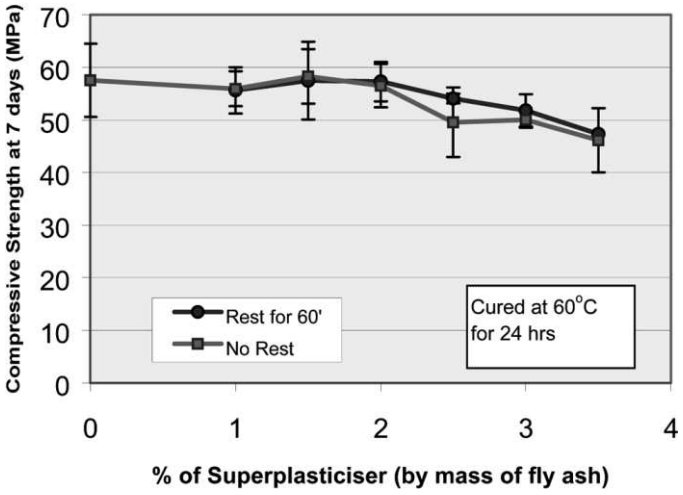

Fig.8. Effect of high-range water-reducing admixture on the *fc′* of the FA-GPC [139]

Furthermore, experimental research work has been conducted to investigate the influence of extra water addition on the workability and compressive strength of FA-GPC. Their results indicated that with increasing the amount of extra water content to the geopolymer concrete mixture, the workability was increased and improved, but the *fc′* was decreased. For instance, the *fc′* was decreased by 32%, 42%, and 71% when the extra water content increased from 0.25 to 0.30, 0.35, and 0.40, respectively [100]. This result attributed to the fact that the evaporation of the water from the GPC, leaving pores and cavities within the geopolymer concrete matrix, when the geopolymer concrete specimens curing at the high temperature inside ovens, and present the extra water may influence the alkalinity environment of the FA-GPC matrix that could cause decreasing the rate of the geopolymerization process between the alkaline materials and source material (fly ash) of the FA-GPC composites [71]. In the same context, a research study has been done to study the effect of extra water and superplasticizer content on the *fc′* of the FA-GPC. They conclude that with the increment of extra water content in the geopolymer concrete mixture, compression strength was decreased as shown in Fig.9 at the age of 7 and 28 days, this decline in the compressive strength was not greater than 10% up to 30 kg/m^3 of extra water, while, reduction in the compressive strength was increased to 24% due to use of 35kg/m^3 of extra water as compared to 10

kg/m^3 of extra water content for the FA-GPC [79]. Similarly, they noticed that the *fc′* of the FA-GPC was slightly decreased as the superplasticiser content increased. For instance, they reported that the value of the compressive strength was decreased by 4.2%, 8.6%, and 24% for the FA-GPC with 5, 7.5, and 10.5 kg/m^3 superplasticiser dosage compared to the same mixture with 2.5 kg/m^3 admixture content [79]. Furthermore, Josef and Mathewb [98] reported that the *fc′* of fly ash-based geopolymer concrete is decreased with the increment of water to geopolymer concrete solids ratio; this reduction in the compressive strength is nearly linear for all values of l/b ratio as presented at Fig.10.

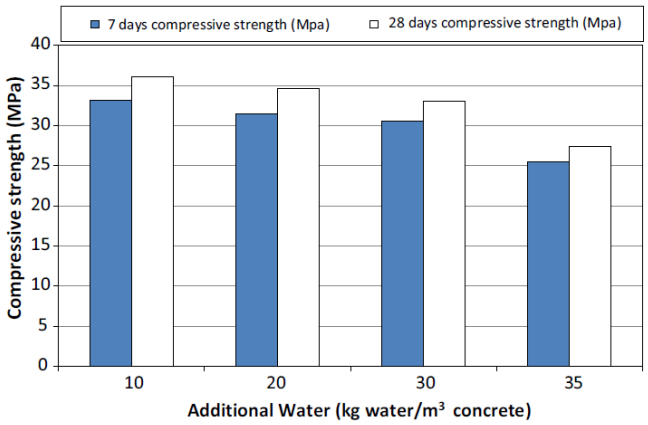

Fig.9. Effect of extra water on the *fc′* of the FA-GPC [79]

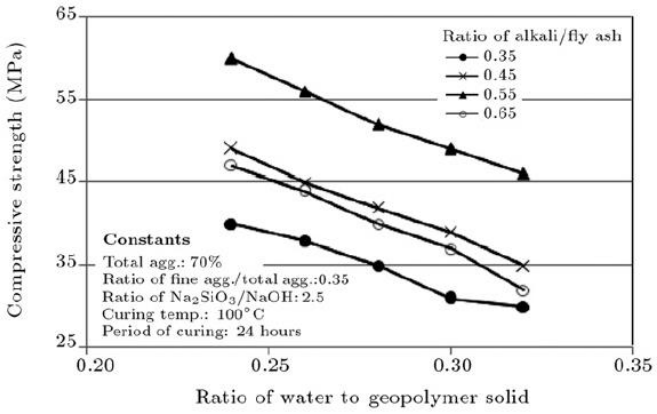

Fig.10. Effect of water to geopolymer solid on the *fc′* of the FA-GPC [98]

Lastly, experimental research work has been carried out to investigate the effect of superplasticizer and water to binder ratio on the *fc′* of FA-GPC. They observed that with increasing the superplasticizer dosage and water to binder ratio, the compressive strength was significantly decreased. For example, the *fc′* was declined by 41% and 50% at 13.92 and 48 kg/m^3 superplasticiser content, respectively, compared to 8.64 kg/m^3 content of superplasticiser. Moreover, the *fc′* was decreased to 46.2 and 27.2 MPa at 45.6 and 60 kg/m^3 extra water content, correspondingly, compared to the 40.8kg/m^3 of extra water content [105]. Similar results have been made by Vora and Dave [114], who observed that the compression strength of FA-GPC was decreased as superplasticiser and water to binder ratio of the concrete mixture increased. This is attributed to the fact that the extra water in the GPC mixture leads to generate large gel crystals with trapped water inside, and then, once the entrapped water evaporated

in the mixture, it produces a highly porous matrix, as a consequence, it causes a decrease in the *fc′* and increases the absorption capacity of the GPC [141]. Overall, high amount of water and superplasticiser content than the solid parts in the geopolymer concrete mixture cause to a reduction in the compression strength of the GPC composite as a result of decreasing contact among activating solution and the source reacting material [26, 142].

4.4 Fly ash content

Fly ash (*FA*) is widely used as a source material for making geopolymer concrete due to its low cost, abundance availability, and higher potential for preparation geopolymers [25, 26]. The content of fly ash in the mixture proportions of different fly ash-based geopolymer concrete for the collected data varied from 254 to 670 kg/m^3. The FAs have different chemical compositions with different specific gravity range from 1.95 to 2.54.

An experimental laboratory research work has been carried out to investigate the influence of different fly ash contents on the bond and compressive strength of FA-GPC; they claimed that with the increment in the fly ash content, bond and compression strength of the GPC were improved. The maximum increment in the *fc′* of three different fly ash content for five different fly ash binder source materials (ER, MP, BW, GL, and CL) were 19%, 23%, 17%, 36%, and 25%, respectively, when the fly ash content changed from 300 kg/m^3 to 500 kg/m^3 [71]. This result (based on their SEM tests) argued the fact that higher content of fly ash in the geopolymer concrete mixture gives denser and compacted microstructure to the geopolymer concrete matrix. Moreover, the particles of fly ash facilitate movement among the aggregate particles owing to the spherical shape and smooth surface of the particles of fly ash [143]; therefore, reducing the fly ash content decreases the capability of the FA-GPC components to consolidate and compact properly, as a consequence bond and compression strength were decreased in one hand, on the other hand, the volume of fine fraction particles in the geopolymer concrete matrix increased as the fly ash content increased, thus in turn fill the voids and pores between the aggregate particles and hence compressive strength was improved [71]. Similar results of increasing *fc′* of FA-GPC with increasing fly ash content were reported at both heat curing and ambient curing regimes [74, 96]. For instance, the value of compression strength changed from 21 MPa to 42 MPa, as the fly ash content increased from 300 to 400 kg/m^3 [96].

In addition, according to the findings of Singhal et al. [73], the compressive strength of FA-GPC was improved as the content of fly ash increased. For example, at the molarity of 16 M, the compression strength was increased by 11% and 32%, when the fly ash content was increased from 350 kg/m^3 to 375 and 400 kg/m^3, correspondingly, at the ambient curing age of 7 days, and increased by 15% and 24% at the age of 28 days. This improvement in the *fc′* of the GPC with the increment of fly ash content was reported for other sodium hydroxide molarities, as shown in Fig.11, at the ambient curing age of 28 days. This result may be attributed to the fact that fly ash is the main source of aluminosilicate source materials in the geopolymer concrete mixture, which silica and alumina increased as the amount of fly ash content increased; thus, they affect the reactions in the polymerization process, which in turn, C-A-

S-H and N-A-S-H gels increased, and finally, compression strength was improved [73]. In the same context, a research study have been conducted to investigate the properties of FA-GPC, they used different contents of fly ash and they observed that the compressive strength of the fly ash-based geopolymer concrete was increased as the fly ash content increased. For example, the compressive strength was 25.44, 36, and 48 MPa, at 356, 408, and 444 kg/m^3 of fly ash content, respectively. These findings are attributed as the same as mentioned before [94]. Similarly, Ramujeea and PothaRajub [77] observed that the compressive strength was increased as fly ash content increased as fly ash content increased in the geopolymer concrete mixture. Overall, most of the researches revealed that the *fc′* of FA-GPC increased with the increment of fly ash content in the geopolymer concrete mixture, and it is obvious that the fly ash with more fineness and glassy phase is more reactive, which leads to accelerating geopolymerization rate and as a consequence produces a high strength geopolymer concrete [20, 144, 145].

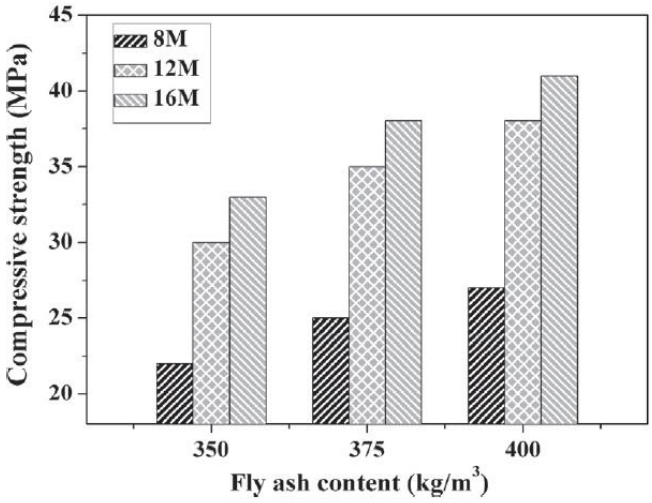

Fig.11. The compression strength of FA-GPC with various FA content and molarity at ambient curing condition [73]

4.5 Aggregate Content

Aggregates in the geopolymer concrete mixtures are the same as a conventional concrete mixture which consists of fine and coarse aggregates. In past studies, river and crushed sand with a maximum particle size of 4.75 mm and a specific gravity of 2.60-2.75 were employed as fine aggregate. Its grade also met the requirements of ASTM C 33 [146]. On the other hand, natural gravel or artificial crushed stone with the nominal aggregate size of 20 mm was used in the previous research as the coarse aggregate to prepare the coarse aggregate to prepare the coarse aggregate to prepare the fly ash-based geopolymer concrete mixtures. Based on the collected datasets from different fly ash-based geopolymer concrete mixture proportions, coarse aggregate content was varying between 394 to 1591 kg/m^3.

A research study had been carried out to show the effect of total aggregate content on the *fc′* of FA-GPC at different molarity and curing temperatures. They used five different volume fractions of total aggregate contents from 74% to 82%. They observed that the compression strength of the FA-GPC was

increased with increasing total aggregate content up to 78%, and they revealed that this result might be argued to the inadequate binding of the aggregate and the matrix phase in the fly ash-based geopolymer concrete mixture. In addition, they reported that the highest compressive strength was achieved for the geopolymer concrete mixture with 78% of total aggregate content at 60 ℃ curing condition as shown if the Fig.12, but this percent of aggregate content leads to a reduction of the workability by 37.5% as compared to the GPC mixture with 76% of aggregate content, so they prefer to use 76% of total aggregate content having the molarity of 12 M and cured at 90 ℃ as it yields low reduction in the compressive strength (about 2.6%) without hindering the slump value of the FA-GPC mixture [75].

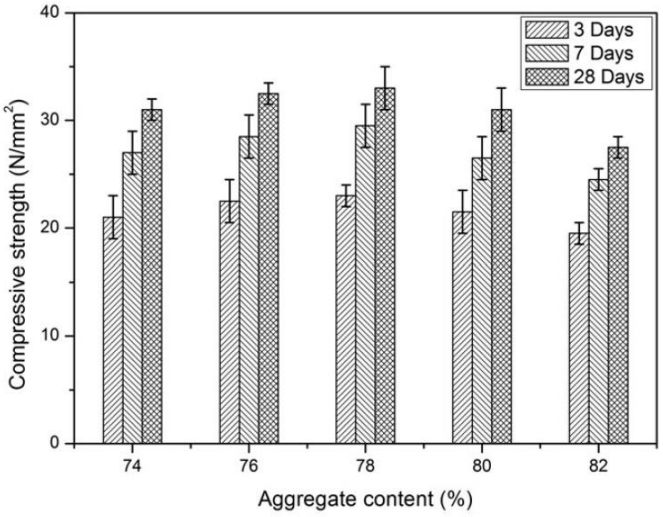

Fig.12. Effect of total aggregate content on the *fc′* of FA-GPC at the age of 3, 7, and 28 days [75]

In addition, experimental research work has been conducted on the effect of aggregate characteristics on the mechanical and absorption properties of fly ash-based geopolymer mortars. They used three different types of aggregates: river sand, crushed sand, and combined river and crushed sand. They reported that the geopolymer mortar mixtures' compression strength was between 28.2 to 47.8 MPa at the age of 1 day when the molarity was 12 M, the ratio of sodium silicate to sodium hydroxide was 2.5, and the specimens cured at 90 ℃ for 24 hr. It was revealed that the geopolymer mixture with crushed sand had higher compression strength as compared to the other aggregates. This result was attributed to the fact that the crushed sand has a rough surface texture with an angular shape which gives a greater surface to volume ratio and, as a consequence, provides better bond properties between the aggregates and the source material pastes [147]. Also, they reported that the highest compressive strength was recorded for the crushed sand with a coarser grade (2-4) mm compared to the other grades, as shown in Fig.13. Similar results have been reported by Mane and Jadhav [148], who observed that the crushed sand gives higher compression strength as compared to the river sand. Furthermore, they reported that the utilization of granite as a coarse aggregate provides better *fc′* to the FA-GPC in compassion to the coarse basalt aggregates. In the same context, another study has been carried out by Nuaklong et al. [149] on the influence of recycled concrete aggregates and crushed limestone aggregates on the FA-GPC properties. They claimed that there is a chance to use recycled concrete aggregates to produce FA-

GPC within the 7-days compression strength of 30-38 MPa; however, this value is slightly smaller than those of FA-GPC with crushed limestone aggregates, which has the compressive strength of 38-41 MPa. Similar results can also be found in other studies, even though different mixture proportions were used [89].

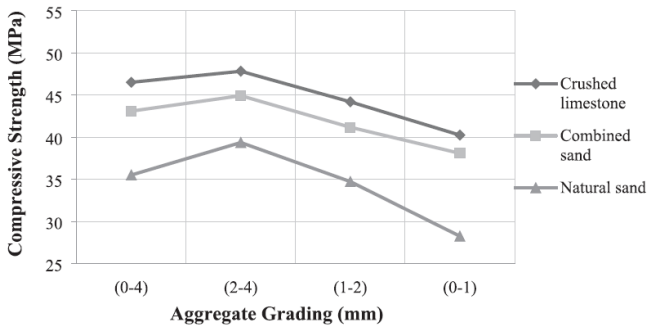

Fig.13. Influence of aggregate type and grading on the *fc′* of FA-GP mortar at the age of 1 day [147]

On the other hand, Sreenivasulu et al. [150] studied the compression strength of blended FA/GGBFS-based geopolymer concrete incorporated various fine aggregate contents and grades. They used granite slurry as a natural sand replacement to produce blended natural sand and granite slurry in different percentages (100:0, 80:20, 60:40, and 40:60). In the circumstances of ambient curing condition with the molarity of 8 M and when the SS/SH was 2, they observed that the *fc′* was significantly increased in the all curing ages of 7, 28, and 90 days until the blend of 60:40 and beyond that decline in the compression strength was reported as depicted in Fig.14. For instance, the compressive strength of blended natural sand and granite slurry proportions of 60:40 was 34, 51, and 59.9 MPa for the curing age of 7, 28, and 90 days, respectively, while this result was decreased to 22.4, 33.6, and 38.6 MPa for the blend of 40:60. These results argued to the fact that the granite slurry act as a filling agent which fills the voids and pores of the geopolymer concrete and hence made the geopolymer concrete dense, as a consequence lead to increase the *fc′* of the GPC until 40% replacement of sand, beyond that lead to decrease in the compression strength because of the high percentages of fine materials in the GPC mixtures [150].

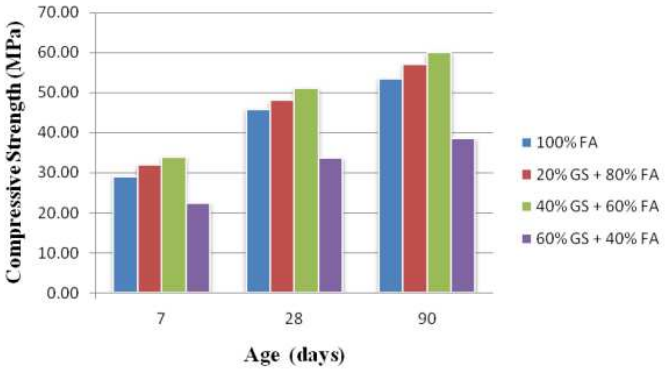

Fig.14. Effect of fine aggregate (F) replacement by granite slurry (GS) on the *fc′* of FA/GBBFS-based geopolymer concrete at the age of 7, 28, and 90 days [150]

Furthermore, according to the findings of Embong et al. [86] who investigated the effect of replacement of coarse granite aggregate by limestone with different percentages. Their experimental woks were carried out by substitute the portion of granite coarse aggregate by (0%, 25%, 50%, 75%, and 100%) with limestone in the GPC mixtures. They noticed that the replacement of limestone has a greater effect on the fc' of the FA-GPC in the ambient curing condition as compared to the oven curing condition. For example, an improvement in the compression strength of 35.3%, 19.5%, and 14.15% was achieved for the replacement level of 25%, 50%, and 75%, respectively, compared to the control GPC mixture without any limestone content. This result attributed to the formation of extra C-A-S-H gels, providing a solid structural framework in the geopolymer concrete [86]. Also, the extra dissolution of *Si* element in the fly ash to generate C-A-S-H gels tackles the drawbacks of the low reactivity in ambient curing conditions [151]. However, a 10.2% reduction in the fc' was reported for the replacement level of 100% of limestone due to lower aggregate packing density provided by uniformly graded limestone in the GPC mixtures [86]. On the other hand, the replacement of granite with limestone in the oven curing condition provides an improvement in the fc' just up to 25% replacement level, and beyond that, reduction in the compressive strength was recorded as shown in Fig.15.

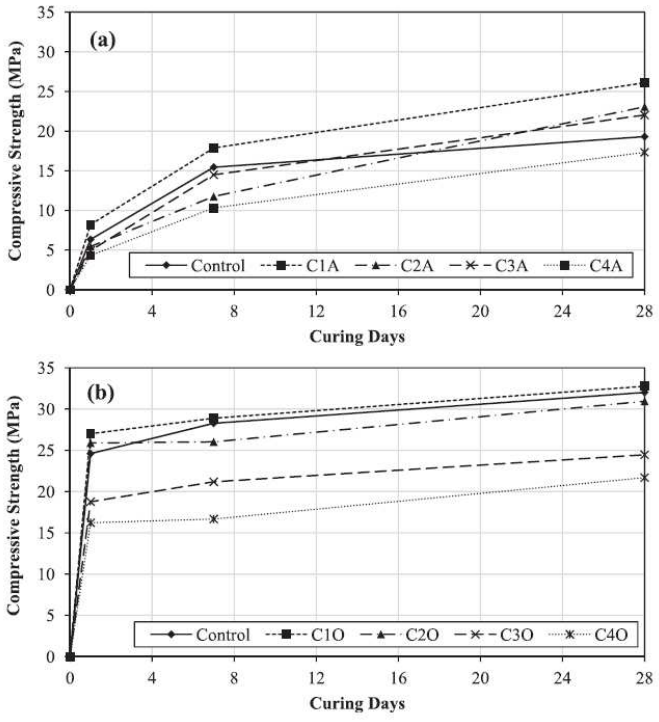

Fig.15. Effect of granite coarse aggregate replacement by limestone on the fc' of FA-GPC at different ages: (a) Ambient curing; (b); Oven curing [86]

Lastly, research work was performed to show the effect of aggregate content on the fresh and mechanical properties of FA-GPC. They used different aggregate contents and various fine aggregate to total aggregate ratios. They concluded that the fc' of the *GPC* mixtures increased with the increment in the total aggregate content up to 70%, and beyond that, it was declined. Also the compression strength was improved by increasing the fine aggregate to total aggregate ratio up

to 0.35% and then it was decreased. So, it is evident that for a given sort of coarse and fine aggregate, there is a limit proportion of fine aggregate and total aggregate content that provided the highest compression strength for the FA-GPC [98].

4.6 (Na_2SiO_3/NaOH) Ratio

Generally, sodium hydroxide (NaOH) and sodium silicate (Na_2SiO_3) is used as the activator solution to prepare the geopolymer concrete mixtures. The content of the sodium hydroxide (*SH*) for the collected literature datasets varied from 25 to 135 kg/m^3. The purity of the *SH* was above 97% of all the fly ash-based geopolymer concrete mixtures, and pellets and flakes were the two main states of the SH in all the mixtures. In addition, the content of sodium silicate (*SS*) was varied between 48 to 342 kg/m^3. The constituents of the *SS* were SiO_2, Na_2O, and water. The range of SiO_2 was varying from 28 to 37%, Na_2O was in the range of 8 to 18%, and the percent of water in the SS was in the range of 45 to 64%. Also, referring to the collected data, the ratio of Na_2SiO_3 to NaOH was varied from 0.4 to 8.8, with an average of 2.34.

In the literature, a variety of researches have been carried out to investigate the effect of alkaline solutions on the engineering properties of FA-GPC mixtures. For instance, experimental laboratory work has been conducted to shows the effect of various sodium silicate to sodium hydroxide ratios on the *fc′* of FA-GPC mixtures. They used two ratios of *SS/SH* which was 0.4 and 2.5 with two different molarity. Their results revealed that with increasing the ratio of *SS/SH* compression strength was significantly increased, for example, when the molarity was 8 M, and the specimens cured at 60 °C for about 24 hr. the *fc′* of FA-GPC was increased from 17.3 MPa to 56.8 MPa just by changing the ratio of *SS/SH* from 0.4 to 2.5. Similarly, the *fc′* was significantly improved from 47.9 MPa to 67.6 MPa when the ratio of *SS/SH* changes from 0.4 to 2.5 when the molarity was 14 M [139]. Similarly, compression strength improvement of FA-GPC was reported by Al-Azzawi et al. [71] as the ratio of *SS/SH* increased at all GPC mixtures even fly ash contents were varying from 300 to 500 kg/m^3. In the same context, based on the findings of Aliabdo et al. [79], who studied the effect of alkaline solution dosages on the performance of FA-GPC, they used three different (0.3, 0.4, and 0.5) sodium hydroxide to sodium silicate ratios. Their results show that with the increment of *SH/SS* ratio, compressive strength was decreased, or with the increment of *SS/SH*, compressive strength was increased, as illustrated in Fig.16. The reduction in the *fc′* of the FA-GPC at the curing age of 28 days was 22.5% and 29.5% at 0.4 and 0.5 of *SH* to *SS* ratio, correspondingly, as compared to the *SH* to *SS* ratio of 0.3. Similar results can also be found in other studies even though different *SS/SH* was used [94, 112, 123, 152].

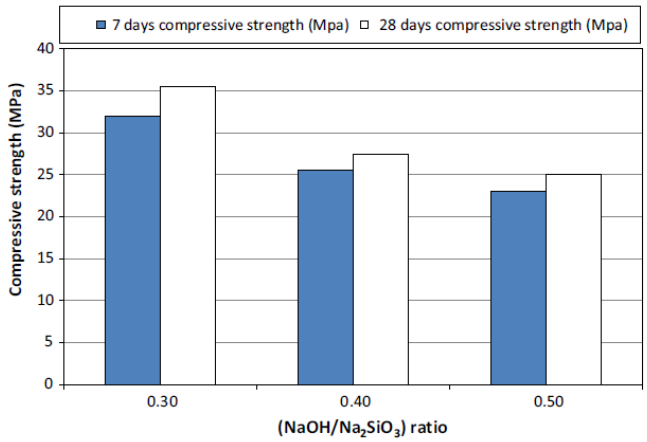

Fig.16. Effect of different *SH/SS* ratios on the *fc′* of FA-GPC at different ages [79]

Furthermore, an experimental research study has been carried out to investigate the effect of various parameters on the performance of FA-GPC. It was observed that the compressive strength was increased with the increment of *SS* to *SH* ratio up to 2.5, and beyond that, decline in the *fc′* was reported as shown in Fig.17. [98]. This result argued to the fact that the microstructure of the geopolymer concrete changes due to the quantity of sodium silicates content, while the reduction in the compressive strength was attributed to the fact that there is not a sufficient amount of sodium hydroxide present in the mixture to completion of dissolution process during the formation of geopolymer [153, 154], or due to the excess OH^- concentration in the GPC mixture [25]. On the other hand, some researchers believed that the excess of sodium content could form sodium carbonate by atmospheric carbonation, and this may disrupt the polymerization process, and as a result, compressive strength was decreased [140]. In the same context, another study has been carried out to investigate the effect of *SS/SH* ratio on the *fc′* of the FA-GPC. They used six different *SS/SH* ratios (0.5, 1.0, 1.5, 2.0, 2.5, and 3.0), and they reported that with the increment of *SS/SH* compressive strength was increased up to the ratio of *SS/SH* of 2.5 and then it was decreased [155]. On the other hand, according to the findings of some researchers, the influence of *SS/SH* on the compression strength of geopolymer concrete was not obvious [99, 118].

In contrast to the above-mentioned results, few studies reported that the compression strength decreased as the ratio of *SS/SH* increased. For instance, a research study was conducted to show the effect of alkaline activators on the mechanical characteristics of FA-GPC at the ambient curing regime. Their results show that with the increase in the *SS/SH* ratio from 1.5 to 2, compressive strength was decreased by 5.2%, 7.6%, 7.6%, 10.8%, and 12.8% at the molarities of 8, 10, 12, 14, and 16, correspondingly. Similar trends were true when the ratio of *SS/SH* changes from 2 to 2.5, as depicted in Fig.18 [117]. This result argued to the reason that the increment in the *SS/SH* ratio would lead to a decrease the amount of sodium hydroxide solution and hydroxide ions (OH^-), which subsequently decreased the formation of N-A-S-H gels, which it is the main 3D network that directly affect the microstructure of the geopolymer concrete and as a consequence *fc′* was decreased [156, 157]. Similarly, a reduction in the compression strength of FA-GPC was reported [114] as *SS/SH* ratio increased from 2 to 2.5, as well

as a reduction in the compression strength of FA-GP mortar was reported as the ratio of *SS/SH* increased from 1.0 to 1.5, 2.0 and 2.5 [158].

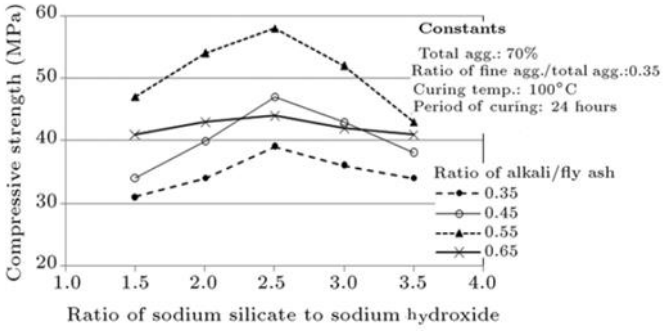

Fig.17. Effect of different *SS/SH* ratios on the *fc'* of FA-GPC [98]

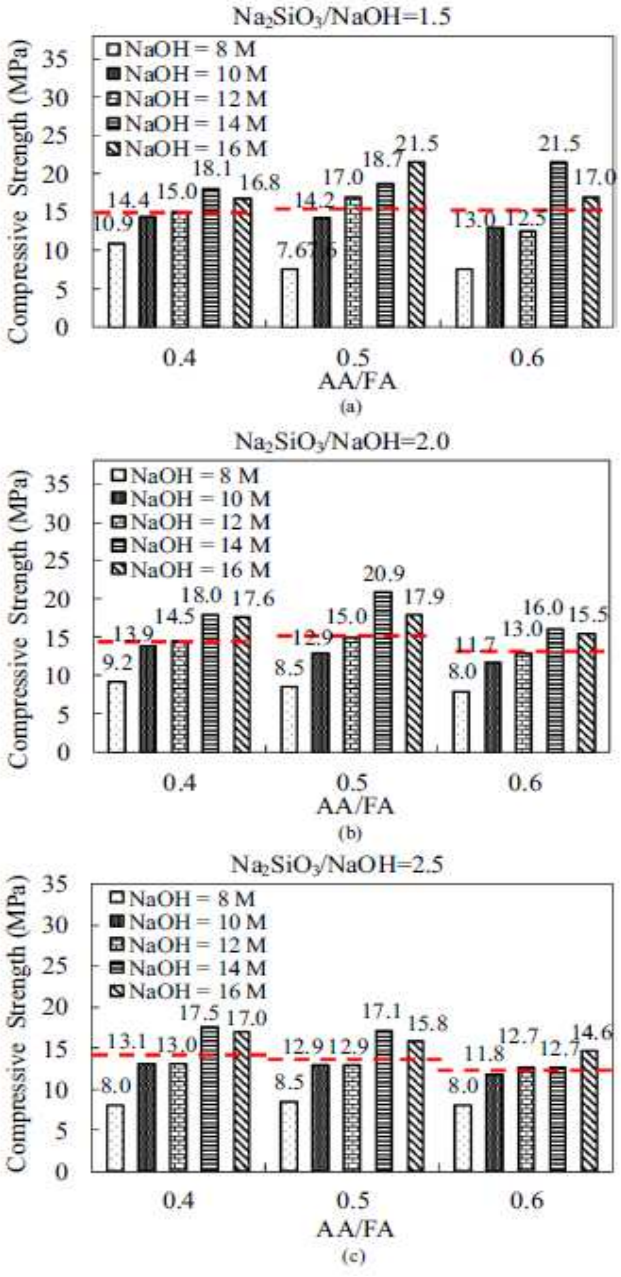

Fig.18. Effect of different *SS/SH* ratios on the *fc′* of FA-GPC at different *M* and *l/b* [117]

4.7 Sodium Hydroxide (NaOH) Concentration (Molarity (M))

The concentration of sodium hydroxide is one of the key parameters that affect the performance of FA-GPC; therefore, a wide range of researches has been conducted to investigate the mentioned phenomena. According to collected datasets from the literature, the sodium hydroxide concentration (molarity) was used to prepare geopolymer concrete in the range between 3 to 20 M. To demonstrate the influence of different molarity on the compression strength of FA-GPC, an experimental laboratory research work was performed by Hardjito et al. [139] and they reported that the compression strength was improved by 176% for the molarity of 14 M as compared to the molarity of 8 M at the ratio of *SS/SH* of 0.4, while this improvement was reduced to 19% at the molarity of 14 M with regarding the molarity of 8 M at the *SS/SH* ratio of 2.5. In the same context, a research study has been carried out to evaluate the effect of different molarities on the *fc′* of the FA-GPC. They observed that the compression strength was improved with the increment in the molarity of sodium hydroxide. For instance, compressive strength improvement of 40% and 8% was reported when the concentration of sodium hydroxide changes from 8 M to 12 M and 12 M to 16 M, correspondingly [73]. This result attributed to the increase of sodium ions in the geopolymer concrete mixture, which was significant for the geopolymerization process, because sodium ions were utilized to balance the charges and formed the alumino-silicate networks as source materials binder in the geopolymer concrete mixture [155] and on the other hand, at low molarity, the geopolymerization process is small due to the less concentration of the base material, and as a consequence, a small amount of *Si* and *Al* are leached from the source base materials [159].

Furthermore, another experimental research work had been conducted by Chithambaram et al. [75] to show the effects of various molarities of sodium hydroxide on the mechanical properties of FA-GPC. They used four different molarities at various curing temperatures, and it was observed that with the increment in the molarity, compression strength was increased up to 12 M, and beyond that, it was declined. For instance, at the curing temperature of 90°C and 28 days of age, the compressive strength was 36, 38.5, 42.5, and 40.9 MPa at 8, 10, 12, and 14 molarities, respectively. Similarly, they reported that the *fc′* was 33.8, 35.9, 40.5, and 39.4 MPa at 8, 10, 12, and 14 molarities, correspondingly, at the curing temperature of 70°C. Also, they claimed that the same trends were true for the curing temperatures of 60 and 80°C. Similar results can also be observed in other studies even though different molarities were used [87, 112]. However, Varaprasad et al. (2010) claimed that the fc′ was improved with increasing molarity. For example, the compression strength of FA-GPC was improved by 8.5%, 14.7%, and 19.2% at 12, 14, and 16 molarities, respectively, as compared to the molarity of 10 M at the age of 28 days with the curing temperature of 60°C. In the same manner, some other research studies claimed that the *fc′* was improved as the molarity of sodium hydroxide increased [88, 114, 122, 123].

According to the findings of Aliabdo et al. [79], the compression strength was increased as the molarity increased in the FA-GPC mixture up to 16 M, and then it was decreased as depicted in Fig.19. Also, they

reported that the optimum concentration of NaOH was 16 M for 48 hr of curing at 50°C. Similar results was observed by Chindaprasirt and Chalee [82], who used different molarities of sodium hydroxide (8, 10, 12, 14, 16, 18, and 20), and they reported that the maximum compression strength was 32.2 MPa at 16 M in the age of 28 days at the ambient curing conditions. In the same context, a research study has been carried out to demonstrate the influence of different NaOH molarities (10, 13, and 16 M) on the *fc′* of FA-GPC at elevated temperatures (200, 400, 600, and 800°C). Their results indicated that the *fc′* was higher for those specimens with higher molarities (13 and 16 M) at all temperature changes than those specimens containing 10 M NaOH solutions as illustrated in Fig.20; on the other hand, interestingly, they observed that the rate of compressive strength loss after 600°C is also high in the FA-GPC mixtures that have a greater concentration of NaOH solution [83].

In addition, a research study has been conducted to show the effect of different molarity of sodium hydroxide solutions (8, 10, 12, 14, and 16 M) on the compression strength of FA-GPC. It was observed that the compressive strength of FA-GPC improved as the molarity of NaOH increased up to 10 M, and then it was decreased as shown in Fig.21 [98]. This result attributed to the fact that during the production of geopolymer concrete, the concentration of sodium hydroxide solution has a positive effect on hydrolysis, dissolution, and condensation reactions but overflowing alkali concentration prohibits the condensation of silicate elements [153, 154, 160].

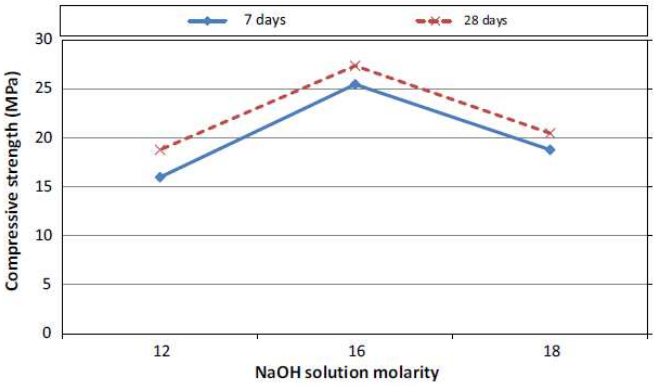

Fig.19. Effect of different molarities of sodium hydroxide on the *fc′* of FA-GPC at the age of 7 and 28 days [79]

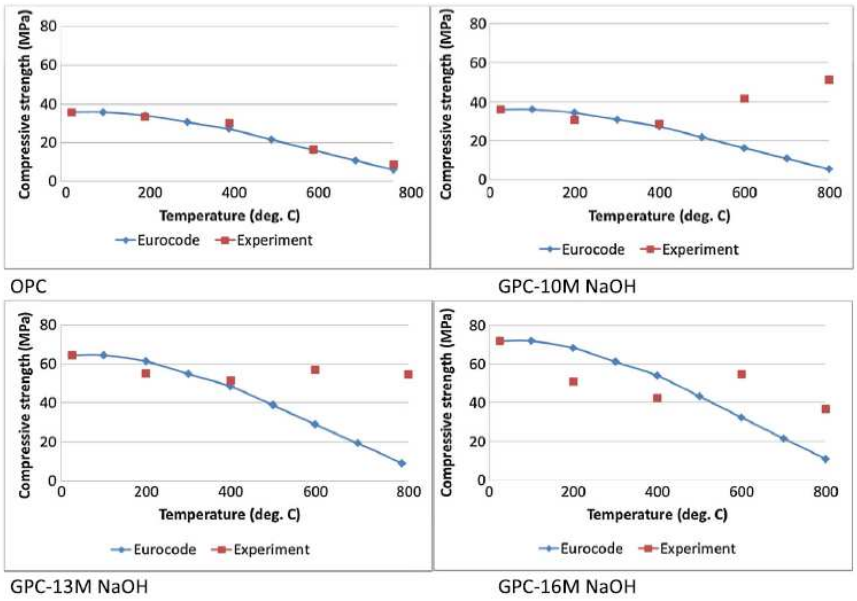

Fig.20. Effect of different molarities of sodium hydroxide on the *fc′* of FA-GPC at various curing temperatures [83]

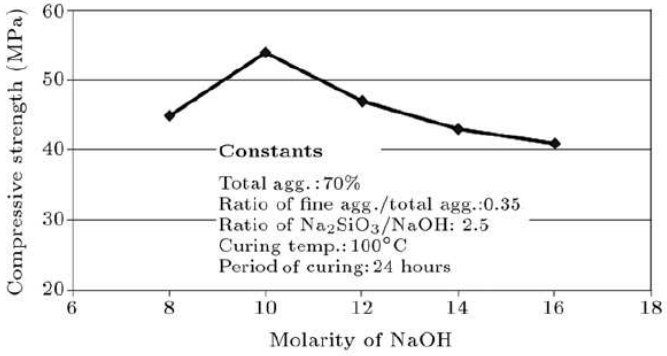

Fig.21. Influence of different molarities of sodium hydroxide on the *fc′* of FA-GPC [98]

Lastly, Ghafoor et al. [117] investigated the effect of alkaline activators on the mechanical characteristics of FA-GPC at the ambient curing conditions. Their results show that the *fc′* of FA-GPC was increased as the molarity of NaOH increased up to 14 M, and beyond that, it was decreased. For instance, an improvement in the compression strength by 55.8%, 10.5%, 33% was reported when the molarity of NaOH changes from 8 to 10 M, 10 to 12 M, and 12 to 14 M, correspondingly. On the other hand, about 9% reduction in the compression strength of the GPC mixture was recorded as the concentration of sodium hydroxide increased from 14 M to 16 M. Generally, an increment in the molarity of sodium hydroxide will lead to improving the *fc′* of FA-GPC composites which could be argued to the full dissolution of aluminum, and silicon particles in the polymerization process [152], the dissolution of *Al* and *Si* particles in the geopolymerization process is dependent of the molarity of sodium hydroxide. The greater the molarity of sodium hydroxide, the greater the dissolution of *Al* and *Si* particles, and as a result, the greater is the compression strength of GPC mixtures [161].

5 Curing Conditions and Specimen Ages

Generally, there are three different curing regimes to cure FA-GPC composites, namely ambient curing, oven curing, and steam curing regimes. In the following paragraph, the effect of these curing conditions on the *fc′* of FA-GPC was provided. The majority of researches used oven curing conditions to cure the FA-GPC as compared to other curing condition types.

A research study has been carried out to show the effect of different oven curing temperatures on the compressive strength of FA-GPC. Their results revealed that the *fc′* was increased as the oven curing temperatures increased, as illustrated in Fig.22. But this improvement in the compression strength did not increase substantially beyond the curing temperature of 60°C [139]. In addition, a research study has been conducted to show the effect of different curing conditions on the mechanical properties of FA-GPC. Their results reported that the *fc′* of heat curing regime was higher than those specimens cured at ambient curing conditions as depicted in Fig.23 at the ages of 3, 7, and 28 days. For instance, the 28 days compression strength of FA-GPC was 22.1 MPa at 90°C of oven curing temperature, while this value decreased to 13.9 MPa at the ambient curing condition [96]. Similar results can be found in other studies even though different ambient and oven curing temperatures were used [81, 83, 86, 88, 105, 112, 113, 119, 122, 162]. In the same context, according to the findings of Chithambaram et al. [75] compression strength of FA-GPC was increased as the oven-cured temperatures increased up to 90°C, and then it was decreased. For example, when the concentration of sodium hydroxide of FA-GPC mixtures was 8M, the 28 days compressive strength was 32.5, 33.8, 35.4, 36, and 33.9 MPa at 60, 70, 80, 90, and 100°C oven curing temperatures, respectively, similar trends were true for the age of 3 and 7 days as well as for the NaOH molarities of 10, 12, and 14M. Similarly, Vora and Dave [114], reported that the compression strength of FA-GPC mixtures was improved as the oven-cured temperature increased. For instance, an increase in the compression strength by 21% and 6.5% was recorded when the oven curing temperature changes of 60 to 75°C, 75 to 90°C, respectively.

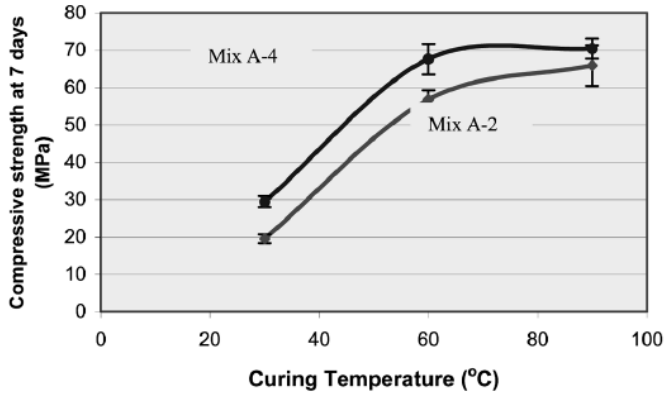

Fig.22. Effect of different oven curing temperatures on the *fc′* of FA-GPC [139]

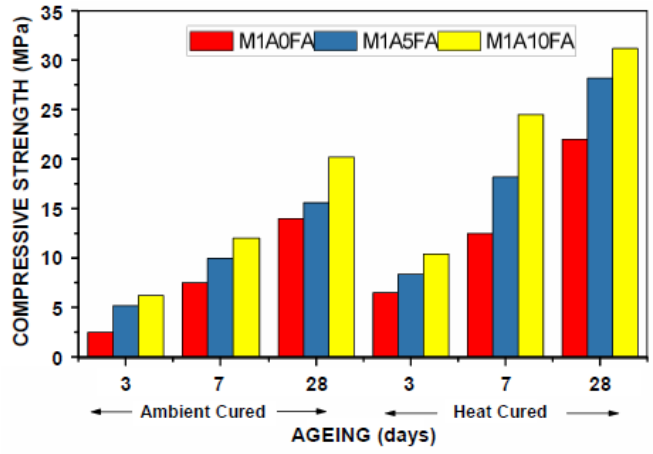

Fig.23. Effect of different curing conditions on the *fc′* of FA-GPC [96]

Furthermore, experimental laboratory research works have been conducted to investigate the effect of ambient and oven curing conditions on the mechanical properties of FA-GPC composites. It was observed that the *fc′* improvement for oven curing conditions was greater than those specimens cured under ambient curing regimes, as shown in Fig.24. This result attributed to the fact that the process of geopolymerization is accelerated as the temperature of the GPC mixtures increased [105]. In the same manner, Joseph and Mathew [98] revealed that the compression strength of FA-GPC was increased with increasing oven curing temperatures up to 100°C, and beyond that, it was decreased as shown in Fig.25. Also, they claimed that this trend was true for the different ratios of alkali solution to the fly ash content. The decrease in the compression strength after 100°C argued to the loss of moisture from the GPC samples even if locked satisfactorily. At temperatures beyond 100°C, the geopolymer samples may dry out and, consequently, lead to a reduction in the *fc′*. Similarly, Thakur and Ghosh [125] and Chindaprasirt et al. [163] reported that the compression strength was improved as the oven curing temperature increased.

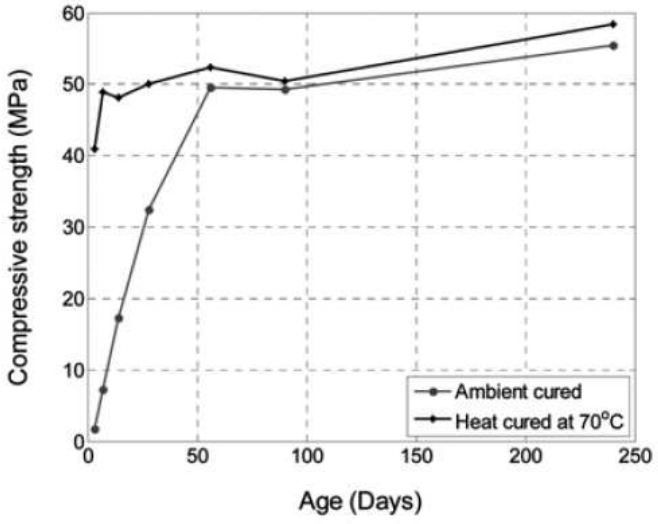

Fig.24. Effect of different curing conditions on the *fc′* of FA-GPC [105]

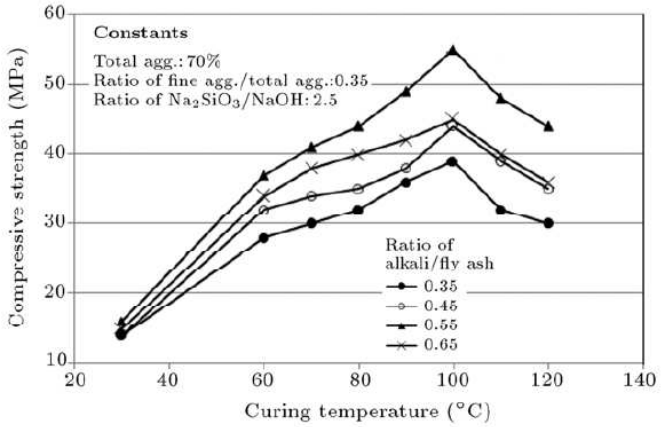

Fig.25. Effect of different oven curing temperatures on the *fc′* of FA-GPC [98]

Furthermore, according to the findings of Hassan et al. [108] who study the influence of curing condition on the mechanical properties of FA-GPC. They reported that the compression strength of FA-GPC was in the range of 10.50-31.11 MPa at the age of 7 and 28 days for heat (75°C) curing regimes, while these values of the *fc′* were reduced to 4.5-10 MPa for ambient curing regimes. Moreover, they observed that the *fc′* of FA-GPC was increased by 67 % at 75°C heat curing as compared to the ambient curing conditions for the age of 28 days. The same trend was observed for various ages of the GPC specimens, as shown in Fig.26. In the same context, a research study had been conducted to show the effect of ambient, steam, and heat curing conditions on the performance of FA-GPC. Their results indicated that the highest compression strength was recorded for heat curing conditions, after that for steam curing, and the last one was observed for the ambient curing condition. For instance, at the age of 3 days, the *fc′* was 20.8, 16.7, and 8.75 MPa at heat, steam, and ambient curing conditions, correspondingly [121]. On the other hand, another research study has been conducted to show the effect of ambient, hot gunny sack, and external exposure curing regimes on the performance of FA-GPC. They observed that the compression strength improvement was greater for external exposure curing condition and then for the ambient condition, while the worth curing condition was recorded for the hot gunny suck curing regimes [124].

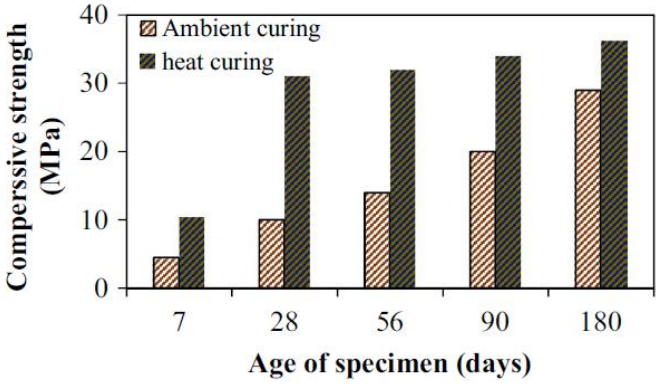

Fig.26. Effect of different curing conditions on the *fc′* of FA-GPC at various ages [108]

The duration of curing FA-GPC specimens inside ovens is one issue that some researchers deal with. For instance, a research study has been carried out to investigate the influence of different mix

compositions on the compression strength and microstructures of FA-GPC composites. It was observed that the *fc′* improved with increment in curing duration inside an oven at a constant temperature. The highest compressive strength (40.8 MPa) for FA-GPC was obtained with 48 hrs of thermal curing. Also, they reported that further increment in the period of curing did not give an appreciable improvement in the compression strength of the FA-GPC, as illustrated in Fig.27 [125]. Similar results have been reported by Hardjito et al. [139]. On the other hand, Joseph and Mathew [98] claimed that the compression strength of FA-GPC was increased as the curing time inside the oven increased at a constant temperature. This strength gain is proportional to the duration of curing and a very small strength gain could be obtained after 24 hrs, as shown in Fig.28; this result may be attributed to the fact that most of the geopolymerization process would have been completed within 24 hrs.

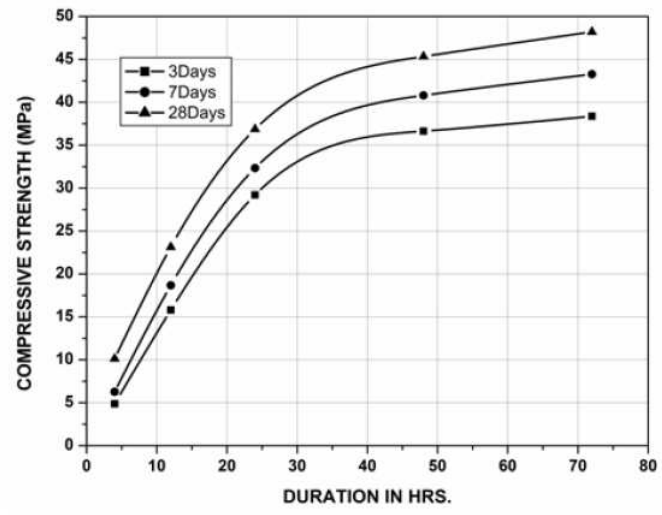

Fig.27. Effect of different period of temperature curing inside an oven on the *fc′* of FA-GPC [125]

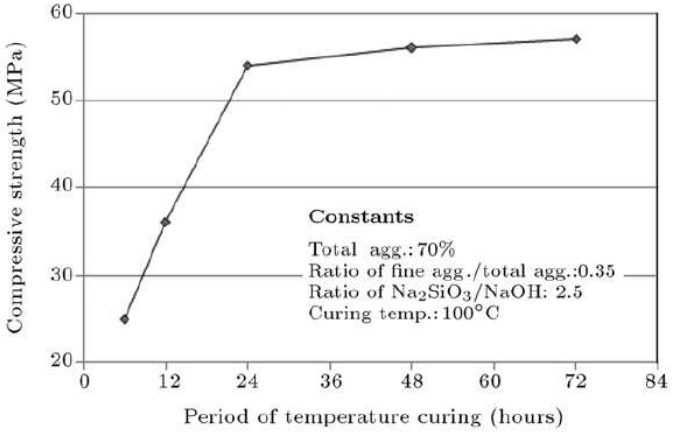

Fig.28. Effect of different period of temperature curing inside an oven on the *fc′* of FA-GPC [98]

6 Statistical assessment

Below sufficient information regarding each variable considered as the input parameter is present. More information on each statistical criterion was reported by Silva et al. [164].

6.1 Alkaline solution/binder (*l/b*)

According to the dataset, which contains 510 data samples from past researches, the *l/b* ratio of the FA-GPC was varied from 0.25 to 0.92 with an average, variance, standard deviation, skewness, and kurtosis of 0.5, 0.01, 0.1, 1.21, and 2.88, respectively. Skewness is belonged to distortion or asymmetry in a symmetrical normal distribution in a dataset. If the curve is moved to the right or the left side, it is stated to be skewed. Also, skewness could be quantified as an impersonation of the range to which a given distribution differs from a normal distribution. For instance, the skew of zero value was measured for normal distribution, while, right skew is an indication of lognormal distribution [165]. Figure 29 is presented the relationship between the compression strength of geopolymer and *l/b*.

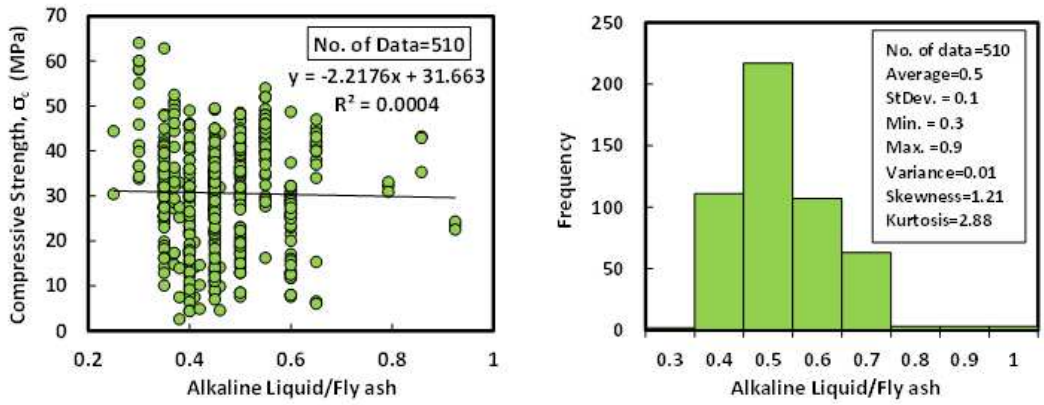

Fig.29. Variation between compression strength and (alkaline liquid/fly ash) ratio with histogram of FA-GPC mixtures

6.2 Fly ash content (*FA*)

The content of fly ash in the mixture proportions of different FA-GPC for the collected data varied from 254 to 670 kg/m^3. The FAs have different chemical compositions as well as different specific gravities ranging from 1.95 to 2.54. The average, standard deviation, variance, skewness, and kurtosis of the FA were 386 kg/m^3, 63 kg/m^3, 3974, 1.51, and 6.18. The kurtosis is a statistical indicator that explains how heavily the tails of a distribution of a set of data are differing from the tails of the normal distribution. In addition, the kurtosis finds the heaviness of the distribution tails, while skewness measures the symmetry of the distribution [66]. Fig.30 illustrated the relationship and a histogram of compression strength and fly ash content of FA-GPC mixes.

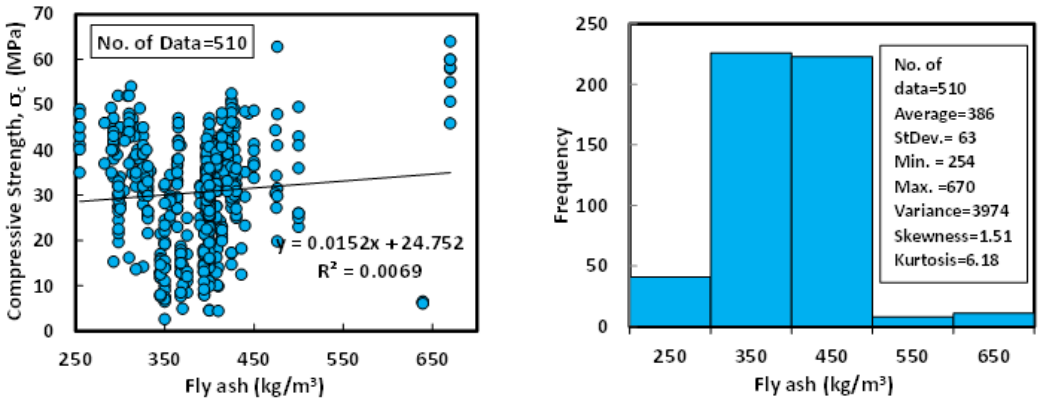

Fig.30. Relationship and a histogram of compression strength and fly ash content of FA-GPC mixtures

6.3 SiO_2/Al_2O_3 (*Si/Al*)

The dataset contains 510 data samples from literature. The *Si/Al* ratio of the fly ash was varied from 0.4 to 7.7 with an average of 2.7, the variance of 2.69, the standard deviation of 1.64, skewness of 2.5 and kurtosis of 5.03. The variance informed of the degree of spread in the dataset; the greater the spread of the data, the greater the variance is about the mean. The relation between compression strength and *Si/Al*, and the histogram analysis of FA-GPC are shown in Fig. 4.

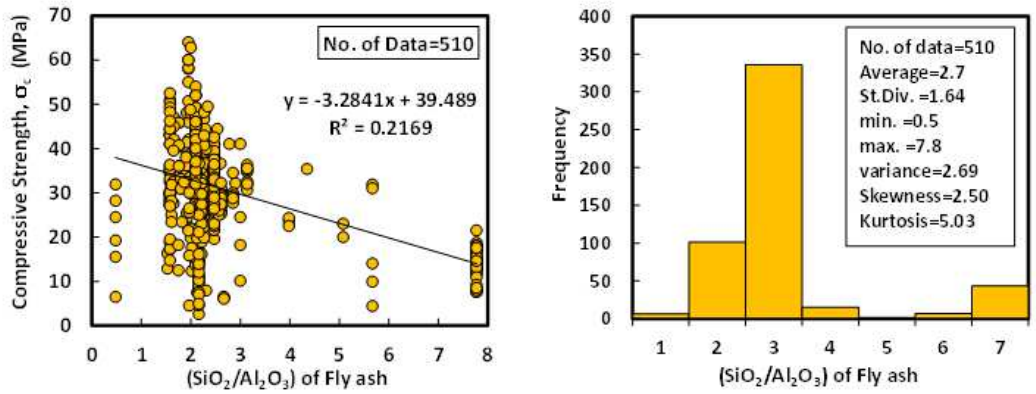

Fig.31. Relationship and a histogram of compression strength and (SiO_2/Al_2O_3) ratio of fly ash of FA-GPC mixtures

6.4 Fine aggregate content (*F*)

In past studies, river and crushed sand with a maximum particle size of 4.75 mm and a specific gravity of 2.60-2.75 were employed as fine aggregate. Its grade also met the requirements of ASTM C 33. The fine aggregate content of the 510 datasets collected ranged from 318 to 1196 kg/m^3 for FA-GPC, with an average of 615 kg/m^3, a standard deviation of 100 kg/m^3, and variance of 10047. Other statistical variables for fine aggregate concentration in FA-GPC mixtures included skewness and kurtosis, which are 1.75 and 5.56, respectively. Figure 32 shows the connection between compressive strength and fine aggregate content using a Histogram of FA-GPC mixture.

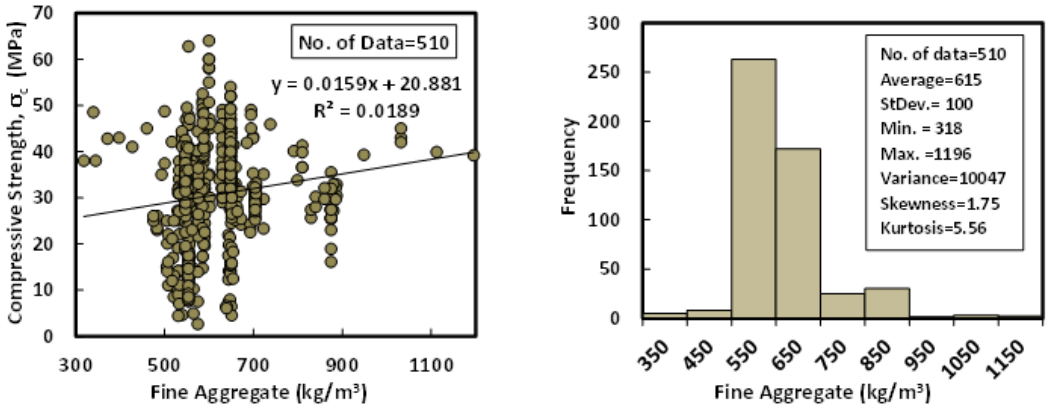

Fig.32. Relationship and a histogram of compression strength and fine aggregate content of FA-GPC mixtures

6.5 Coarse aggregate content (*C*)

In the literature, coarse aggregate for FA-GPC was crushed stone or gravel with a nominal aggregate size of 20 mm. The coarse aggregate content ranged from 394 to 1591 kg/m^3 based on the 510 datasets available from different FA-GPC admixture proportions. Based on the current dataset's statistical analysis, the average coarse aggregate content was 1187 kg/m^3, the skewness was -1.69, and the kurtosis was 4.5. The standard deviation was 146.8 kg/m^3, and the variance was 21557. Figure 33 shows the relationship between compression strength and coarse aggregate content using a Histogram of FA-GPC mixes.

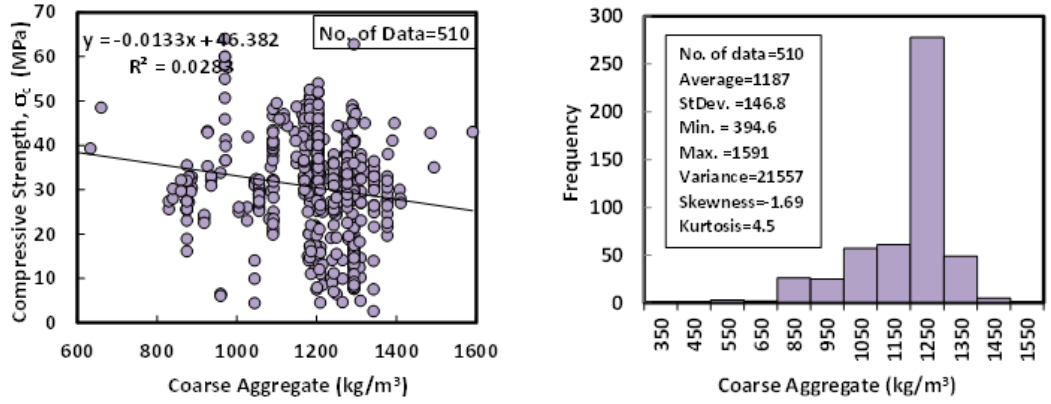

Fig.33. Relationship and a histogram of compression strength and coarse aggregate content of FA-GPC

6.6 Sodium hydroxide (*SH*)

The sodium hydroxide (NaOH) content for the collected 510 datasets varied from 25 to 135 kg/m^3, with an average of 54.3 kg/m^3, the standard deviation of 16.11 kg/m^3, and a variance of 259. The skewness and kurtosis were 1.69 and 4.55, respectively. The purity of the SH was above 97% of all the FA-GPC mixtures, and pellets and flakes were the two main states of the SH in all the mixtures. The relationship between compressive strength and sodium hydroxide with the Histogram of FA-GPC mixtures is illustrated in Fig.34.

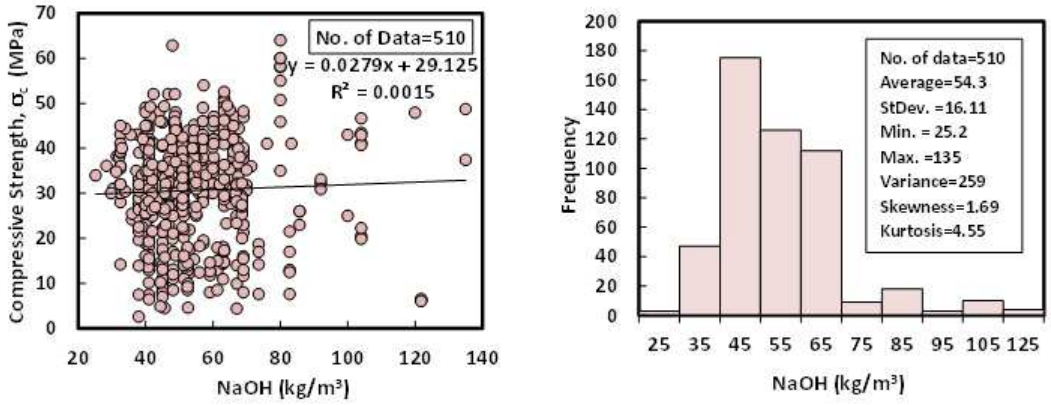

Fig.34. Relationship and a histogram of compression strength and sodium hydroxide content of FA-GPC

6.7 Sodium silicate (*SS*)

Based on the dataset, which contains 510 data samples from literature, the content of SS was varied between 48 to 342 kg/m^3. The constituents of the SS were SiO_2, Na_2O, and water. The range of SiO_2 was varying from 28 to 37%, Na_2O was in the range of 8 to 18%, and the percent of water in the SS was in the range of 45 to 64%. The statistical analysis for the collected data of SS revealed that the average content of SS in the FA-GPC was 123.4 kg/m^3, the standard deviation was 36.2 kg/m^3, the variance was 1313, skewness was 2.89, and kurtosis was 12.8. (Fig.35).

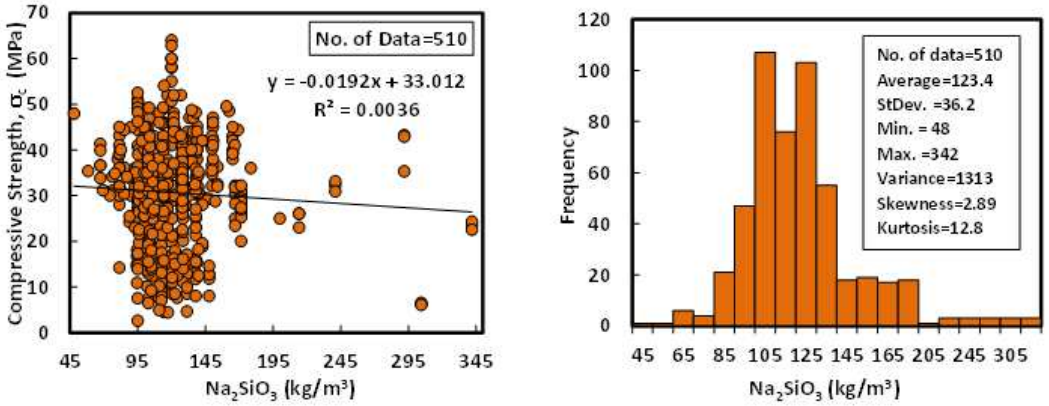

Fig.35. Relationship and a histogram of compression strength and sodium silicate content of FA-GPC

6.8 SS/SH

Referring to the collected data, the ratio of Na_2SiO_3 to NaOH was varied from 0.4 to 8.8, with an average of 2.4. The standard deviation, variance, skewness, and kurtosis were 0.68, 0.47, 4.71, and 45.9, respectively. The relationship between compression strength and SS/SH with the histogram of FA-GPC mixtures is presented in Fig.36.

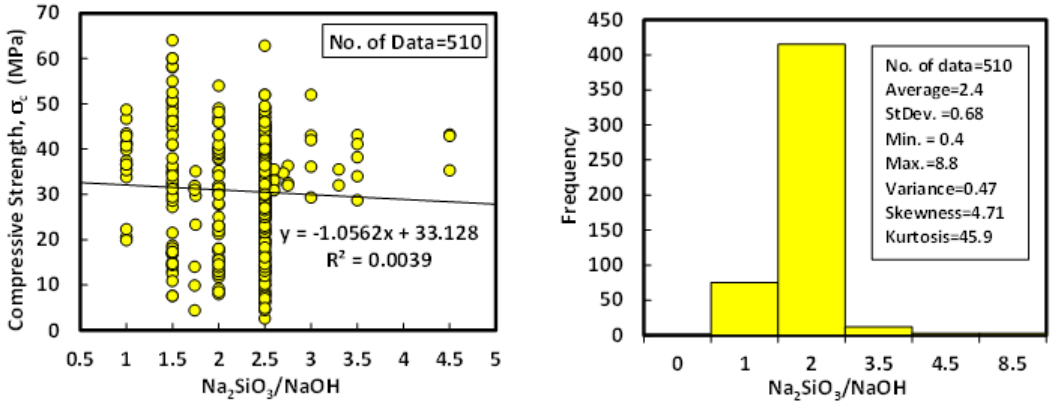

Fig.36. Relationship and a histogram of compression strength and (SS/SH) ratio of FA-GPC mixtures

6.9 Molarity (*M*)

According to the 510 datasets from previous research studies, the sodium hydroxide concentration (molarity) was varying from 3 to 20 M, with an average of 11.9 M, the standard deviation of 2.8 M, the variance of 7.83, the skewness of 0.14, and the kurtosis of -0.41. Variation between compressive strength and molarity with the Histogram of FA-GPC mixtures is illustrated in Fig.37.

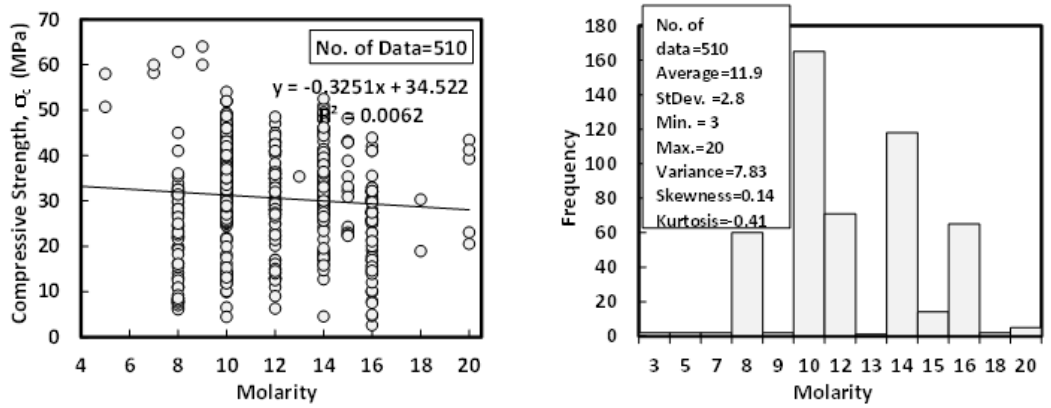

Fig.37. Relationship and a histogram of compression strength and molarity with a histogram of FA-GPC mixtures

6.10 Curing temperature (*T*)

The statistical analysis for the total collected data of the 510 dataset shows that the range of the curing temperature was varied from 23 to 120 ℃, with an average of 58.6 ℃ and standard deviations of 27.9 ℃. Besides, the variance, skewness, and kurtosis were 7, 0.05, and -1.16, correspondingly. The relationship and a histogram of compression strength and curing temperature of FA-GPC mixtures are illustrated in Fig.38.

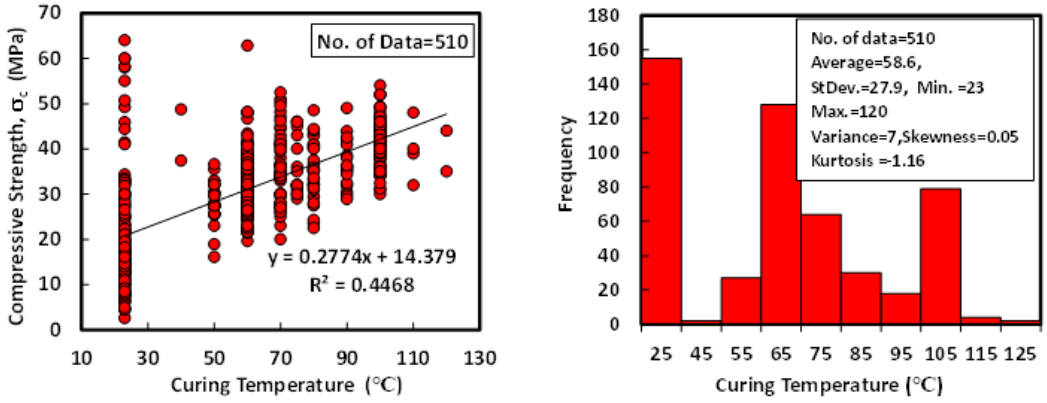

Fig.38. Relationship and a histogram of compression strength and curing temperature of FA-GPC mixtures

6.11 Oven curing duration (*CD*)

The duration of heating samples in the oven with the selected temperatures was another independent variable that is collected from the past different research studies. The statistical analysis revealed that the minimum curing duration of the collected data set was 8 hr., while the maximum CD inside ovens was 168 hr. Moreover, the average of CD was measured as 29 hr. the other stats indications such as standard deviation, variance, skewness, and kurtosis were recorded as 19.86 hr, 395, 5.66, and 35.6, respectively. Relationship and a histogram of compressive strength and the oven curing duration of FA-GPC mixtures are depicted in Fig.39.

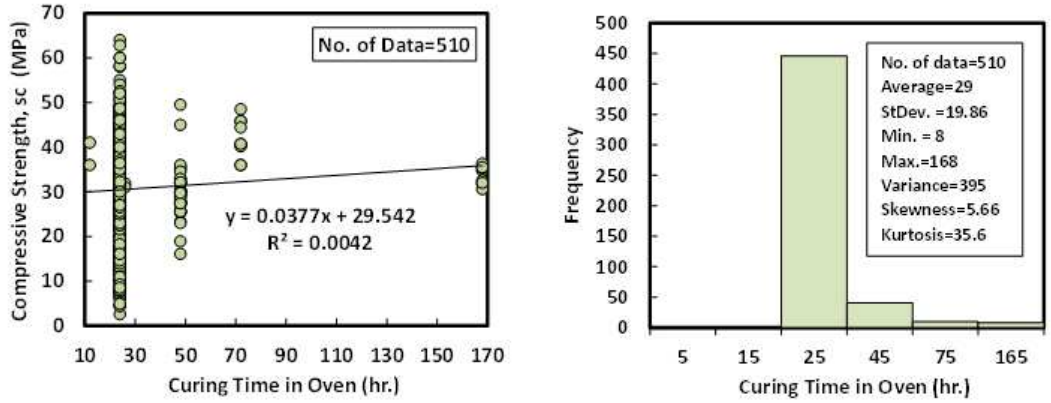

Fig.39. Relationship and a histogram of compression strength and curing duration of FA-GPC mixtures

6.12 Specimens ages (*A*)

Another independent variable collected in the literature papers is the age of FA-GPC specimens. The collected data contain the ages of the specimens range from 3 up to 112 days. Other statistical measuring devices such as standard deviation, variance, skewness, and kurtosis were calculated as 15.65 days, 245, 2.67, and 10.75, correspondingly. Relationship and a histogram of compressive strength and specimens ages of FA-GPC mixtures are presented in Fig.40.

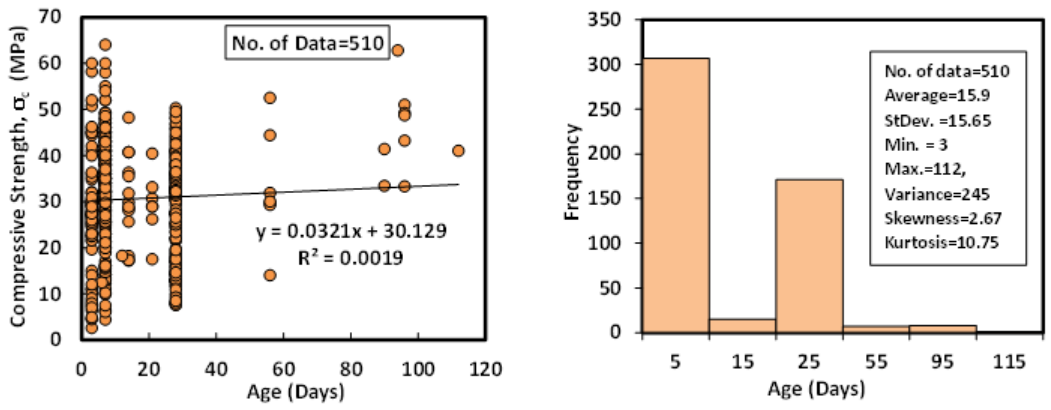

Fig.40. Relationship and a histogram of compression strength and specimens ages of FA-GPC mixtures

6.13 Compression strength (*fc′*)

The measured *fc′* of the 510 collected data from the literature studies was shown in Table 3; the *fc′* of the FA-GPC was in the range of 2 to 64 MPa, with an average of 30.6 MPa. The statistical analysis for the other dataset distribution indications such as standard deviation, variance, skewness, and kurtosis was 11.6 MPa, 133.8, -0.16, and -0.3, respectively.

7 Modeling

Based on the coefficient of determination (R^2) and statistical analysis, there are no direct relationships between the *fc′* and the constituents of the FA-GPC, as shown in Fig.29 to Fig.40.

As a result, four different models are proposed to examine the effects of the above mixture proportions on the *fc′* of FA-GPC, as shown below.

The models suggested in this paper are used to forecast the *fc′* of the FA-GPC and choose the optimum solution that delivers a better estimate of *fc′* than the experimentally determined *fc′*. All the collected datasets were randomly split into three parts: training, testing,, and validating datasets [57, 69]. 340 training dataset is used to train the LR, MLR, ANN, and M5P-tree model and obtain the optimal weights and biases, while 85 testing dataset is used to confirm the fulfillment of the proposed models. Moreover, 85 validating datasets are used to explore the generality of the models and prohibition of the over-fitting problem in the case of classical training algorithms. Comparisons of model predictions were made using the following evaluation criteria: The model should be scientifically accurate, with a smaller proportion of error between observed and projected data, as well as lower RMSE, OBJ, SI, and higher R^2 values.

7.1 Linear regression model (LR)

One of the most common methods to predict the *fc′* of concrete is the linear regression model (LR) [166], as shown in *Eq.1*, and it is considered as a general form of the linear regression model [66, 69, 165].

$$fc' = a + b(l/b) \qquad (1)$$

Where fc', l/b, $a\ and\ b$ represents compressive strength, liquid to binder ratio, and equation parameters, respectively. However, other components of FA-GPC mixtures that influence the compressive strength such as fly ash content and SS content and other mix proportions are not included in the calculation above. As a result, *Eq.2* is recommended to incorporate all other mix proportions and factors that may affect the fc' of FA-GPC in order to have more reliable and scientific observations.

$$fc' = a + b\left(\frac{l}{b}\right) + c(FA) + d\left(\frac{Si}{Al}\right) + e(F) + f(C) + g(SH) + h(SS) + i\left(\frac{SS}{SH}\right) + j(M) + k(T) + l(CD) + m(A) \quad (2)$$

Where: *l/b* is the alkaline solution to the binder ratio, *FA* is the fly ash (kg/m^3) content, *Si/Al* is the ratio of SiO_2 to Al_2O_3 of the fly ash, *F* is the fine aggregate (kg/m^3) content, *C* is the coarse aggregate (kg/m^3) content, *SH* is the sodium hydroxide (kg/m^3) content, *SS* is the sodium silicate (kg/m^3) content, *SS/SH* is the ratio of sodium silicate to the sodium hydroxide, *M* is the sodium hydroxide concentration (Molarity), *T* is the curing temperature (°C), a *CD* is the curing duration inside ovens (hr), and *A* is the ages of the specimens (days). While *a, b, c, d, e, f, g, h, i, j, k, l,* and *m* are the model parameters. This developed equation is a unique equation that involves a wide range of independent variables to produce FA-GPC that may be very useful for the construction industry.

7.2 Multilogistic model (MLR)

Same as the former models, a multi-logistic regression analysis model was carried out for the collected datasets, and the general form of the MLR is shown in *Eq.3* based on the research studied that had been conducted by Mohammed et al. [66] and Faraj et al. [69]. MLR is used to clarify the difference between a nominal predictor variable and one or more independent variables.

$$fc' = a * \left(\frac{l}{b}\right)^b * (FA)^c * \left(\frac{Si}{Al}\right)^d * (F)^e * (C)^f * (SH)^g * (SS)^h * \left(\frac{SS}{SH}\right)^i * (M)^j * (T)^k * (CD)^l * (A)^m \quad (3)$$

Where: *l/b* is the alkaline solution to the binder ratio, *FA* is the fly ash (kg/m^3) content, *Si/Al* is the ratio of SiO_2 to Al_2O_3 of the fly ash, *F* is the fine aggregate (kg/m^3) content, *C* is the coarse aggregate (kg/m^3) content, *SH* is the sodium hydroxide (kg/m^3) content, *SS* is the sodium silicate (kg/m^3) content, *SS/SH* is the ratio of sodium silicate to the sodium hydroxide, *M* is the sodium hydroxide concentration (Molarity), *T* is the curing temperature (°C), the *CD* is the curing duration inside ovens (hr), and *A* is the ages of the specimens (days). While *a, b, c, d, e, f, g, h, i, j, k, l,* and *m* are the model parameters.

7.3 Artificial Intelligence network (ANN)

ANN is a powerful simulation software designed for data analysis and computation to think as a human brain in terms of processing and analyses. This machine learning tool is widely used in construction engineering for predicting the future behavior of several numerical problems [60, 167, 168]. ANN model is generally divided into three main layers, which are input, hidden, output layers. Each of the

input and output layers can be one or more layers depending on the proposed problem. However, the hidden layer is usually ranged for two or more layers. Although the input and output layers are usually depending on the collected data and the designed model purpose, the hidden layer is determined by rated weight, transfer function, and the bias of each layer to other layers. A multi-layer feed-forward network is built based on a mixture of pro-portions, weight/bias, several parameters including (*l/b, FA, Si/Al,* …) as inputs, and the output of ANN here is the compressive strength. There is no standard approach to designing the network architecture. Therefore, the number of hidden layers and neurons is determined based on a trial and error test. One of the main objectives of the training process of the network is to determine the optimum number of iteration (epochs) that provide the minimum mean absolute error (MAE), and root mean square error (RMSE) and best R-value that close to one. The effect of several epochs on reducing the MAE and RMSE has been studied. The collected data set (a total of 510 data) has been divided into three parts for the training purpose of the designed ANN. Around 70th percent of the collected data was used as a trained data for training the network, 15th percent of overall data was used for testing the dada set, and the rest of the remaining data was used to validate the trained network [167]. The designed ANN was trained and tested for various hidden layers to determine optimal network structure based on the fitness of the predicted compression strength of FA-GPC with the fc' of the real collected data. It was observed that the ANN structure with two hidden layers, twenty neurons, and a hyperbolic tangent transfer function was a best-trained network that provides a maximum R^2 and minimum both MAE and RMSE (shown in Table 4). As a part of this study, an ANN model has been used to predict the future value of the compressive strength of FA-GPC. The general equation of the ANN model is shown in *Eq.4*, *Eq.5*, and *Eq.6*

From linear node 0:

$$fc' = Threshold + \left(\frac{Node\ 1}{1 + e^{-B1}}\right) + \left(\frac{Node\ 2}{1 + e^{-B2}}\right) + \cdots \quad (4)$$

From sigmoid node 1:

$$B1 = Threshold + \Sigma\ (Attribute * Variable) \quad (5)$$

From sigmoid node 2:

$$B2 = Threshold + \Sigma\ (Attribute * Variable) \quad (6)$$

Table 4. The tested ANN architectures

No. of Hidden layers	No. of Neurons in left side	No. of Neurons in right side	R^2	MAE (MPa)	RMSE (MPa)
1	1	0	0.9196	3.8723	4.8722

1	2	0	0.9327	3.4534	4.3788
1	3	0	0.9343	3.4433	4.3535
1	5	0	0.9479	3.1805	4.0428
1	7	0	0.9533	3.0219	3.8181
1	9	0	0.9562	2.8841	3.6957
1	11	0	0.9574	2.7475	3.5838
1	15	0	0.9591	2.5443	3.3819
1	17	0	0.9608	2.6331	3.4333
2	1	1	0.9186	3.9349	4.9583
2	2	2	0.9305	3.4333	4.2936
2	4	4	0.9524	2.815	3.579
2	5	5	0.9555	2.8434	3.5767
2	6	6	0.9598	2.9021	3.7213
2	6	5	0.9587	2.8525	3.6551
2	7	7	0.9619	2.5111	3.2843
2	8	8	0.9615	2.6078	3.3435
2	**10**	**10**	**0.9647**	**2.5853**	**3.332**
2	15	15	0.9628	2.7318	3.5506
2	10	9	0.9639	2.5132	3.2834
2	9	5	0.9615	2.4835	3.2599
2	12	7	0.9618	3.1656	3.9592
2	6	9	0.9576	2.8395	3.6575
2	7	10	0.9639	2.5955	3.4115

7.4 M5P-tree model

The M5P model tree is a reconstruction of Quinlan's M5 algorithm [169] that is based on the conventional decision tree with the addition of a linear regression function to the leaves nodes. The decision tree is a representation of the algorithms by a tree form trained through a data to form nodes. The nodes constituting the decision tree are divided into three types namely; root nodes, internal nodes, and leaves nodes. Nodes are interconnected to each other through branches until the leaves reached [170, 171]. Furthermore, M5P-tree, introduced by Mohammed [168], is a robust decision tree learner model to study regression analysis. This learner algorithm puts linear regression functions at the terminal nodes and places a multivariate linear regression model to each sub-space by classifying all data sets into multiple sub-spaces. The M5P-tree works on continuous class problems rather than discrete segments and can handle tasks with high dimensional features. It reveals the developed information of each linear model component constructed to estimate the nonlinear correlation of the data sets. The information about division criteria for the M5-tree model is obtained through the error calculation at each node. At each node, errors are analyzed by the standard deviation of the class entering that node. The attribute that maximize the reduction of estimated error at each node is used to evaluate any task of that node. As a result of this division in the M5P tree, a large tree likes structure

that leads to overfitting will be created. In the followed step, the enormous tree is trimmed, and the pruned subtrees are restored by linear regression functions. The general equation form of the M5P-tree model is the same as the linear regression equation, as shown in *Eq. 7*

$$fc' = a + b\left(\frac{l}{b}\right) + c(FA) + d\left(\frac{Si}{Al}\right) + e(F) + f(C) + g(SH) + h(SS) + i\left(\frac{SS}{SH}\right) + j(M) + k(T) + l(CD) + m(A) \quad (7)$$

Where: *l/b* is the alkaline solution to the binder ratio, *FA* is the fly ash (kg/m^3) content, *Si/Al* is the ratio of SiO_2 to Al_2O_3 of the fly ash, *F* is the fine aggregate (kg/m^3) content, *C* is the coarse aggregate (kg/m^3) content, *SH* is the sodium hydroxide (kg/m^3) content, *SS* is the sodium silicate (kg/m^3) content, *SS/SH* is the ratio of sodium silicate to the sodium hydroxide, *M* is the sodium hydroxide concentration (Molarity), *T* is the curing temperature (°C), the *CD* is the curing duration inside ovens (hr) and *A* is the ages of the specimens (days). While *a, b, c, d, e, f, g, h, i, j, k, l,* and *m* are the model parameters.

8 Model performance assessment criteria

Various performance indicators, including the coefficient of determination (R^2), Root Mean Squared Error (RMSE), Mean Absolute Error (MAE), Scatter Index (SI), and OBJ, were employed to analyze and analyze the effectiveness of the presented models. :

$$R^2 = \left(\frac{\sum_{p=1}^{p}(t_p - t')(y_p - y')}{\sqrt{\left[\sum_{p=1}^{p}(t_p - t')^2\right]\left[\sum_{p=1}^{p}(y_p - y')^2\right]}}\right)^2 \quad (8)$$

$$RMSE = \sqrt{\frac{\sum_{p=1}^{p}(y_p - t_p)^2}{p}} \quad (9)$$

$$MAE = \frac{\sum_{p=1}^{p}|(y_p - t_p)|}{p} \quad (10)$$

$$SI = \frac{RMSE}{t'} \quad (11)$$

$$OBJ = \left(\frac{n_{tr}}{n_{all}} * \frac{RMSE_{tr} + MAE_{tr}}{R^2_{tr}+1}\right) + \left(\frac{n_{tst}}{n_{all}} * \frac{RMSE_{tst} + MAE_{tst}}{R^2_{tst}+1}\right) + \left(\frac{n_{val}}{n_{all}} * \frac{RMSE_{val} + MAE_{val}}{R^2_{val}+1}\right) \quad (12)$$

Where: $\boldsymbol{y_p}$ and $\boldsymbol{t_p}$ are the estimated and the tested compression strength values and $\boldsymbol{t'}$ and $\boldsymbol{y'}$ are the averages of the experimentally tested and the predicted values from the models, respectively. ***tr***, ***tst,*** and ***val*** are referred to as training, testing, and validating datasets, respectively, and ***n*** is the number of datasets.

With the exception of the R^2 value, zero is the optimal value for all other evaluation parameters. However, one is the highest benefit for R^2. When it came to the SI parameter, a model has bad performance when it is > 0.3, acceptable performance when it is 0.2 SI 0.3, great performance when it is 0.1 SI 0.2, and great performance when it is 0.1 SI 0.1 [57, 69, 172]. Furthermore, the OBJ parameter

was employed as a performance measurement parameter in *Eq.12* to measure the efficiency of the suggested models.

9 Results and Analysis of all Models

9.1 LR model

Figures 41a, b, and c show the comparison of forecasted and measured compression strength of FA-GPC for training, testing, and validating datasets, respectively. The model parameters *l/b* and *SS/SH* all have a substantial impact on the mechanical properties, such as the fc' of FA-GPC. The weight of each parameter on the fc' of the FA-GPC was determined for the current model by optimizing the sum of error squares and the least square method in Excel using Optimizer to compute the ideal value (a certain value, minimum or maximum) for the equation in one cell named the objective cell [66]. Based on the linear regression analysis model, it was observed that, among the whole model input parameters, the ratio of alkaline liquid to the binder ration and the sodium silicate to the sodium hydroxide ratio of the GPC mixture have a great influence on the fc' of the FA-GPC which it is matched with the experimental results presented in the literature [71, 73, 79, 98, 139].The equation for the LR model with different weight parameters can be written as follows (*Eq.13)*.

$$fc' = -66.8 + 187.75\left(\frac{l}{b}\right) + 0.246(FA) - 1.697\left(\frac{Si}{Al}\right) - 0.016(F) - 0.012(C) - 0.334(SH) - 0.538(SS) + 0.942\left(\frac{SS}{SH}\right) + 0.179(M) + 0.228(A) + 0.342(T) + 0.01(CD) \quad (13)$$

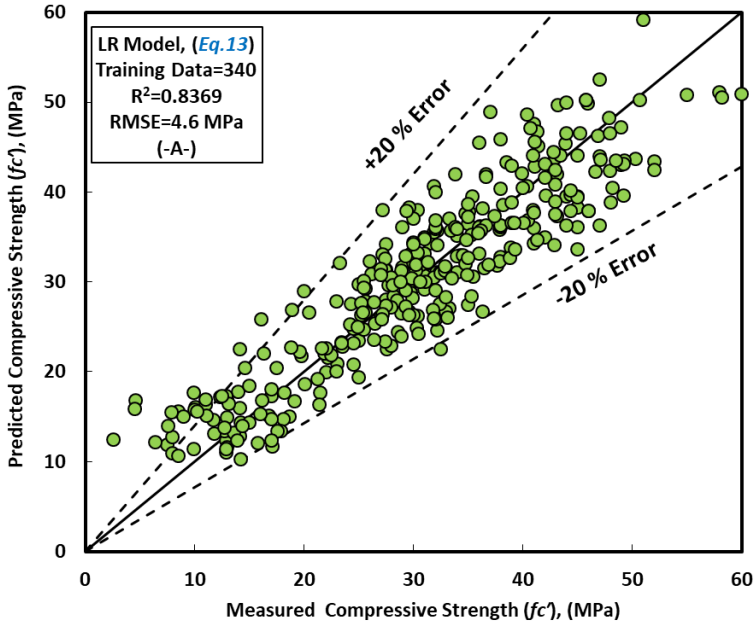

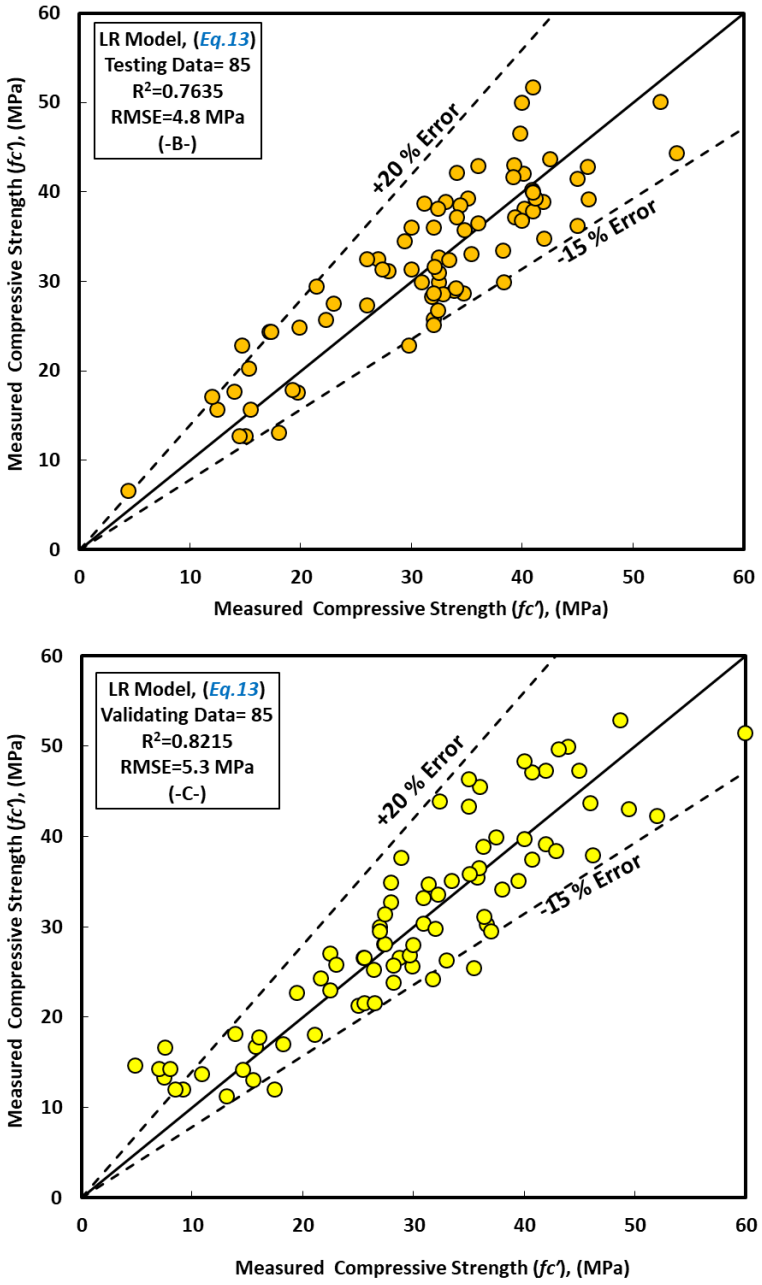

Fig.41. Comparison between measured and predicted *fc'* of the FA-GPC using LR model, (a) training, (b) testing, and (c) validating datasets

The studied datasets have a ±20% error line for the training data and -15% and +20% error lines for both testing and validating datasets. Nevertheless, the developed model slightly overestimated the low-strength FA-GPC mixes and underestimated the high-strength FA-GPC. Also, the residual *fc'* between the predicted and measured compression strength for the LR model using training, testing, and validating dataset was compared as shown in Fig.42.

The R^2, RMSE, and MAE evaluation variables for this model are the same as the values of 0.8369, 4.65 MPa, and 3.76 MPa, correspondingly. Furthermore, as shown in Fig. 43 and 44, the current model's OBJ and SI values for the training dataset are 3.09 and 0.15, respectively.

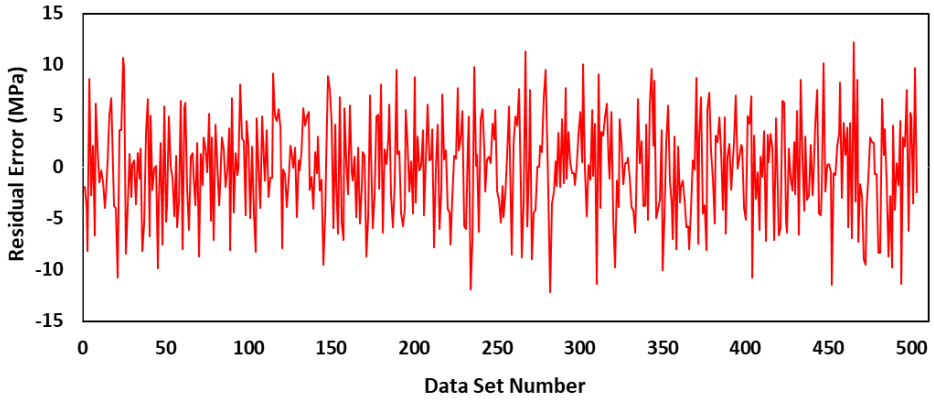

Fig.42. Residual error diagram of *fc'* of the FA-GPC using training, testing, and validating dataset for LR model

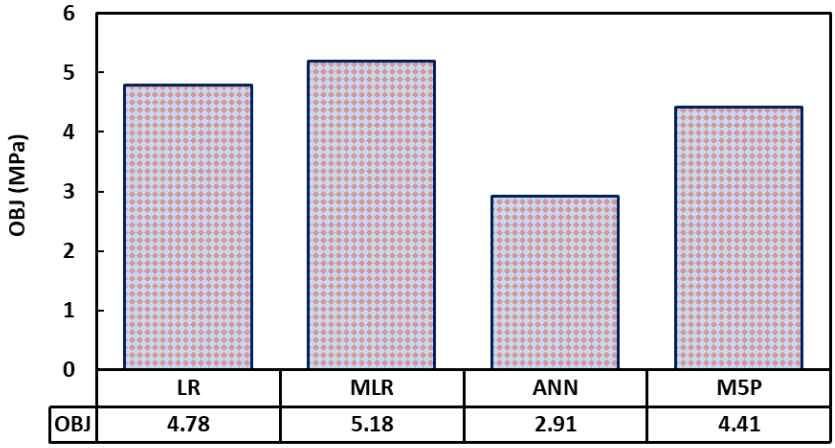

Fig.43. The value of OBJ for the whole proposed models

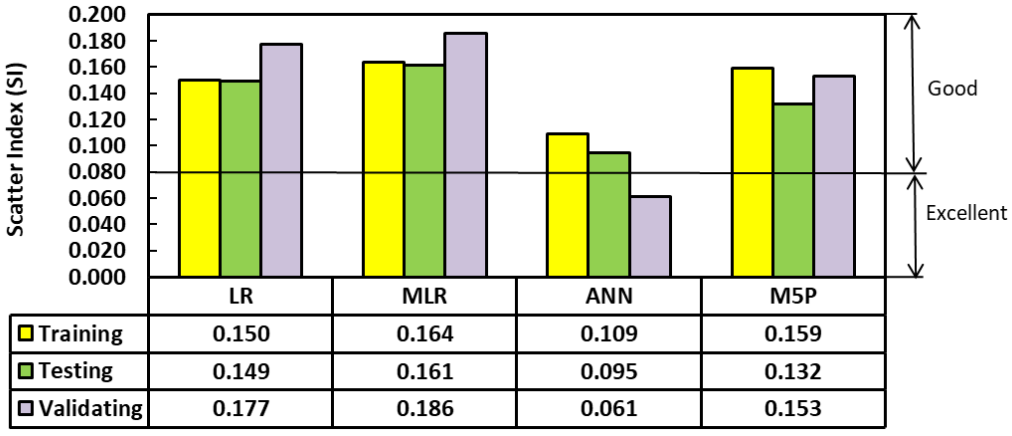

Fig.44. The SI statistical criteria for the whole proposed models

9.2 MLR model

The developed models for the MLR model with various variable parameters presented in *Eq.14*. In the MLR model, like other developed models, the curing temperature, sodium silicate content, and alkaline liquid to the binder ratio were the most significant independent variables that affect on the *fc'* of the

FA-GPC that is matched with the experimental works presented in the literature [71, 73, 79, 96, 98, 105, 108, 112, 113, 121, 122, 139]. The relationships between the predicted and measured fc' of the training data set for the FA-GPC was shown in Fig.45a. Further, same as the previous model, this model was checked by two sets of data (testing and validating dataset) to show their efficiency for other data out of the model data (training data); the results show that this model can be used to predict the fc' of FA-GPC just by substitute the independent variables into the developed equation as shown in Fig.45b and Fig.45c.

$$f_{c'} = 147.14 * (\frac{l}{b})^{0.350} * (FA)^{0.195} * \left(\frac{Si}{Al}\right)^{-0.383} * (F)^{-0.212} * (C)^{-0.236} * (SH)^{-0.715} * (SS)^{0.393} * \left(\frac{SS}{SH}\right)^{-0.81} * (M)^{0.086} * (A)^{0.128} * (T)^{0.534} * (CD)^{-0.046} \quad (14)$$

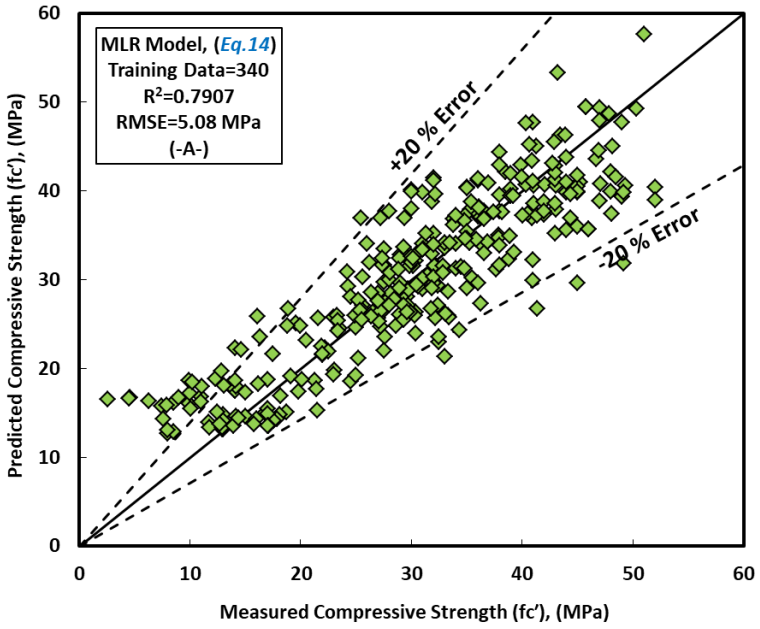

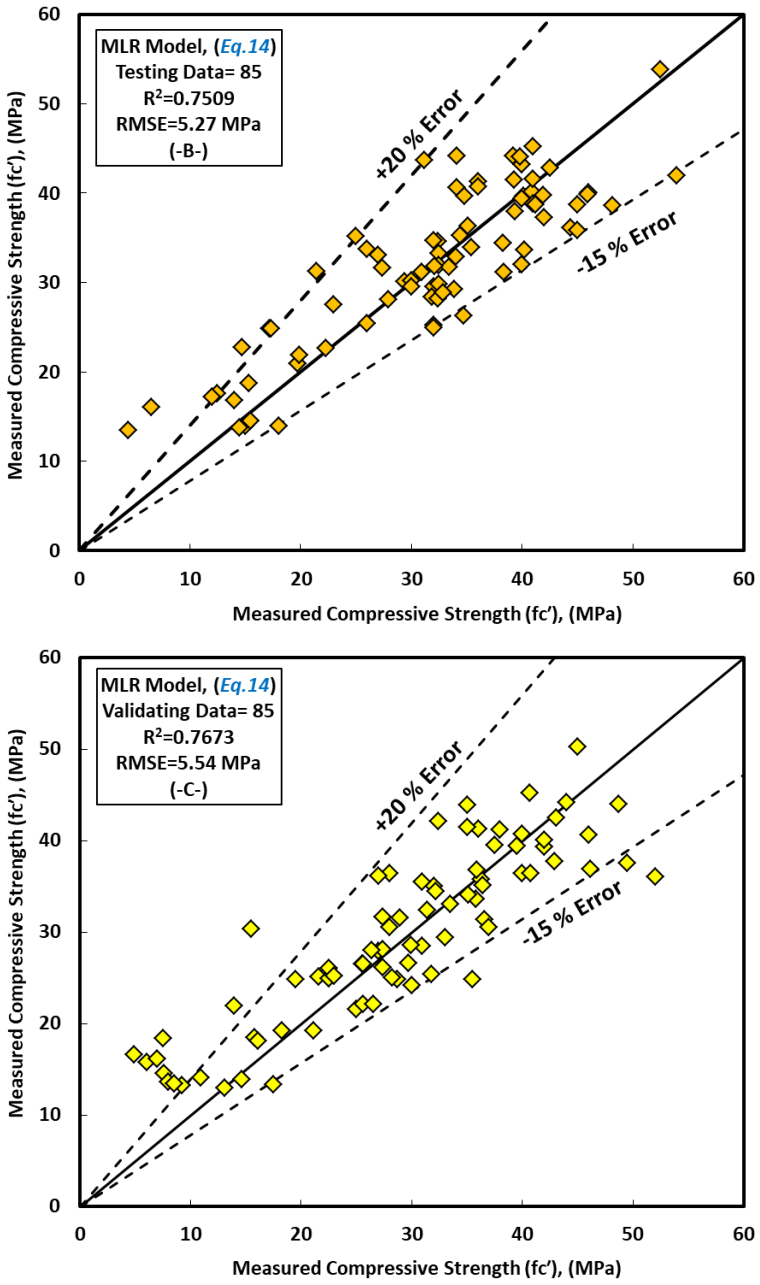

Fig.45. Comparison between examined and predicted *fc′* of the FA-GPC using MLR model, (a) training, (b) testing, and (c) validating datasets

Like other models, the studied datasets have a ±20% error line for the training data and -15% and +20% error lines for both testing and validating dataset, indicating that almost all checked results were in ± 20% error lines. Finally, the residual compression strength for the MLR model was shown in Fig.46 for the predicted and measured *fc′* by using training, testing, and validating datasets. Furthermore, the assessment criteria for this model, such as R^2, RMSE, MAE, OBJ, and SI are 0.7907, 5.08 MPa, 3.95 MPa, 3.4, and 0.17, respectively, for the training dataset.

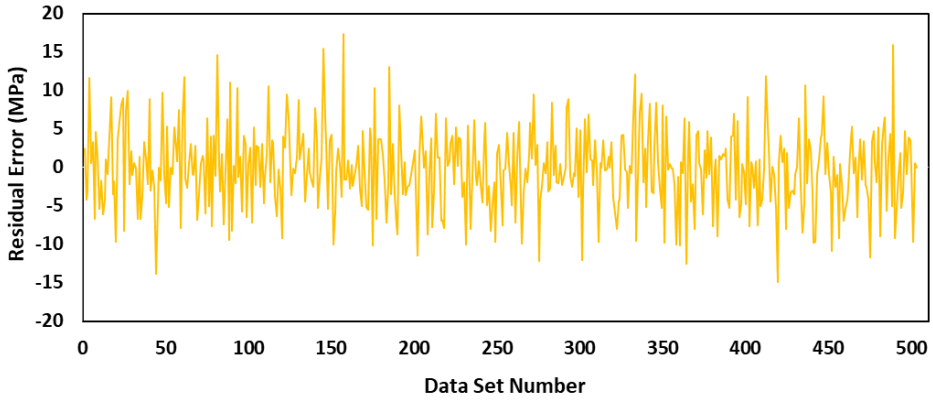

Fig.46. Residual error diagram of fc' of the FA-GPC mixtures using training, testing and validating dataset for MLR model

9.3 ANN model

In this study, the authors tried a lot to get the high efficiency of the ANN by applying different numbers of the hidden layer, neurons, momentum, learning rate, and iteration. Lastly, they observed that when the ANN has two hidden layers, 20 neurons (10 for left side and 10 for the right side as shown in Fig. 48), 0.2 momentum, 0.1 learning rate, and 2000 iteration give best-predicted values of the fc' of the FA-GPC composites. The ANN model was equipped with the training datasets, accompanied by both the testing and validating datasets to predict the compression strength values for the correct input parameters. The comparison between predicted and measured fc's of FA-GPC for training, testing, and validating datasets are presented in Figures 47a, b, and c. The studied datasets have a +15% and -20% error line for the training data, +10% and -20% error lines for testing data, and +15% and -10% for the validating datasets, which it is better than the other developed models. Furthermore, this model has a better performance compared to other models to predict the fc' of the FA-GPC based on the value of OBJ and SI that illustrated in Fig. 43 and Fig. 44, also, the value of $R^2 = 0.9647$, MAE = 2.5853 MPa, and RMSE = 2.332 MPa. Finally, the residual compression strength for the ANN model was shown in Fig.49 for the predicted and measured fc' by using all datasets.

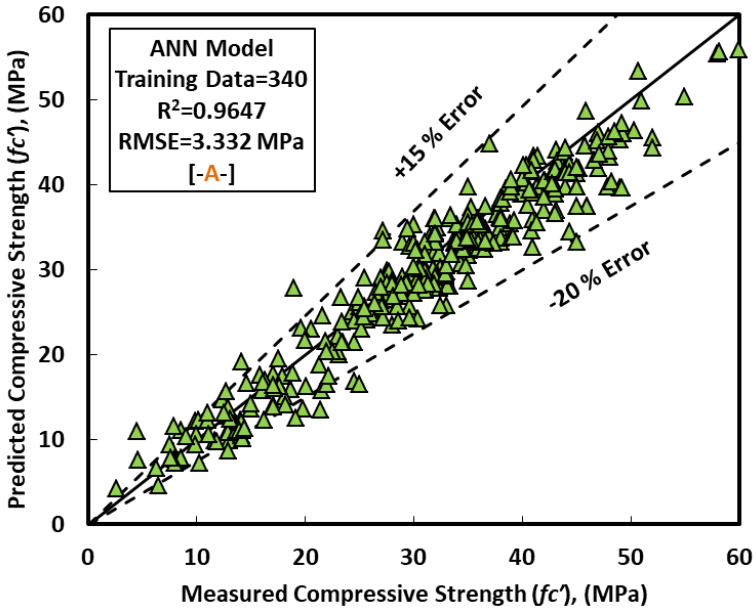
ANN Model
Training Data=340
R²=0.9647
RMSE=3.332 MPa
[-A-]
+15 % Error
-20 % Error
Predicted Compressive Strength (fc'), (MPa)
Measured Compressive Strength (fc'), (MPa)
0
10
20
30
40
50
60

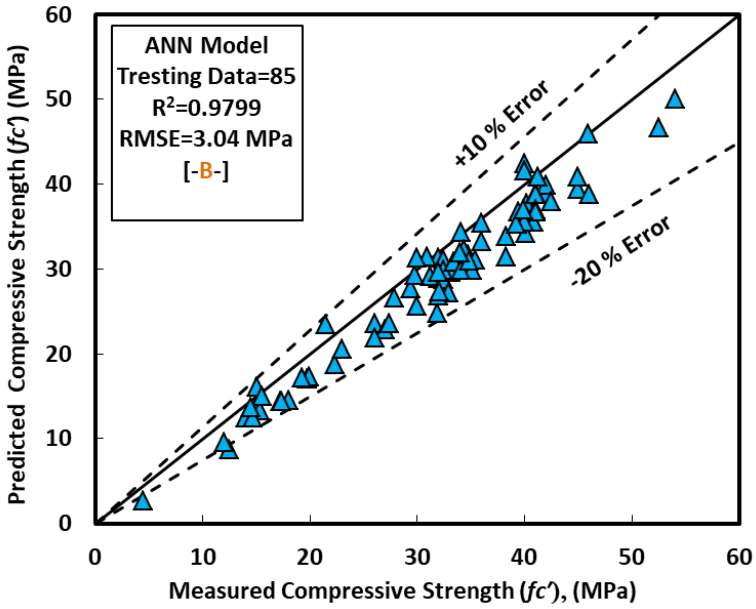
ANN Model
Tresting Data=85
R²=0.9799
RMSE=3.04 MPa
[-B-]
+10 % Error
-20 % Error
Predicted Compressive Strength (fc') (MPa)
Measured Compressive Strength (fc'), (MPa)
0
10
20
30
40
50
60

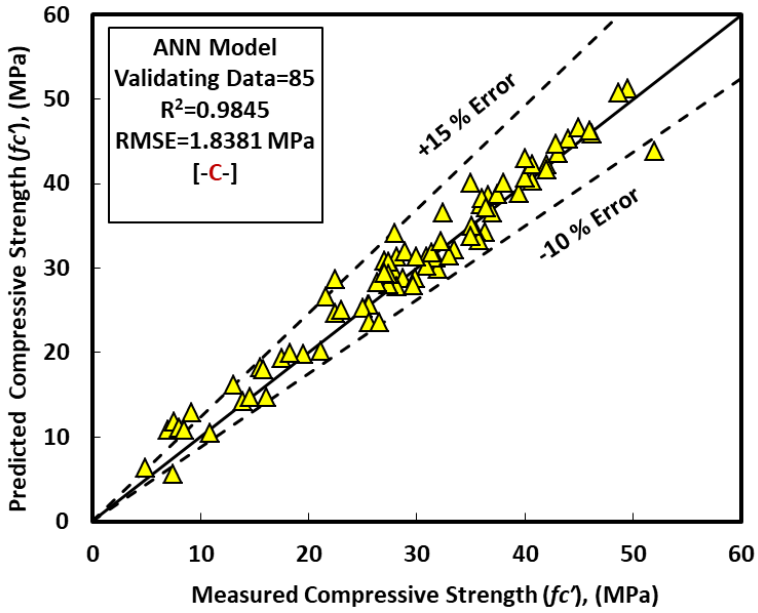

Fig.47. Measured-predicted *fc'* of the FA-GPC mixture using ANN model, (a) training, (b) testing, and (c) validating datasets

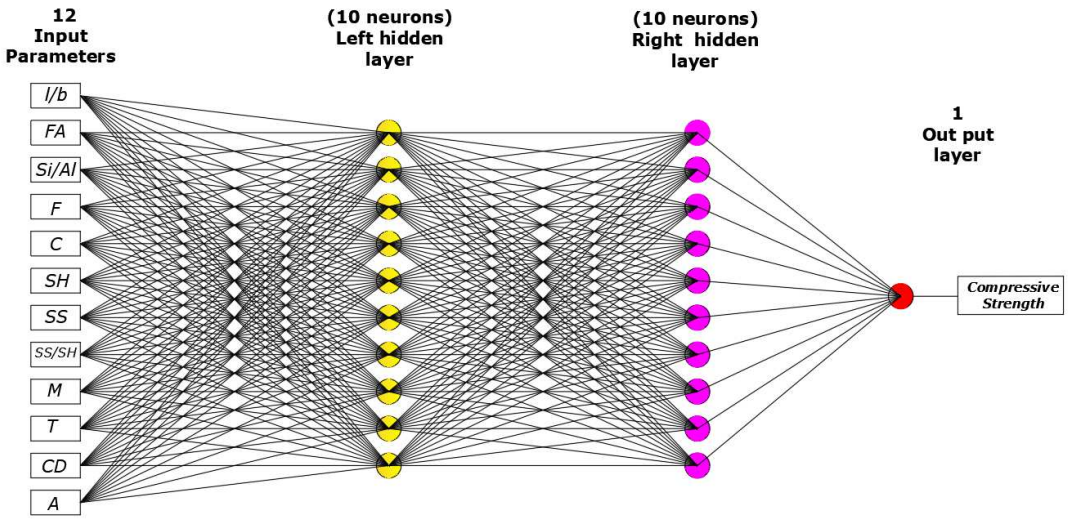

Fig. 48. Optimal Network Structures of the ANN Model.

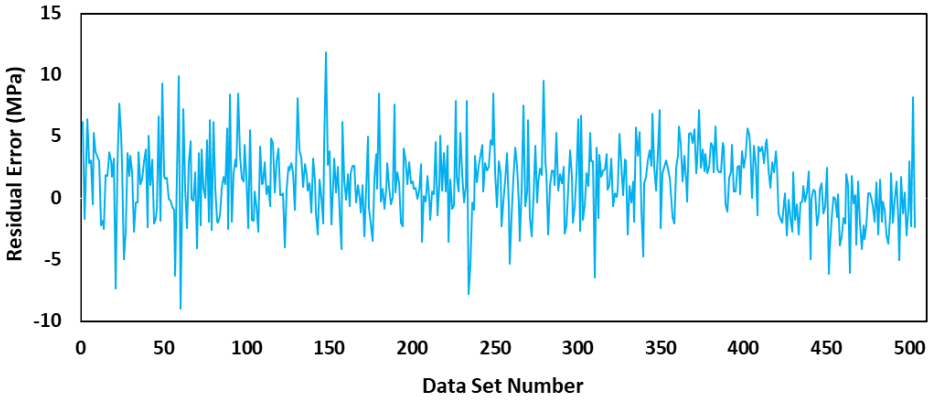

Fig.49. Residual error diagram of *fc'* of the FA-GPC mixtures using training, testing and validating dataset for ANN model

9.4 M5P model

Figures 50a, b, and c are shown a comparison between the predicted and measured *fc'*s of the FA-GPC for training, testing, and validating datasets. Same as other models, it was observed that the ratio of alkaline liquid to the binder ratio and the sodium silicate to the sodium hydroxide ratio of the FA-GPC mixture have a great influence on the compression strength of the FA-GPC, which it is matching with the experimental results presented in the literature [71, 73, 79, 98, 139]. Fig.51 indicates the tree-shaped branch relationship, and the model (*Eq.15*) parameters are summarized in *Table 5,* and based on the linear tree registration function, the model variables will be selected.

$$fc' = a + b\left(\frac{l}{b}\right) + c(FA) + d\left(\frac{Si}{Al}\right) + e(F) + f(C) + g(SH) + h(SS) + i\left(\frac{SS}{SH}\right) + j(M) + k(T) + l(CD) + m(A) \quad (15)$$

Table 5. M5P-tree Model parameters (Eq.15).

	(LM) num:	**1**	**2**	**3**	**4**	**5**
Model Parameters	***a***	41.6064	11.7823	95.402	32.4732	31.5933
	b	-88.116	-58.4305	-4.1404	-4.1404	1.7345
	c	0.0104	0.0433	0.0104	0.0104	0.0053
	d	-0.3919	-0.3919	-0.9358	-2.621	-3.4389
	e	-	-	-	-	-0.0096
	f	-0.0147	-0.0147	-0.0728	-0.0122	-0.0054
	g	0.149	0.149	0.0673	0.0673	0.0482
	h	0.2003	0.1005	-0.0402	-0.0667	-
	i	2.5613	2.5613	-0.3196	1.0122	-1.8158
	j	-0.3463	0.4596	0.5641	0.1147	-
	k	0.0405	0.0405	0.0405	0.0405	0.281
	l	-	-	-	-	-
	m	0.1782	0.2279	0.4176	0.2897	0.1787

The studied datasets have a ±20% error line for all the training, testing, and validating datasets. Finally, the residual compression strength for the M5P model was shown in Fig.52 for the predicted and examined fc' by using all datasets. Furthermore, the assessment criteria for this model, such as R^2, RMSE, MAE, OBJ, and SI, are 0.9078, 4.8432 MPa, 3.7864 MPa, 4.41, and 0.159, respectively, for the training datasets.

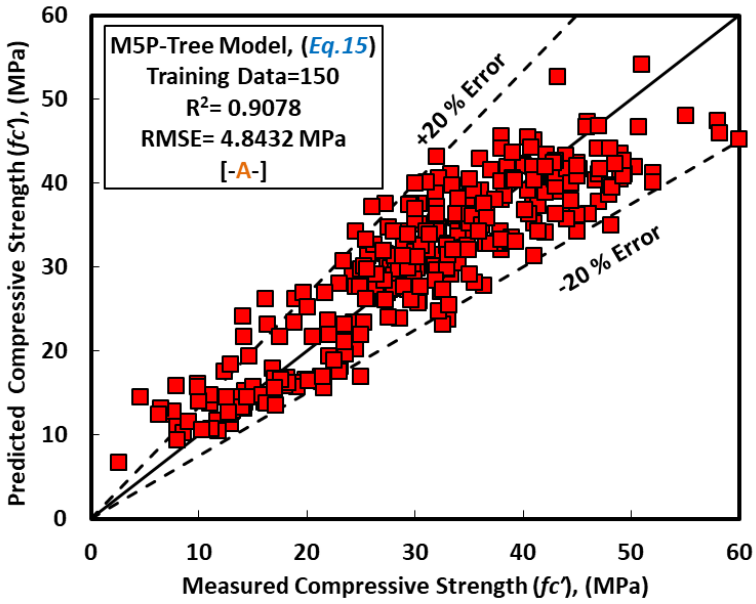
M5P-Tree Model, (Eq.15)
Training Data=150
R²= 0.9078
RMSE= 4.8432 MPa
[-A-]
+20 % Error
-20 % Error
Predicted Compressive Strength (fc'), (MPa)
Measured Compressive Strength (fc'), (MPa)
0
10
20
30
40
50
60

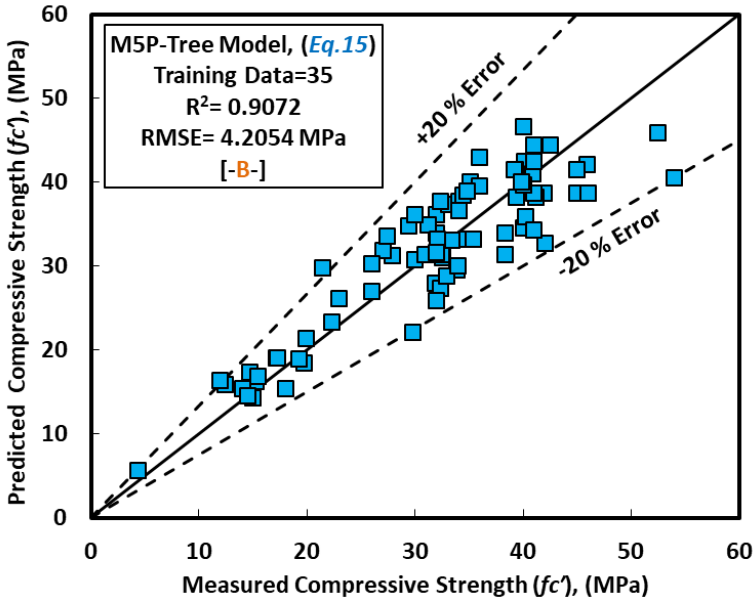
M5P-Tree Model, (Eq.15)
Training Data=35
R²= 0.9072
RMSE= 4.2054 MPa
[-B-]
+20 % Error
-20 % Error
Predicted Compressive Strength (fc'), (MPa)
Measured Compressive Strength (fc'), (MPa)
0
10
20
30
40
50
60

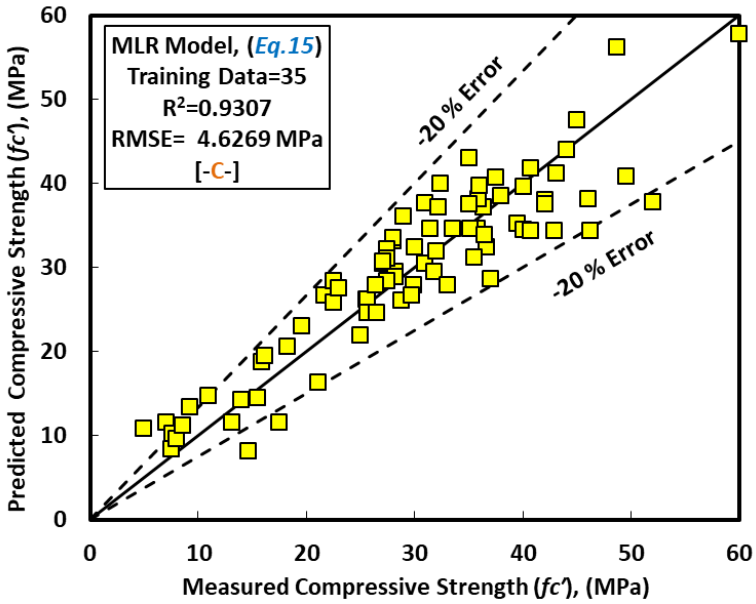

Fig.50. Relationship between examined and predicted *fc′* of the FA-GPC using M5P model, (a) training, (b) testing, and (c) validating datasets

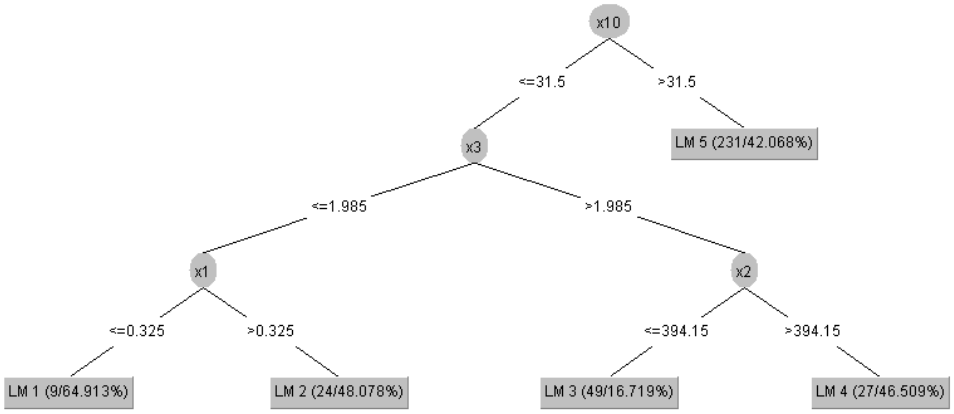

Fig.51. M5P-tree Pruned model tree.

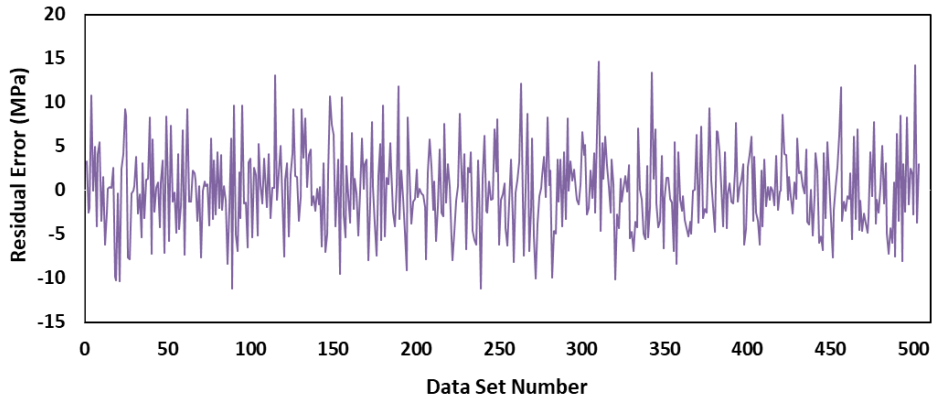

Fig.52. Residual error diagram of *fc′* of the FA-GPC mixtures using training, testing and validating dataset for M5P model

10 Developed models Performance

The efficiency of the proposed models was evaluated using five different statistical tools: RMSE, MAE, SI, OBJ, and R^2. Among the four models, the ANN model has a stronger R^2 and lower RMSE and MAE values than the LR, MLR, and M5P models. In addition, Fig.53 shows a comparison of model predictions of FA-GPC mixture *fc′* vs. validating results. Furthermore, utilizing training, testing, and validating datasets, Figures 42, 46, 49, and 52 displays the residual error for all models. The ANN model's predicted and observed compressive strength values are closer in both figures, indicating that the ANN model outperforms other models. Figure 43 shows the OBJ values for all of the suggested models. OBJ is 4.78, 5.18, 2.91, and 4.41 for LR, MLR, ANN, and M5P, respectively. The ANN model's OBJ value is 64.2 percent less than the LR model, 78 percent less than the MLR model, and 51.5 percent less than the M5P model. This also shows that the ANN model is better at forecasting the *fc′* of the FA-GPC mixes. In addition, Fig.44 shows the SI assessment model parameters for the proposed models through the training, validating, and testing stages. The SI values for all models and stages (training, testing, and validating) were between 0.1 and 0.2, suggesting good performance for all models, as shown in Fig.44. The ANN model, like the other performance parameters, has lower SI values than the other models. The ANN model has lower SI values than the LR, MLR, and M5P models by 37.6%, 50.5%, and 45.8%, respectively. This also demonstrated that when forecasting the *fc′* of the FA-GPC, the ANN model is more efficient and performs better than the LR, MLR, and M5P models.

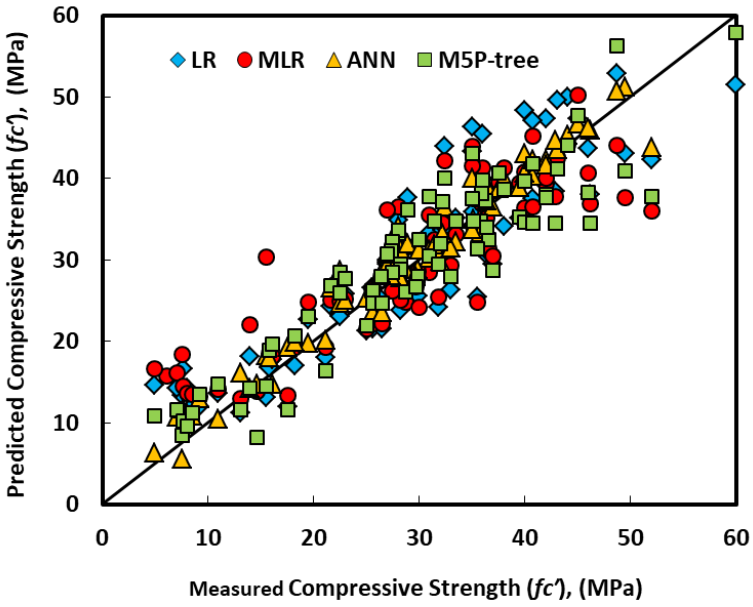

Fig.53. Model projections of *fc′* of the FA-GPC mixtures using validating datasets

11 Discussion

- As a result of the modeling and comprehensive systematic review of the literature above, it can be said that the geopolymer concrete is a cementless concrete that use industrial or agro by-product ashes as main binder instead of ordinary Portland cement, this is leads to the geopolymer concrete to be an eco-efficient and environmentally friendly construction materials. Further, this type of

concrete lead to a reduction of the carbon dioxide percent in the air, energy consumption, as well as waste disposal and the cost of the construction. This type of concrete is affected by many mixed proportion parameters as well as curing conditions.

- , The alkaline solution to the binder ratio (l/b), is the ratio of the summation of sodium hydroxide and sodium silicate content to the total weight or volume of the fly ash or other source binder materials in the mixture proportions of the geopolymer concrete mixtures. This ratio has a significant impact on the compressive strength of the fly ash-based geopolymer concrete. Some researchers believed that the compressive strength was improved as the l/b increased up to a limited amount, then it was decreased. While many researchers reported reduction in the compressive strength as the l/b was increased. Because of the fact that with decreasing l/b ratio will lead to accelerating in the alkaline activation process of fly ash geopolymer concrete due to the decrease of consistency of the geopolymer concrete mixture and in this case, the Calcium Aluminate Silicate Hydrate (C-A-S-H) gel and Sodium Aluminate Silicate Hydrate (N-A-S-H) gel can be generated quickly in the geopolymer concrete mixture with low l/b ratio and as a consequence participated in the development of early-age compressive strength of fly ash-based geopolymer concrete
- Superplasticizer and water content are two key parameters that govern the workability behavior of the fly ash-based geopolymer concrete and hence affect on the hardened characteristics of the geopolymer concrete. Same as conventional concrete, increasing water content or extra water to the fly ash-based geopolymer concrete will lead to decreasing the compressive strength of the geopolymer concrete, this is due to the evaporation of water in the geopolymer concrete mixture will lead to leaving pores and cavities with in the geopolymer concrete matrix, when the geopolymer concrete specimens curing at the high temperature inside ovens, moreover, the presence of extra water may influence the alkalinity environment of the fly ash-based geopolymer concrete matrix that could cause decreasing the rate of the geopolymerization process between the alkaline materials and the source materials. While superplasticizer content improves the compressive strength of the fly ash-based geopolymer concrete composites up to a limited amount and beyond that has a negative effect on the compressive strength.
- Fly ash is one of the most common types of source material binders to produce geopolymer concrete composites. The amount of fly ash content in the geopolymer concrete mixture influences the composite's compressive strength. As the fly ash content increased in the geopolymer concrete mixture, then compressive strength was improved. This is because the higher content of fly ash in the geopolymer concrete mixture gives denser and compacted microstructure to the geopolymer concrete matrix. Moreover, the particles of fly ash facilitate movement among the aggregate particles owing to the spherical shape and smooth surface of the particles of fly ash; on the other hand, the volume of fine fraction particles in the geopolymer concrete matrix increased as the fly ash content increased, thus, in turn, fill the voids and pores between the aggregate particles and hence compressive strength was improved. In addition, fly ash is the main source of aluminosilicate

source materials in the geopolymer concrete mixture, which silica and alumina increased as the amount of fly ash content increased; thus, they affect the reactions in the polymerization process, which in turn, C-A-S-H and N-A-S-H gels increased, and finally, compressive strength was improved

- The effects of fine and coarse aggregates on the geopolymer concrete mixture performances are the same as conventional concrete mixtures. Therefore, it was suggested to use good quality of aggregates to produce good geopolymer concrete composites, and hence about 70-80% of total aggregate content is required to produce 1.0 m^3 of fly ash-based geopolymer concrete.
- The alkaline solution content and the ratio of sodium silicate to sodium hydroxide significantly influence the compressive strength of fly ash-based geopolymer concrete. Compressive strength of fly ash-based geopolymer concrete increases as the ratio of SS/SH increased up to a limited amount; this increase in the compressive strength is due to the improvement in the microstructure of geopolymer concrete at the required quantity of sodium silicates contents, while, at a high ratio of SS/SH, reduction in the compressive strength happened due to the fact that there is not sufficient amount of sodium hydroxide present in the mixture to completion of dissolution process during the formation of geopolymer or due to the excess OH^- concentration in the geopolymer concrete mixture. On the other hand, the excess of the sodium content can form sodium carbonate by atmospheric carbonation, and this may disrupt the polymerization process, and as a result, compressive strength was decreased. Therefore, it is suggested to use the ratio of SS/SH in the range of 1.5-2.5 for getting fly ash-based geopolymer concrete with superior compressive strength
- The value of the concentration of sodium hydroxide solution has an appreciable effect on the compressive strength of fly ash-based geopolymer concrete. Because it is leads to an increase of sodium ions in the geopolymer concrete mixture, which was significant for the geopolymerization process, and hence, sodium ions were used to balance the charges and formed alumino-silicate networks as a source materials binder in the geopolymer concrete mixture. So, it was suggested to use the molarity of sodium hydroxide in the range of 10-16M to produce the fly ash-based geopolymer concrete mixtures with acceptable compressive strength behavior.
- The compressive strength of fly ash-based geopolymer concrete is significantly affected by the curing temperature and duration. Longer curing time and curing at high temperatures (50-100 °C) increases the compressive strength of fly ash-based geopolymer concrete, although the increase in strength may be insignificant for curing at more than 60°C and for periods longer than 48 hrs. Therefore, for heat curing regimes, temperatures between 50-80°C and curing time of 24 hr are widely accepted values used for successful geopolymerization process. In addition, among the curing condition methods (oven, steam, and ambient), oven curing techniques has a better influence on the compressive strength of fly ash-based geopolymer concrete composites.
- As a result of the comprehensive systematic review that had been carried out in this study on the factors that affect on the compressive strength of FA-GPC, different mixture proportions, curing

conditions, and age of the concrete specimens influence the compressive strength. Therefore, developing multi-scale models to predict this important property of the geopolymer concrete by considering a wide range of input parameters is essential regarding knowing the effect of each parameter on the compressive strength of the FA-GPC as well as modeling will be helpful for the concrete and construction industry regarding saving in time, energy, cost-effectiveness, and it gives guidance about scheduling for the construction process and removal of formwork elements.

12 Conclusions

Based on the extensive literature review and discussions made in this study, the following conclusions can be reached:

I. Geopolymer concrete with acceptable compressive strength values could be produced by using fly ash as source binder materials.

II. , The alkaline solution to the binder ratio (l/b), has a significant impact on the compressive strength of the fly ash-based geopolymer concrete. Some researches believed that the compressive strength was improved as the l/b increased. While, many researchers reported a reduction in the compressive strength as the l/b was increased.

III. Increasing water content or extra water to the fly ash-based geopolymer concrete will lead to decreasing the compressive strength of the geopolymer concrete. While superplasticizer content improves the compressive strength of the fly ash-based geopolymer concrete composites up to a limited value around 2% of fly ash content.

IV. strength of fly ash-based geopolymer concrete increases as the ratio of SS/SH increased up to around 2.5, and then it decreased.

V. It was suggested to use the molarity of sodium hydroxide in the range of 10-16M to produce the fly ash-based geopolymer concrete mixtures with acceptable compressive strength behavior.

VI. Among the curing methods, the heat curing regime is the best one for getting early and high compressive strength of fly ash-based geopolymer concrete.

VII. It was suggested to use the oven curing temperatures between 50-80°C and curing time of 24 hr for successful geopolymerization process as well as getting acceptable compressive strength of fly ash-based geopolymer concrete.

VIII. Different models could be successfully used to predict the compressive strength of FA-GPC with different mixture proportions, curing regimes, and concrete ages.

IX. All the used models LR, MLR, ANN, and M5P could be successfully used to develop predictive models for the compressive strength of the FA-GPC. Overall, the ANN model has better performance than the other two models. The R^2 values for this model are 0.96, 0.98, and 0.98 for the training, testing, and validating datasets, respectively. In addition, other sensitivity indicators for the training dataset for the ANN model are 3.33 MPa, 2.58 MPa, 2.91 and 0.109 for the RMSE, MAE, OBJ, and SI, respectively.

Recommendation

Detailed investigations on the fresh and mechanical properties of fly ash-based geopolymer concrete can be found in the literature. However, studies which are focused on the other properties of this composite are still limited. In order for this composite to be acceptable by the construction industry, some durability properties such as water permeability, gas permeability, chloride resistance, fatigue performance, and freeze-thaw resistance should further be examined comprehensively.

Author Declarations

We wish to draw the attention of the Editor to the following facts which may be considered as potential conflicts of interest and to significant financial contributions to this work. [OR] We wish to confirm that there are no known conflicts of interest associated with this publication and there has been no significant financial support for this work that could have influenced its outcome. We confirm that the manuscript has been read and approved by all named authors and that there are no other persons who satisfied the criteria for authorship but are not listed. We further confirm that the order of authors listed in the manuscript has been approved by all of us. We confirm that we have given due consideration to the protection of intellectual property associated with this work and that there are no impediments to publication, including the timing of publication, with respect to intellectual property. In so doing, we confirm that we have followed the regulations of our institutions concerning intellectual property. We further confirm that any aspect of the work covered in this manuscript that has involved either experimental animals or human patients has been conducted with the ethical approval of all relevant bodies and that such approvals are acknowledged within the manuscript. [CAN BE DELETED IF NOT RELEVANT] We understand that the Corresponding Author is the sole contact for the Editorial process (including Editorial Manager and direct communications with the office). He/she is responsible for communicating with the other authors about progress, submissions of revisions and final approval of proofs. We confirm that we have provided a current, correct email address which is accessible by the Corresponding Author.

Consent for publication

I (Ahmed S. Mohammed) hereby declare that I participated in this study and the manuscript's development (Compressive strength of Geopolymer concrete composites: Modeling and comprehensive systematic review). I have read the final version and give my consent for the article to be published in Silicon Journal.

Availability of data and materials

The data supporting the conclusions of this article are included with the article.

Competing interests

The authors declare that they have no competing interests.

Funding

This work had no finding.

Authors' contributions

Hemn Unis Ahmed and Ahmed S. Mohammed is collecting data, planning, and writing. Azad Mohammed, results and analysis. Hemn and Ahmed did the conclusions and editing.

Acknowledgment

The University of Sulaimani, College of Engineering, supported this work.

References

[1] Mahasenan, N., Smith, S., & Humphreys, K. (2003, January). The cement industry and global climate change: current and potential future cement industry CO2 emissions. In Greenhouse Gas Control Technologies-6th International Conference (pp. 995-1000). Pergamon, https://doi.org/10.1016/B978-008044276-1/50157-4

[2] Madheswaran, C. K., Gnanasundar, G., & Gopalakrishnan, N. (2013). Effect of molarity in geopolymer concrete. *International Journal of Civil & Structural Engineering*, *4*(2), 106-115, https://doi.org/10.6088/ijcser.20130402001

[3] Yu, Q. L. (2019). Application of nanomaterials in alkali-activated materials. In *Nanotechnology in Eco-efficient Construction* (pp. 97-121). Woodhead Publishing, https://doi.org/10.1016/B978-0-08-102641-0.00005-0

[4] Guo, X., Shi, H., & Dick, W. A. (2010). Compressive strength and microstructural characteristics of class C fly ash geopolymer. Cement and Concrete Composites, 32(2), 142-147, https://doi.org/10.1016/j.cemconcomp.2009.11.003

[5] Mehta, P. K. (2001). Reducing the environmental impact of concrete. Concrete international, 23(10), 61-66.

[6] Mejeoumov, G. G. (2007). Improved cement quality and grinding efficiency by means of closed mill circuit modeling. Texas A&M University, https://core.ac.uk/download/pdf/4276576.pdf

[7] Shaikh, F. U. A. (2016). Mechanical and durability properties of fly ash geopolymer concrete containing recycled coarse aggregates. *International Journal of Sustainable Built Environment*, *5*(2), 277-287, https://doi.org/10.1016/j.ijsbe.2016.05.009

[8] Shalini, A., Gurunarayanan, G., & Sakthivel, S. (2016). Performance of rice husk ash in geopolymer concrete. *Int J Innov Res Sci Tech*, *2*, 73-77.

[9] Han, B., Yu, X., & Ou, J. (2014). *Self-sensing concrete in smart structures*. Butterworth-Heinemann.

[10] Provis, J. L., Palomo, A., & Shi, C. (2015). Advances in understanding alkali-activated materials. *Cement and Concrete Research*, *78*, 110-125, https://doi.org/10.1016/j.cemconres.2015.04.013

[11] Abdel-Gawwad, H. A., & Abo-El-Enein, S. A. (2016). A novel method to produce dry geopolymer cement powder. *HBRC journal*, *12*(1), 13-24, https://doi.org/10.1016/j.hbrcj.2014.06.008

[12] Davidovits, J. (2015). Geopolymer Chemistry and Applications. 4-th edition. *J. Davidovits.–Saint-Quentin, France*.

[13] Davidovits, J. (2008). Geoplolymer chemistry and application. institute Geopolymer Saint-Quentin.

[14] Palomo, A., Blanco-Varela, M. T., Granizo, M. L., Puertas, F., Vazquez, T., & Grutzeck, M. W. (1999). Chemical stability of cementitious materials based on metakaolin. Cement and Concrete Research, 29(7), 997-1004, https://doi.org/10.1016/S0008-8846(99)00074-5

[15] Abdullah, M. M. A., Hussin, K., Bnhussain, M., Ismail, K. N., & Ibrahim, W. M. W. (2011). Mechanism and chemical reaction of fly ash geopolymer cement-a review. Int. J. Pure Appl. Sci. Technol, 6(1), 35-44.
[16] Palomo, A., Grutzeck, M. W., & Blanco, M. T. (1999). Alkali-activated fly ashes: A cement for the future. Cement and concrete research, 29(8), 1323-1329, https://doi.org/10.1016/S0008-8846(98)00243-9
[17] Liew, Y. M., Heah, C. Y., & Kamarudin, H. (2016). Structure and properties of clay-based geopolymer cements: A review. Progress in Materials Science, 83, 595-629, https://doi.org/10.1016/j.pmatsci.2016.08.002
[18] Duxson, P., Fernández-Jiménez, A., Provis, J. L., Lukey, G. C., Palomo, A., & van Deventer, J. S. (2007). Geopolymer technology: the current state of the art. Journal of materials science, 42(9), 2917-2933, https://doi.org/10.1007/s10853-006-0637-z
[19] Ravitheja, A., & Kumar, N. K. (2019). A study on the effect of nano clay and GGBS on the strength properties of fly ash based geopolymers. Materials Today: Proceedings, 19, 273-276, https://doi.org/10.1016/j.matpr.2020.06.292
[20] Diaz, E. I., Allouche, E. N., & Eklund, S. (2010). Factors affecting the suitability of fly ash as source material for geopolymers. Fuel, 89(5), 992-996, https://doi.org/10.1016/j.fuel.2009.09.012
[21] Yip, C. K., Lukey, G. C., Provis, J. L., & van Deventer, J. S. (2008). Effect of calcium silicate sources on geopolymerisation. Cement and Concrete Research, 38(4), 554-564, https://doi.org/10.1016/j.cemconres.2007.11.001
[22] Sumesh, M., Alengaram, U. J., Jumaat, M. Z., Mo, K. H., & Alnahhal, M. F. (2017). Incorporation of nano-materials in cement composite and geopolymer based paste and mortar–A review. *Construction and Building Materials*, *148*, 62-84, https://doi.org/10.1016/j.conbuildmat.2017.04.206
[23] Weil, M., Dombrowski, K., & Buchwald, A. (2009). Life-cycle analysis of geopolymer. In Geopolymers (pp. 194-210). Woodhead Publishing, https://doi.org/10.1533/9781845696382.2.194
[24] Omer, S. A., Demirboga, R., & Khushefati, W. H. (2015). Relationship between compressive strength and UPV of GGBFS based geopolymer mortars exposed to elevated temperatures. Construction and Building Materials, 94, 189-195, https://doi.org/10.1016/j.conbuildmat.2015.07.006
[25] Xu, H., & Van Deventer, J. S. J. (2000). The geopolymerisation of alumino-silicate minerals. International journal of mineral processing, 59(3), 247-266, https://doi.org/10.1016/S0301-7516(99)00074-5
[26] Pavithra, P. E., Reddy, M. S., Dinakar, P., Rao, B. H., Satpathy, B. K., & Mohanty, A. N. (2016). A mix design procedure for geopolymer concrete with fly ash. Journal of cleaner production, 133, 117-125, https://doi.org/10.1016/j.jclepro.2016.05.041
[27] Gorai, B., & Jana, R. K. (2003). Characteristics and utilisation of copper slag—a review. Resources, Conservation and Recycling, 39(4), 299-313, https://doi.org/10.1016/S0921-3449(02)00171-4
[28] Ahmaruzzaman, M. (2010). A review on the utilization of fly ash. Progress in energy and combustion science, 36(3), 327-363, https://doi.org/10.1016/j.pecs.2009.11.003
[29] ASTM-C618 (1999) Standard specification for coal fly ash and raw or calcined natural pozzolan for use as a mineral admixture in Concretein concrete, ASTM International, West Conshohocken, PA, USA.
[30] Bankowski, P., Zou, L., & Hodges, R. (2004). Reduction of metal leaching in brown coal fly ash using geopolymers. Journal of hazardous materials, 114(1-3), 59-67, https://doi.org/10.1016/j.jhazmat.2004.06.034
[31] Antiohos, S. K., & Tsimas, S. (2007). A novel way to upgrade the coarse part of a high calcium fly ash for reuse into cement systems. Waste Management, 27(5), 675-683, https://doi.org/10.1016/j.wasman.2006.03.016
[32] Neupane, G., & Donahoe, R. J. (2013). Leachability of elements in alkaline and acidic coal fly ash samples during batch and column leaching tests. Fuel, 104, 758-770, https://doi.org/10.1016/j.fuel.2012.06.013
[33] Nyale, S. M., Eze, C. P., Akinyeye, R. O., Gitari, W. M., Akinyemi, S. A., Fatoba, O. O., & Petrik, L. F. (2014). The leaching behaviour and geochemical fractionation of trace elements in hydraulically disposed weathered coal fly ash. Journal of Environmental Science and Health, Part A, 49(2), 233-242, https://doi.org/10.1080/10934529.2013.838929
[34] Yao, Z. T., Ji, X. S., Sarker, P. K., Tang, J. H., Ge, L. Q., Xia, M. S., & Xi, Y. Q. (2015). A comprehensive review on the applications of coal fly ash. Earth-Science Reviews, 141, 105-121, https://doi.org/10.1016/j.earscirev.2014.11.016

[35] Shibayama, A., Kim, Y., Harjanto, S., Sugai, Y., Okada, K., & Fujita, T. (2005). Remediation of contaminated soil by fly ash containing dioxins from incineration by using flotation. Materials transactions, 46(5), 990-995, https://doi.org/10.2320/matertrans.46.990

[36] Nomura, Y., Fujiwara, K., Terada, A., Nakai, S., & Hosomi, M. (2010). Prevention of lead leaching from fly ashes by mechanochemical treatment. Waste Management, 30(7), 1290-1295, https://doi.org/10.1016/j.wasman.2009.11.025

[37] Boiny, H. U., Alshkane, Y. M., & Rafiq, S. K. (2016, October). Mechanical properties of cement mortar by using polyethylene terephthalate fibers. In 5th National and 1st International Conference on Modern Materials and Structures in Civil Engineering, Iran (Islamic Republic of Iran).

[38] Alshkane, Y. M., Rafiq, S. K., & Boiny, H. U. (2017). Correlation between Destructive and Non-Destructive Tests on the Mechanical Properties of Different Cement Mortar Mixtures incorporating Polyethylene Terephthalate Fibers. Sulaimania Journal for Engineering Sciences, 4(5), https://doi.org/10.17656/sjes.10058

[39] Ahmed, H. U., Faraj, R. H., Hilal, N., Mohammed, A. A., & Sherwani, A. F. H. (2021). Use of recycled fibers in concrete composites: A systematic comprehensive review. Composites Part B: Engineering, 108769, https://doi.org/10.1016/j.compositesb.2021.108769

[40] Anjos, M. A., Camões, A., Campos, P., Azeredo, G. A., & Ferreira, R. L. (2020). Effect of high volume fly ash and metakaolin with and without hydrated lime on the properties of self-compacting concrete. Journal of Building Engineering, 27, 100985, https://doi.org/10.1016/j.jobe.2019.100985

[41] Barbhuiya, S. (2011). Effects of fly ash and dolomite powder on the properties of self-compacting concrete. Construction and Building Materials, 25(8), 3301-3305, https://doi.org/10.1016/j.conbuildmat.2011.03.018

[42] Bouzoubaa, N., & Lachemi, M. (2001). Self-compacting concrete incorporating high volumes of class F fly ash: Preliminary results. Cement and concrete research, 31(3), 413-420, https://doi.org/10.1016/S0008-8846(00)00504-4

[43] Dinakar, P., Babu, K. G., & Santhanam, M. (2008). Mechanical properties of high-volume fly ash self-compacting concrete mixtures. Structural concrete, 9(2), 109-116, https://www.icevirtuallibrary.com/doi/abs/10.1680/stco.2008.9.2.109

[44] Moffatt, E. G., Thomas, M. D., & Fahim, A. (2017). Performance of high-volume fly ash concrete in marine environment. Cement and Concrete Research, 102, 127-135, https://doi.org/10.1016/j.cemconres.2017.09.008

[45] Roychand, R., Li, J., De Silva, S., Saberian, M., Law, D., & Pramanik, B. K. (2021). Development of zero cement composite for the protection of concrete sewage pipes from corrosion and fatbergs. Resources, Conservation and Recycling, 164, 105166, https://doi.org/10.1016/j.resconrec.2020.105166

[46] Yildirim, G., Sahmaran, M., & Ahmed, H. U. (2015). Influence of hydrated lime addition on the self-healing capability of high-volume fly ash incorporated cementitious composites. Journal of Materials in Civil Engineering, 27(6), 04014187, https://doi.org/10.1061/(ASCE)MT.1943-5533.0001145

[47] Jiang, X., Xiao, R., Ma, Y., Zhang, M., Bai, Y., & Huang, B. (2020). Influence of waste glass powder on the physico-mechanical properties and microstructures of fly ash-based geopolymer paste after exposure to high temperatures. Construction and Building Materials, 262, 120579, https://doi.org/10.1016/j.conbuildmat.2020.120579

[48] Wulandari, K. D., Ekaputri, J. J., Kurniawan, S. B., Primaningtyas, W. E., Abdullah, S. R. S., Ismail, N. I., & Imron, M. F. (2021). Effect of microbes addition on the properties and surface morphology of fly ash-based geopolymer paste. Journal of Building Engineering, 33, 101596, https://doi.org/10.1016/j.jobe.2020.101596

[49] Shill, S. K., Al-Deen, S., Ashraf, M., & Hutchison, W. (2020). Resistance of fly ash based geopolymer mortar to both chemicals and high thermal cycles simultaneously. Construction and Building Materials, 239, 117886, https://doi.org/10.1016/j.conbuildmat.2019.117886

[50] Sivasakthi, M., Jeyalakshmi, R., & Rajamane, N. P. (2021). Fly ash geopolymer mortar: Impact of the substitution of river sand by copper slag as a fine aggregate on its thermal resistance properties. Journal of Cleaner Production, 279, 123766, https://doi.org/10.1016/j.jclepro.2020.123766

[51] Noushini, A., Castel, A., Aldred, J., & Rawal, A. (2020). Chloride diffusion resistance and chloride binding capacity of fly ash-based geopolymer concrete. Cement and Concrete Composites, 105, 103290, https://doi.org/10.1016/j.cemconcomp.2019.04.006

[52] Morla, P., Gupta, R., Azarsa, P., & Sharma, A. (2021). Corrosion Evaluation of Geopolymer Concrete Made with Fly Ash and Bottom Ash. Sustainability, 13(1), 398, https://doi.org/10.3390/su13031469

[53] Zhuang, X. Y., Chen, L., Komarneni, S., Zhou, C. H., Tong, D. S., Yang, H. M., ... & Wang, H. (2016). Fly ash-based geopolymer: clean production, properties and applications. Journal of Cleaner Production, 125, 253-267, https://doi.org/10.1016/j.jclepro.2016.03.019

[54] ASTM C39/C39M (2017) Standard Test Method for Compressive Strength of Cylindrical Concrete Specimens, ASTM International, West Conshohocken, PA, USA.

[55] The European Standard BS EN12390-3, 2009, testing on hardned concrete:part-3: compressive strength of test specimens

[56] Neville, A. M., & Brooks, J. J. (2010). Concrete technology.

[57] Golafshani, E. M., Behnood, A., & Arashpour, M. (2020). Predicting the compressive strength of normal and High-Performance Concretes using ANN and ANFIS hybridized with Grey Wolf Optimizer. Construction and Building Materials, 232, 117266, https://doi.org/10.1016/j.conbuildmat.2019.117266

[58] George, U. A., & Elvis, M. M. (2019). Modelling of the mechanical properties of concrete with cement ratio partially replaced by aluminium waste and sawdust ash using artificial neural network. SN Applied Sciences, 1(11), 1514, https://doi.org/10.1007/s42452-019-1504-2

[59] Mehdipour, V., Stevenson, D. S., Memarianfard, M., & Sihag, P. (2018). Comparing different methods for statistical modeling of particulate matter in Tehran, Iran. Air Quality, Atmosphere & Health, 11(10), 1155-1165, https://doi.org/10.1007/s11869-018-0615-z

[60] Sihag, P., Jain, P., & Kumar, M. (2018). Modelling of impact of water quality on recharging rate of storm water filter system using various kernel function based regression. Modeling earth systems and environment, 4(1), 61-68, https://doi.org/10.1007/s40808-017-0410-0

[61] Shahmansouri, A. A., Bengar, H. A., & Ghanbari, S. (2020). Compressive strength prediction of eco-efficient GGBS-based geopolymer concrete using GEP method. Journal of Building Engineering, 101326, https://doi.org/10.1016/j.jobe.2020.101326

[62] Velay-Lizancos, M., Perez-Ordoñez, J. L., Martinez-Lage, I., & Vazquez-Burgo, P. (2017). Analytical and genetic programming model of compressive strength of eco concretes by NDT according to curing temperature. Construction and Building Materials, 144, 195-206, https://doi.org/10.1016/j.conbuildmat.2017.03.123

[63] Gholampour, A., Mansouri, I., Kisi, O., & Ozbakkaloglu, T. (2020). Evaluation of mechanical properties of concretes containing coarse recycled concrete aggregates using multivariate adaptive regression splines (MARS), M5 model tree (M5Tree), and least squares support vector regression (LSSVR) models. Neural Computing and Applications, 32(1), 295-308, https://doi.org/10.1007/s00521-018-3630-y

[64] Behnood, A., Olek, J., & Glinicki, M. A. (2015a). Predicting modulus elasticity of recycled aggregate concrete using M5′ model tree algorithm. Construction and Building Materials, 94, 137-147, https://doi.org/10.1016/j.conbuildmat.2015.06.055

[65] Golafshani, E. M., & Behnood, A. (2018). Application of soft computing methods for predicting the elastic modulus of recycled aggregate concrete. Journal of cleaner production, 176, 1163-1176, https://doi.org/10.1016/j.jclepro.2017.11.186

[66] Mohammed, A., Rafiq, S., Sihag, P., Kurda, R., & Mahmood, W. (2020). Soft computing techniques: systematic multiscale models to predict the compressive strength of HVFA concrete based on mix proportions and curing times. Journal of Building Engineering, 101851, https://doi.org/10.1016/j.jobe.2020.101851

[67] Shahmansouri, A. A., Yazdani, M., Ghanbari, S., Bengar, H. A., Jafari, A., & Ghatte, H. F. (2020). Artificial neural network model to predict the compressive strength of eco-friendly geopolymer concrete incorporating silica fume and natural zeolite. Journal of Cleaner Production, 279, 123697, https://doi.org/10.1016/j.jclepro.2020.123697

[68] Behnood, A., Verian, K. P., & Gharehveran, M. M. (2015b). Evaluation of the splitting tensile strength in plain and steel fiber-reinforced concrete based on the compressive strength. Construction and Building Materials, 98, 519-529, https://doi.org/10.1016/j.conbuildmat.2015.08.124

[69] Faraj, R. H., Mohammed, A. A., Mohammed, A., Omer, K. M., & Ahmed, H. U. (2021). Systematic multiscale models to predict the compressive strength of self-compacting concretes modified with nanosilica at different curing ages. *Engineering with Computers*, 1-24, https://doi.org/10.1007/s00366-021-01385-9

[70] Hardjito, D., Wallah, S. E., Sumajouw, D. M. J., & Rangan, B. V. (2005, August). Introducing fly ash-based geopolymer concrete: manufacture and engineering properties. In 30th conference on our world in concrete & structures (Vol. 24).

[71] Al-Azzawi, M., Yu, T., & Hadi, M. N. (2018, June). Factors affecting the bond strength between the fly ash-based geopolymer concrete and steel reinforcement. In *Structures* (Vol. 14, pp. 262-272). Elsevier, https://doi.org/10.1016/j.istruc.2018.03.010

[72] Zhao, R., Yuan, Y., Cheng, Z., Wen, T., Li, J., Li, F., & Ma, Z. J. (2019). Freeze-thaw resistance of class F fly ash-based geopolymer concrete. Construction and Building Materials, 222, 474-483, https://doi.org/10.1016/j.conbuildmat.2019.06.166

[73] Singhal, D., Junaid, M. T., Jindal, B. B., & Mehta, A. (2018). Mechanical and microstructural properties of fly ash based geopolymer concrete incorporating alccofine at ambient curing. *Construction and building materials*, *180*, 298-307, https://doi.org/10.1016/j.conbuildmat.2018.05.286

[74] Shehab, H. K., Eisa, A. S., & Wahba, A. M. (2016). Mechanical properties of fly ash based geopolymer concrete with full and partial cement replacement. *Construction and building materials*, *126*, 560-565, https://doi.org/10.1016/j.conbuildmat.2016.09.059

[75] Chithambaram, S. J., Kumar, S., Prasad, M. M., & Adak, D. (2018). Effect of parameters on the compressive strength of fly ash based geopolymer concrete. *Structural Concrete*, *19*(4), 1202-1209, https://doi.org/10.1002/suco.201700235

[76] Wardhono, A., Gunasekara, C., Law, D. W., & Setunge, S. (2017). Comparison of long term performance between alkali activated slag and fly ash geopolymer concretes. *Construction and Building materials*, *143*, 272-279, https://doi.org/10.1016/j.conbuildmat.2017.03.153

[77] Ramujee, K., & PothaRaju, M. (2017). Mechanical properties of geopolymer concrete composites. *Materials Today: Proceedings*, *4*(2), 2937-2945, https://doi.org/10.1016/j.matpr.2017.02.175

[78] Wallah, S. E. (2010). Creep behaviour of fly ash-based geopolymer concrete. *Civil Engineering Dimension*, *12*(2), 73-78.

[79] Aliabdo, A. A., Abd Elmoaty, M., & Salem, H. A. (2016). Effect of water addition, plasticizer and alkaline solution constitution on fly ash based geopolymer concrete performance. *Construction and Building Materials*, *121*, 694-703, https://doi.org/10.1016/j.conbuildmat.2016.06.062

[80] Xie, T., & Ozbakkaloglu, T. (2015). Behavior of low-calcium fly and bottom ash-based geopolymer concrete cured at ambient temperature. *Ceramics International*, *41*(4), 5945-5958, https://doi.org/10.1016/j.ceramint.2015.01.031

[81] Sarker, P. K. (2011). Bond strength of reinforcing steel embedded in fly ash-based geopolymer concrete. *Materials and structures*, *44*(5), 1021-1030, https://doi.org/10.1617/s11527-010-9683-8

[82] Chindaprasirt, P., & Chalee, W. (2014). Effect of sodium hydroxide concentration on chloride penetration and steel corrosion of fly ash-based geopolymer concrete under marine site. *Construction and Building Materials*, *63*, 303-310, https://doi.org/10.1016/j.conbuildmat.2014.04.010

[83] Shaikh, F. U. A., & Vimonsatit, V. (2015). Compressive strength of fly-ash-based geopolymer concrete at elevated temperatures. *Fire and materials*, *39*(2), 174-188, https://doi.org/10.1002/fam.2240

[84] Sastry, K. G. K., Sahitya, P., & Ravitheja, A. (2020). Influence of nano TiO2 on strength and durability properties of geopolymer concrete. *Materials Today: Proceedings*, https://doi.org/10.1016/j.matpr.2020.03.139

[85] Çevik, A., Alzeebaree, R., Humur, G., Niş, A., & Gülşan, M. E. (2018). Effect of nano-silica on the chemical durability and mechanical performance of fly ash based geopolymer concrete. *Ceramics International*, *44*(11), 12253-12264, https://doi.org/10.1016/j.ceramint.2018.04.009

[86] Embong, R., Kusbiantoro, A., Shafiq, N., & Nuruddin, M. F. (2016). Strength and microstructural properties of fly ash based geopolymer concrete containing high-calcium and water-absorptive aggregate. *Journal of cleaner production*, *112*, 816-822, https://doi.org/10.1016/j.jclepro.2015.06.058

[87] Sumajouw, D. M. J., Hardjito, D., Wallah, S. E., & Rangan, B. V. (2007). Fly ash-based geopolymer concrete: study of slender reinforced columns. *Journal of materials science*, *42*(9), 3124-3130, https://doi.org/10.1007/s10853-006-0523-8

[88] Jaydeep, S., & Chakravarthy, B. J. (2013). Study on fly ash based geo-polymer concrete using admixtures. *International Journal of Engineering Trends and Technology*, *4*(10), 4614-4617, https://ijettjournal.org/archive/ijett-v4i10p161

[89] Nuaklong, P., Jongvivatsakul, P., Pothisiri, T., Sata, V., & Chindaprasirt, P. (2020). Influence of rice husk ash on mechanical properties and fire resistance of recycled aggregate high-calcium fly ash geopolymer concrete. *Journal of Cleaner Production*, *252*, 119797, https://doi.org/10.1016/j.jclepro.2019.119797

[90] Okoye, F. N., Durgaprasad, J., & Singh, N. B. (2016). Effect of silica fume on the mechanical properties of fly ash based-geopolymer concrete. *Ceramics International*, *42*(2), 3000-3006, https://doi.org/10.1016/j.ceramint.2015.10.084

[91] Okoye, F. N., Prakash, S., & Singh, N. B. (2017). Durability of fly ash based geopolymer concrete in the presence of silica fume. *Journal of cleaner Production*, *149*, 1062-1067, https://doi.org/10.1016/j.jclepro.2017.02.176

[92] Sarker, P. K., Haque, R., & Ramgolam, K. V. (2013). Fracture behaviour of heat cured fly ash based geopolymer concrete. *Materials & Design*, *44*, 580-586, https://doi.org/10.1016/j.matdes.2012.08.005

[93] Junaid, M. T., Kayali, O., & Khennane, A. (2017). Response of alkali activated low calcium fly-ash based geopolymer concrete under compressive load at elevated temperatures. *Materials and Structures*, *50*(1), 50, https://doi.org/10.1617/s11527-016-0877-6

[94] Olivia, M., Sarker, P., & Nikraz, H. (2008). Water penetrability of low calcium fly ash geopolymer concrete. *Proc. ICCBT2008-A*, *46*, 517-530.

[95] Abhilash, P., Sashidhar, C., & Reddy, I. R. (2016). Strength properties of Fly ash and GGBS based Geo-polymer Concrete. *International Journal of ChemTech Research, ISSN*, 0974-4290.

[96] Jindal, B. B., Parveen, Singhal, D., & Goyal, A. (2017). Predicting relationship between mechanical properties of low calcium fly ash-based geopolymer concrete. *Transactions of the Indian Ceramic Society*, *76*(4), 258-265, https://doi.org/10.1080/0371750X.2017.1412837

[97] Vignesh, P., & Vivek, K. (2015). An experimental investigation on strength parameters of flyash based geopolymer concrete with GGBS. *International Research Journal of Engineering and Technology*, *2*(2), 135-142, https://www.irjet.net/archives/V2/i2/Irjet-v2i224.pdf

[98] Joseph, B., & Mathew, G. (2012). Influence of aggregate content on the behavior of fly ash based geopolymer concrete. *Scientia Iranica*, *19*(5), 1188-1194, https://doi.org/10.1016/j.scient.2012.07.006

[99] Nath, P., & Sarker, P. K. (2014). Effect of GGBFS on setting, workability and early strength properties of fly ash geopolymer concrete cured in ambient condition. Construction and Building Materials, 66, 163-171, https://doi.org/10.1016/j.conbuildmat.2014.05.080

[100] Patankar, S. V., Jamkar, S. S., & Ghugal, Y. M. (2013). Effect of water-to-geopolymer binder ratio on the production of fly ash based geopolymer concrete. *Int. J. Adv. Technol. Civ. Eng*, *2*(1), 79-83.

[101] Adak, D., Sarkar, M., & Mandal, S. (2017). Structural performance of nano-silica modified fly-ash based geopolymer concrete. *Construction and Building Materials*, *135*, 430-439, https://doi.org/10.1016/j.conbuildmat.2016.12.111

[102] Gunasekara, C., Law, D. W., & Setunge, S. (2016). Long term permeation properties of different fly ash geopolymer concretes. *Construction and Building Materials*, *124*, 352-362, https://doi.org/10.1016/j.conbuildmat.2016.07.121

[103] Mehta, A., & Siddique, R. (2017). Sulfuric acid resistance of fly ash based geopolymer concrete. *Construction and Building Materials*, *146*, 136-143, https://doi.org/10.1016/j.conbuildmat.2017.04.077

[104] Cui, Y., Gao, K., & Zhang, P. (2020). Experimental and Statistical Study on Mechanical Characteristics of Geopolymer Concrete. *Materials*, *13*(7), 1651, https://doi.org/10.3390/ma13071651

[105] Albitar, M., Visintin, P., Ali, M. M., & Drechsler, M. (2015). Assessing behaviour of fresh and hardened geopolymer concrete mixed with class-F fly ash. *KSCE Journal of Civil Engineering*, *19*(5), 1445-1455, https://doi.org/10.1007/s12205-014-1254-z

[106] Bhogayata, A. C., & Arora, N. K. (2019). Utilization of metalized plastic waste of food packaging articles in geopolymer concrete. *Journal of Material Cycles and Waste Management*, *21*(4), 1014-1026, https://doi.org/10.1007/s10163-019-00859-9

[107] Gomaa, E., Sargon, S., Kashosi, C., Gheni, A., & ElGawady, M. A. (2020). Mechanical Properties of High Early Strength Class C Fly Ash-Based Alkali Activated Concrete. *Transportation Research Record*, 0361198120915892, https://doi.org/10.1177%2F0361198120915892

[108] Hassan, A., Arif, M., & Shariq, M. (2019). Effect of curing condition on the mechanical properties of fly ash-based geopolymer concrete. *SN Applied Sciences*, *1*(12), 1694, https://doi.org/10.1007/s42452-019-1774-8

[109] Kurtoglu, A. E., Alzeebaree, R., Aljumaili, O., Nis, A., Gulsan, M. E., Humur, G., & Cevik, A. (2018). Mechanical and durability properties of fly ash and slag based geopolymer concrete. *Advances in Concrete Construction*, *6*(4), 345, http://dx.doi.org/10.12989/acc.2018.6.4.345

[110] Nath, P., & Sarker, P. K. (2015). Use of OPC to improve setting and early strength properties of low calcium fly ash geopolymer concrete cured at room temperature. *Cement and concrete composites*, *55*, 205-214, https://doi.org/10.1016/j.cemconcomp.2014.08.008

[111] Saravanan, S., & Elavenil, S. (2018). Strength Properties of Geopolymer Concrete using M Sand by Assessing their Mechanical Characteristics. *ARPN Journal of Engineering and Applied Sciences*, *13*(13), 4028-4041.

[112] Topark-Ngarm, P., Chindaprasirt, P., & Sata, V. (2015). Setting time, strength, and bond of high-calcium fly ash geopolymer concrete. *Journal of Materials in Civil Engineering*, *27*(7), 04014198, https://doi.org/10.1061/(ASCE)MT.1943-5533.0001157

[113] Vijai, K., Kumutha, R., & Vishnuram, B. G. (2011). Experimental investigations on mechanical properties of geopolymer concrete composites, http://dl.lib.mrt.ac.lk/handle/123/9265

[114] Vora, P. R., & Dave, U. V. (2013). Parametric studies on compressive strength of geopolymer concrete. *Procedia Engineering*, *51*, 210-219, https://doi.org/10.1016/j.proeng.2013.01.030

[115] Wang, Y., Hu, S., & He, Z. (2019). Mechanical and Fracture Properties of Fly Ash Geopolymer Concrete Addictive with Calcium Aluminate Cement. *Materials*, *12*(18), 2982, https://doi.org/10.3390/ma12182982

[116] Ibrahim, M., Johari, M. A. M., Maslehuddin, M., & Rahman, M. K. (2018). Influence of nano-SiO2 on the strength and microstructure of natural pozzolan based alkali activated concrete. *Construction and Building Materials*, *173*, 573-585, https://doi.org/10.1016/j.conbuildmat.2018.04.051

[117] Ghafoor, M. T., Khan, Q. S., Qazi, A. U., Sheikh, M. N., & Hadi, M. N. S. (2021). Influence of alkaline activators on the mechanical properties of fly ash based geopolymer concrete cured at ambient temperature. Construction and Building Materials, 273, 121752, https://doi.org/10.1016/j.conbuildmat.2020.121752

[118] Fang, G., Ho, W. K., Tu, W., & Zhang, M. (2018). Workability and mechanical properties of alkali-activated fly ash-slag concrete cured at ambient temperature. *Construction and Building Materials*, *172*, 476-487, https://doi.org/10.1016/j.conbuildmat.2018.04.008

[119] Vijai, K., Kumutha, R., & Vishnuram, B. G. (2010). Effect of types of curing on strength of geopolymer concrete. *International journal of physical sciences*, *5*(9), 1419-1423, https://doi.org/10.5897/IJPS.9000200

[120] Krishnaraja, A. R., Sathishkumar, N. P., Kumar, T. S., & Kumar, P. D. (2014). Mechanical behaviour of geopolymer concrete under ambient curing. *International Journal of Scientific Engineering and Technology*, *3*(2), 130-132.

[121] Kumaravel, S. (2014). Development of various curing effect of nominal strength Geopolymer concrete. *Journal of Engineering Science and Technology Review*, *7*(1), 116-119.

[122] Muhammad, N., Baharom, S., Ghazali, N. A. M., & Alias, N. A. (2019). Effect of Heat Curing Temperatures on Fly Ash-Based Geopolymer Concrete. *Int. J. Eng. Technol*, *8*, 15-19.

[123] Das, S. K., & Shrivastava, S. (2020). Siliceous fly ash and blast furnace slag based geopolymer concrete under ambient temperature curing condition. *Structural Concrete*, https://doi.org/10.1002/suco.201900201

[124] Nuruddin, M. N., Kusbiantoro, A. K., Qazi, S. Q., Darmawan, M. D., & Husin, N. H. (2011). Development of geopolymer concrete with different curing conditions. *IPTEK The Journal for Technology and Science*, *22*(1), https://doi.org/10.21833/ijaas.2018.01.005

[125] Thakur, R. N., & Ghosh, S. (2009). Effect of mix composition on compressive strength and microstructure of fly ash based geopolymer composites. ARPN Journal of Engineering and Applied Sciences, 4(4), 68-74, http://www.arpnjournals.com/jeas/research_papers/rp_2009/jeas_0609_200.pdf

[126] Dombrowski, K., Buchwald, A., & Weil, M. (2007). The influence of calcium content on the structure and thermal performance of fly ash based geopolymers. Journal of Materials Science, 42(9), 3033-3043, https://doi.org/10.1007/s10853-006-0532-7

[127] Chi, M., & Huang, R. (2013). Binding mechanism and properties of alkali-activated fly ash/slag mortars. Construction and building materials, 40, 291-298, https://doi.org/10.1016/j.conbuildmat.2012.11.003

[128] Fernandez-Jimenez, A. M., Palomo, A., & Lopez-Hombrados, C. (2006). Engineering properties of alkali-activated fly ash concrete. ACI Materials Journal, 103(2), 106, https://www.concrete.org/publications/internationalconcreteabstractsportal/m/details/id/15261

[129] Ryu, G. S., Lee, Y. B., Koh, K. T., & Chung, Y. S. (2013). The mechanical properties of fly ash-based geopolymer concrete with alkaline activators. Construction and Building Materials, 47, 409-418, https://doi.org/10.1016/j.conbuildmat.2013.05.069

[130] Khale, D., & Chaudhary, R. (2007). Mechanism of geopolymerization and factors influencing its development: a review. Journal of materials science, 42(3), 729-746, https://doi.org/10.1007/s10853-006-0401-4

[131] Thokchom, S., Mandal, K. K., & Ghosh, S. (2012). Effect of Si/Al ratio on performance of fly ash geopolymers at elevated temperature. Arabian Journal for Science and Engineering, 37(4), 977-989, https://doi.org/10.1007/s13369-012-0230-5

[132] Garcia-Lodeiro, I., Palomo, A., Fernández-Jiménez, A., & Macphee, D. E. (2011). Compatibility studies between NASH and CASH gels. Study in the ternary diagram Na2O–CaO–Al2O3–SiO2–H2O. Cement and Concrete Research, 41(9), 923-931, https://doi.org/10.1016/j.cemconres.2011.05.006

[133] Sathonsaowaphak, A., Chindaprasirt, P., & Pimraksa, K. (2009). Workability and strength of lignite bottom ash geopolymer mortar. Journal of Hazardous Materials, 168(1), 44-50, https://doi.org/10.1016/j.jhazmat.2009.01.120

[134] Rafeet, A., Vinai, R., Soutsos, M., & Sha, W. (2017). Guidelines for mix proportioning of fly ash/GGBS based alkali activated concretes. Construction and Building Materials, 147, 130-142, https://doi.org/10.1016/j.conbuildmat.2017.04.036

[135] Lloyd, R. R., Provis, J. L., & van Deventer, J. S. (2009). Microscopy and microanalysis of inorganic polymer cements. 1: remnant fly ash particles. Journal of materials science, 44(2), 608-619, https://doi.org/10.1007/s10853-008-3077-0

[136] Saha, S., & Rajasekaran, C. (2017). Enhancement of the properties of fly ash based geopolymer paste by incorporating ground granulated blast furnace slag. Construction and Building Materials, 146, 615-620, https://doi.org/10.1016/j.conbuildmat.2017.04.139

[137] Hu, W., Nie, Q., Huang, B., Su, A., Du, Y., Shu, X., & He, Q. (2018). Mechanical property and microstructure characteristics of geopolymer stabilized aggregate base. Construction and Building Materials, 191, 1120-1127, https://doi.org/10.1016/j.conbuildmat.2018.10.081

[138] Deb, P. S., Nath, P., & Sarker, P. K. (2014). The effects of ground granulated blast-furnace slag blending with fly ash and activator content on the workability and strength properties of geopolymer concrete cured at ambient temperature. Materials & Design (1980-2015), 62, 32-39, https://doi.org/10.1016/j.matdes.2014.05.001

[139] Hardjito, D., Wallah, S. E., Sumajouw, D. M., & Rangan, B. V. (2004). On the development of fly ash-based geopolymer concrete. ACI *Materials Journal*, *101*(6), 467-472, https://www.concrete.org/publications/internationalconcreteabstractsportal.aspx?m=details&ID=13485

[140] Barbosa, V. F., MacKenzie, K. J., & Thaumaturgo, C. (2000). Synthesis and characterisation of materials based on inorganic polymers of alumina and silica: sodium polysialate polymers. International Journal of Inorganic Materials, 2(4), 309-317, https://doi.org/10.1016/S1466-6049(00)00041-6

[141] Van Jaarsveld, J. G. S., Van Deventer, J. S. J., & Lukey, G. C. (2002). The effect of composition and temperature on the properties of fly ash-and kaolinite-based geopolymers. Chemical Engineering Journal, 89(1-3), 63-73, https://doi.org/10.1016/S1385-8947(02)00025-6

[142] He, J., Jie, Y., Zhang, J., Yu, Y., & Zhang, G. (2013). Synthesis and characterization of red mud and rice husk ash-based geopolymer composites. Cement and Concrete Composites, 37, 108-118, https://doi.org/10.1016/j.cemconcomp.2012.11.010

[143] Rickard, W. D., Williams, R., Temuujin, J., & Van Riessen, A. (2011). Assessing the suitability of three Australian fly ashes as an aluminosilicate source for geopolymers in high temperature applications. Materials Science and Engineering: A, 528(9), 3390-3397, https://doi.org/10.1016/j.msea.2011.01.005

[144] Komljenović, M., Baščarević, Z., & Bradić, V. (2010). Mechanical and microstructural properties of alkali-activated fly ash geopolymers. Journal of Hazardous Materials, 181(1-3), 35-42, https://doi.org/10.1016/j.jhazmat.2010.04.064

[145] Kumar, S., & Kumar, R. (2011). Mechanical activation of fly ash: Effect on reaction, structure and properties of resulting geopolymer. Ceramics International, 37(2), 533-541, https://doi.org/10.1016/j.ceramint.2010.09.038

[146] ASTM Designation C33/C33M (2018). Standard specification of concrete aggregates, Annual Book of ASTM Standard.

[147] Mermerdaş, K., Manguri, S., Nassani, D. E., & Oleiwi, S. M. (2017). Effect of aggregate properties on the mechanical and absorption characteristics of geopolymer mortar. Engineering science and Technology, an international Journal, 20(6), 1642-1652, https://doi.org/10.1016/j.jestch.2017.11.009

[148] Mane, S., & Jadhav, H. S. (2012). Investigation of geopolymer mortar and concrete under high temperature. International Journal of Emerging Technology and Advanced Engineering, 2 (12), 384-390.

[149] Nuaklong, P., Sata, V., & Chindaprasirt, P. (2016). Influence of recycled aggregate on fly ash geopolymer concrete properties. Journal of Cleaner Production, 112, 2300-2307, https://doi.org/10.1016/j.jclepro.2015.10.109

[150] Sreenivasulu, C., GURU, J. J., SEKHAR, R. M. V., & PAVAN, K. D. (2016). Effect of fine aggregate blending on short-term mechanical properties of geopolymer concrete. Asian Journal of Civil Engineering, 17 (5), 537–550, https://www.sid.ir/en/Journal/ViewPaper.aspx?ID=484795

[151] Puligilla, S., & Mondal, P. (2013). Role of slag in microstructural development and hardening of fly ash-slag geopolymer. Cement and Concrete Research, 43, 70-80, https://doi.org/10.1016/j.cemconres.2012.10.004

[152] Nath, P., & Sarker, P. K. (2017). Flexural strength and elastic modulus of ambient-cured blended low-calcium fly ash geopolymer concrete. *Construction and Building Materials*, *130*, 22-31, https://doi.org/10.1016/j.conbuildmat.2016.11.034

[153] Weng, L., & Sagoe-Crentsil, K. (2007). Dissolution processes, hydrolysis and condensation reactions during geopolymer synthesis: Part I—Low Si/Al ratio systems. Journal of materials science, 42(9), 2997-3006, https://doi.org/10.1007/s10853-006-0820-2

[154] Sagoe-Crentsil, K., & Weng, L. (2007). Dissolution processes, hydrolysis and condensation reactions during geopolymer synthesis: Part II. High Si/Al ratio systems. Journal of materials science, 42(9), 3007-3014, https://doi.org/10.1007/s10853-006-0818-9]

[155] Mustafa Al Bakri, A. M., Kamarudin, H., Bnhussain, M., Rafiza, A. R., & Zarina, Y. (2012). Effect of Na_2 SiO_3/NaOH Ratios and NaOH Molarities on Compressive Strength of Fly-Ash-Based Geopolymer. ACI Materials Journal, 109(5), https://www.concrete.org/publications/internationalconcreteabstractsportal/m/details/id/51684080

[156] Ridtirud, C., Chindaprasirt, P., & Pimraksa, K. (2011). Factors affecting the shrinkage of fly ash geopolymers. International Journal of Minerals, Metallurgy, and Materials, 18(1), 100-104, https://doi.org/10.1007/s12613-011-0407-z

[157] Phoo-ngernkham, T., Maegawa, A., Mishima, N., Hatanaka, S., & Chindaprasirt, P. (2015). Effects of sodium hydroxide and sodium silicate solutions on compressive and shear bond strengths of FA–GBFS geopolymer. Construction and Building Materials, 91, 1-8, https://doi.org/10.1016/j.conbuildmat.2015.05.001

[158] Morsy, M. S., Alsayed, S. H., Al-Salloum, Y., & Almusallam, T. (2014). Effect of sodium silicate to sodium hydroxide ratios on strength and microstructure of fly ash geopolymer binder. Arabian Journal for science and engineering, 39(6), 4333-4339, https://doi.org/10.1007/s13369-014-1093-8

[159] Alonso, S., & Palomo, A. (2001). Alkaline activation of metakaolin and calcium hydroxide mixtures: influence of temperature, activator concentration and solids ratio. Materials Letters, 47(1-2), 55-62, https://doi.org/10.1016/S0167-577X(00)00212-3

[160] Duxson, P., Lukey, G. C., Separovic, F., & Van Deventer, J. S. J. (2005). Effect of alkali cations on aluminum incorporation in geopolymeric gels. Industrial & Engineering Chemistry Research, 44(4), 832-839, https://doi.org/10.1021/ie0494216

[161] Görhan, G., & Kürklü, G. (2014). The influence of the NaOH solution on the properties of the fly ash-based geopolymer mortar cured at different temperatures. Composites part b: engineering, 58, 371-377, https://doi.org/10.1016/j.compositesb.2013.10.082

[162] Ramujee, K. (2014). Development of low calcium flyash based geopolymer concrete. *International Journal of Engineering and Technology*, *6*(1), 1.

[163] Chindaprasirt, P., Chareerat, T., Hatanaka, S., & Cao, T. (2011). High-strength geopolymer using fine high-calcium fly ash. Journal of Materials in Civil Engineering, 23(3), 264-270, https://doi.org/10.1061/(ASCE)MT.1943-5533.0000161

[164] Silva, R. V., De Brito, J., & Dhir, R. K. (2014). Properties and composition of recycled aggregates from construction and demolition waste suitable for concrete production. Construction and Building Materials, 65, 201-217, https://doi.org/10.1016/j.conbuildmat.2014.04.117

[165] Mohammed, A., Rafiq, S., Sihag, P., Kurda, R., Mahmood, W., Ghafor, K., & Sarwar, W. (2020). ANN, M5P-tree and nonlinear regression approaches with statistical evaluations to predict the compressive strength of cement-based mortar modified with fly ash. Journal of Materials Research and Technology, 9(6), 12416-12427, https://doi.org/10.1016/j.jmrt.2020.08.083

[166] FM Zain, M., & M Abd, S. (2009). Multiple regression model for compressive strength prediction of high performance concrete. JApSc, 9(1), 155-160.

[167] Demircan, E., Harendra, S., & Vipulanandan, C. (2011). Artificial neural network and nonlinear models for gelling time and maximum curing temperature rise in polymer grouts. *Journal of materials in civil engineering*, *23*(4), 372-377, https://doi.org/10.1061/(ASCE)MT.1943-5533.0000172

[168] Mohammed, A. S. (2018). Vipulanandan model for the rheological properties with ultimate shear stress of oil well cement modified with nanoclay. *Egyptian journal of petroleum*, *27*(3), 335-347, https://doi.org/10.1016/j.ejpe.2017.05.007

[169] *Quinlan Ross J., 1992. Learning with continuous classes. In: 5th Australian Joint Conference on Artificial Intelligence, Singapore, pp. 343–348.*

[170] Wang, Y., & Witten, I. H. 1997. Induction of model trees for predicting continuous classes. In *Poster papers of the 9th European Conference on Machine Learning*, https://hdl.handle.net/10289/1183

[171] Malerba, D., Esposito, F., Ceci, M., & Appice, A. (2004). Top-down induction of model trees with regression and splitting nodes. *IEEE Transactions on Pattern Analysis and Machine Intelligence*, *26*(5), 612-625, https://doi.org/10.1109/TPAMI.2004.1273937

[172] Li, M. F., Tang, X. P., Wu, W., & Liu, H. B. (2013). General models for estimating daily global solar radiation for different solar radiation zones in mainland China. Energy conversion and management, 70, 139-148, https://doi.org/10.1016/j.enconman.2013.03.004